ENTRAINED-BED COAL GASIFICATION MODELLING. INTERIM REPORT

WEST VIRGINIA UNIV., MORGANTOWN. DEPT. OF CHEMICAL ENGINEERING

1978

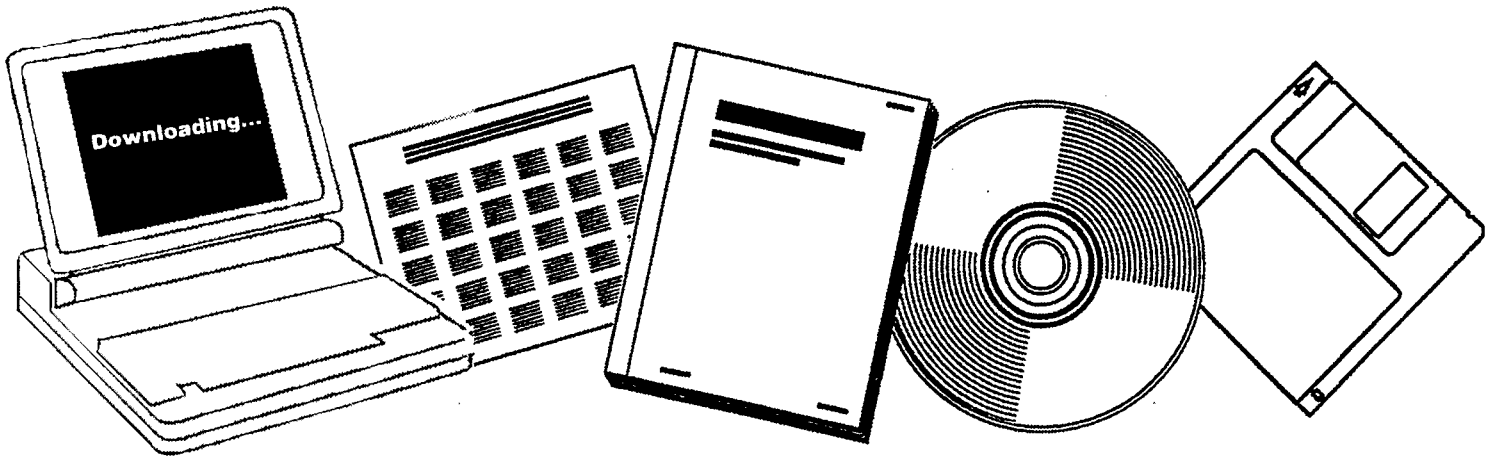

One Source. One Search. One Solution.

NTIS

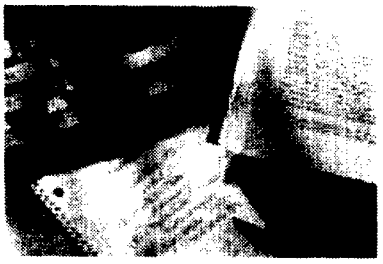

Providing Permanent, Easy Access to U.S. Government Information

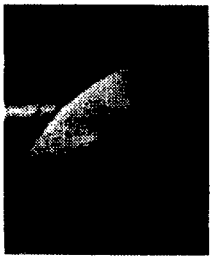

National Technical Information Service is the nation's largest repository and disseminator of government-initiated scientific, technical, engineering, and related business information. The NTIS collection includes almost 3,000,000 information products in a variety of formats: electronic download, online access, CD-ROM, magnetic tape, diskette, multimedia, microfiche and paper.

Search the NTIS Database from 1990 forward

NTIS has upgraded its bibliographic database system and has made all entries since 1990 searchable on **www.ntis.gov.** You now have access to information on more than 600,000 government research information products from this web site.

Link to Full Text Documents at Government Web Sites

Because many Government agencies have their most recent reports available on their own web site, we have added links directly to these reports. When available, you will see a link on the right side of the bibliographic screen.

Download Publications (1997 - Present)

NTIS can now provides the full text of reports as downloadable PDF files. This means that when an agency stops maintaining a report on the web, NTIS will offer a downloadable version. There is a nominal fee for each download for most publications.

For more information visit our website:

www.ntis.gov

U.S. DEPARTMENT OF COMMERCE
Technology Administration
National Technical Information Service
Springfield, VA 22161

ENTRAINED-BED COAL GASIFICATION MODELLING

Report submitted to

Department of Energy

Contract
E(49-18)2274

INTERIM REPORT

by

C. Y. Wen & T. Z. Chuang
Dept. of Chemical Engineering
West Virginia University
Morgantown
West Virginia
1978

TABLE OF CONTENTS

		page
	ABSTRACT	
I.	Introduction	1
	1. Texaco Entrained-Bed Pilot Plant Gasifier	2
	2. Raw Material Properties	2
II.	Reactions in and Entrained-Bed Gasifier	5
	1. Pyrolysis and Volatile Combustion Zone	5
	2. Combustion and Gasification Zone	5
	3. Gasification Zone	6
III.	Coal Gasification Reaction Kinetics	7
	1. Pyrolysis	7
	2. Volatile Combustion	9
	3. Char-Gas Reactions	11
	4. Char-Oxygen Reaction	12
	5. Char-Steam Reaction	17
	6. Char-Carbon Dioxide Reaction	20
	7. Char-Hydrogen Reaction	20
	8. Water-Gas Reaction	25
	9. Methane-Steam Reaction	25
IV.	Model Development	28
	1. Hydrodynamics	28
	2. Heat and Mass Balances	29
V.	Results and Discussion	34
VI.	Conclusion and Recommendation	38
VII.	Notation	40
VIII.	Literature Cited	42
IX.	APPENDICES	
	1. Reactions in each zone	46
	2. Rate Expressions	48
	3. Typical Ultimate Analysis for the Feedstock used in Texaco's Pilot Plant Tests	55
	4. Operating Conditions for Five Typical Runs of Texaco's Pilot Plant Tests	56
	5. Typical Temperature and Concentration Profiles in the Texaco Downflow Entrained-Bed Gasifier calculated from the Model	57
	6. Comparison of Computational Results from the model with Experimental Results from Texaco Entrained-Bed Pilot Plant Gasifier	72
	7. Parameter Studies of the Reactor Performance at Various Operating Conditions	76
	8. Computer Program	94

ABSTRACT

A mathematical model has been developed to simulate the Texaco Downflow Entrained-Bed Pilot Plant Gasifier using coal liquefaction residues and coal-water slurries as feedstocks. The entrained-bed gasifier was conceptually divided into three zones: the Pyrolysis and Volatile Combustion Zone, the Gasification and Combustion Zone, and the Gasification Zone. The gas phase was assumed to be completely mixed at the entrance region followed by a region approximating plug flow. The solid phase was assumed to be a plug flow throughout the reactor. Temperature and concentration profiles along the reactor were obtained by solving the material and energy balances and taking into consideration the gasification kinetics, the transport rates and the hydrodynamics of the gasifier. The results of computation from the proposed model were compared with the experimental data. Sensitivity of the parameters used in the model was tested and optimum operating conditions were searched to provide a better understanding of the performance under various operating conditions utilizing the model.

I. Introduction

Entrained-bed gasifiers are co-current flow reactors in which pulverized or atomized hydrocarbons react with oxygen and steam to produce gaseous fuels of low to high heating range values. The residence time in an entrained bed system is approximately five seconds and is much shorter than in a fluidized bed or a fixed bed system. To achieve a high conversion rate the reactor must either have a recycling of unreacted hydrocarbons or a more substantial amount of feed oxygen to react with parts of the feed hydrocarbons in order to provide a high temperature environment for promoting gasification rates. Furthermore, most gasification reactions in the reactor are endothermic and require a large amount of heat which must be provided either from combustion reactions or from outside heat sources.

The Texaco Synthesis Gas Generation Process [1] contains a downflow entrained-bed gasifier which was first designed to convert natural gas to synthesis gas ($CO+H_2$). Further developments enable the use of light oils, asphalts and coal-water slurries as feedstocks. Recently Texaco demonstrated that it is possible to gasify molten coal liquefaction residues into synthesis gas ($CO-H_2$) by an entrained bed gasifier. Most of the liquefaction processes currently being developed require hydrogen or synthesis gas (a mixture of hydrogen and carbon monoxide) to solubilize the coal. This entrained bed system is able to produce the needed hydrogen or synthesis gas for liquefaction processes primarily from the non-liquefied fraction of the coal with very high carbon conversions (91-99%).

The entrained-bed gasifiers currently being developed have several advantages over other proposed and existing gasification processes:

1. ability to utilize any type of coal or coal residues irrespective of swelling and caking including fines;
2. high coal throughput capacity particularly at high pressure;
3. product gas free of tars and phenols;
4. high carbon utilization due to high reaction rates.

However the required high temperature operating condition also means disadvantages such as:

1. difficulty in the selection of refractories and construction material in the combustion zone;
2. problem of sensible heat recovery in order to efficiently utilize the high temperature outlet gas;
3. large amounts of oxygen needed to maintain such a high temperature operating condition.

This paper reports on the development of a steady state model for the non-recycling entrained-bed gasifiers. The results reported here will compare with the pilot plant results of the Texaco Synthesis Gas Generator which use several kinds of coal liquefaction residues and coal-water slurries as feedstocks. This model also assesses the importance of each input parameter and provides criteria for scale-up purposes.

1.1 Texaco Entrained-Bed Pilot Plant Gasifier

The Texaco pilot plant gasifier shown schematically in Figure 1 is described in detail in a report by Texaco's Montebello Research Laboratory [1]. The 5 ft. fiameter by 20 ft. long steel vessel is dived internally into two sections. The top section is lined with a special refractory material specifically designed to withstand the severe operating environment expected. In this section, combustion and gasification reactions take place. The lower section is a quench vessel. A reservoir of water is maintained in the bottom of this vessel at all times by continuous injection of cooling water. Syngas leaving the top section of the gasifier passes through a water cooled dip tube into the water reservoir in the quench vessel. Slag, most of the soot, and unreacted hydrocarbon carried with the syngas remain in the water and are then removed. The saturated syngas is removed from the gas space above the water.

The pulverized coal liquefaction residue is made pumpable by melting the residue which is kept at 400°F-500°F and then blended with 2-7% aromatic solvent. The molten residue, oxygen and steam are fed through a proprietary Texaco Burner into the top of the pilot plant gasifier. All of the experimental runs with coal liquefaction residues were conducted at a pressure of 24 atmospheres.

For coal-water slurry runs, the coal is mixed with water and preheated to a temperature below saturation point so that water in the slurry enters the reactor as a liquid. It has been reported that the slurry can be mixed and pumped at solid loading as high as 70%, i.e., at a water/coal ratio of 0.4 [74]. The operating pressure for coal-water slurry runs is about 21 atm.

1.2 Raw Material Properties

Table I lists the ultimate analysis and some physical properties of the two coal liquefaction residues as received at the Montebello Research Laboratory [1]. The Wyodak coal residue, on the average, was much more viscous than the Illinois No. 6 coal residue at the operating temperatures. It is therefore expected that the particle size of Wyodak coal residue after being sprayed through the inlet nozzle is larger than that of Illinois No. 6 residue.

Appendix 3 and 4 give the ultimate analysis of the input fuel and the operating conditions respectively for seven typical runs at Texaco's pilot plant testing facility.

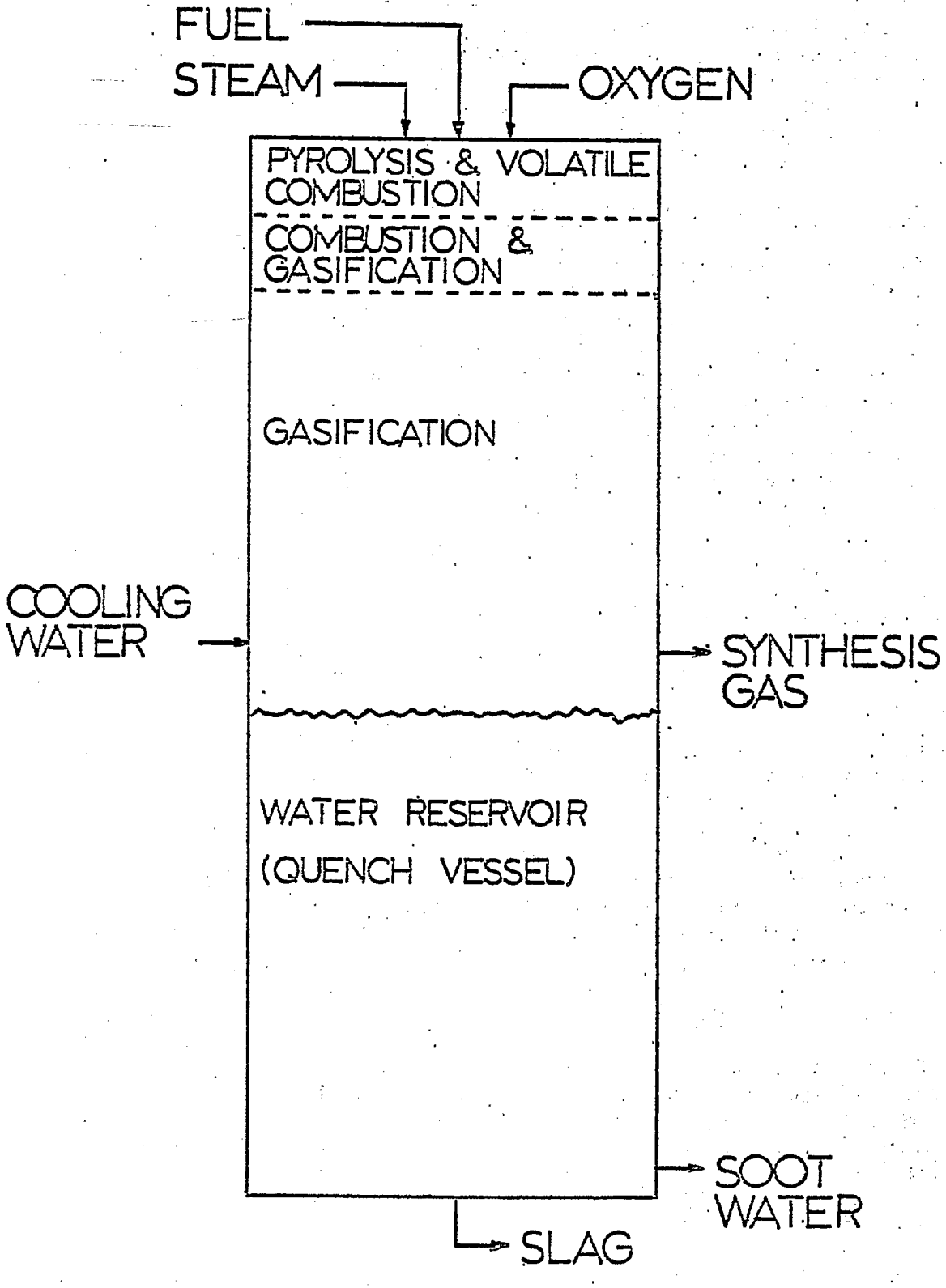

FIGURE 1. TEXACO DOWNFLOW ENTRAINED BED PILOT PLANT GASIFIER

TABLE I

Average Analysis of H-Coal Liquefaction Residues as Received [1]

Ultimate Analysis Wt. Pct.	Illinois No. 6	Wyodak
C	69.73	78.06
H	5.21	5.32
N	0.81	0.93
S	1.38	0.05
Ash	19.96	10.86
Cl	0.21	0.03
O (by diff.)	2.70	4.75
Typical Viscosity		
CP @ 177°C (350°F)	1,700	-----
CP @ 204°C (400°F)	440	5,900
CP @ 232°C (450°F)	150	2,000
Specific Gravity		
@ 232°C (450°F)	1.18	1.01
Gross Heating Value		
Cal/gm	7,333	7,722
BTU/lb	13,200	13,900

II. Reactions in an Entrained-Bed Gasifier

In an entrained-bed gasifier, oxygen (or air), steam and hydrocarbons are introduced simultaneously either from the top or from the bottom of the reactor and travel in the same direction. Extremely high temperature is to be expected in the gas phase near the fuel due to the inlet combination of a high oxygen concentration and the subsequent combustion of volatiles produced by rapid pyrolysis which is enhanced by such a high temperature environment. This phenomena is very similar to that which occurs near the inlet of a coal combustor or a utility boiler. The heat produced by combustion will thereafter support the endothermic gasification reactions.

Fuel traveling along the reactor is successively devolatilized, burned and gasified. The gasifier can be conceptually divided into three zones:

1. Pyrolysis and Volatile Combustion Zone
2. Combustion and Gasification Zone
3. Gasification Zone

2.1 Pyrolysis and Volatile Combustion Zone

Both coal and coal liquefaction residues that have been used in an entrained bed system are polymeric compounds consisting of C, H, O, N, S and ash. The input fuel, when heated to high temperatures, decomposes and produces volatiles which consist of a mixture of combustible gases, carbon dioxide, water vapor and tar. The pyrolysis reaction can be represented as follows:

$$\underset{\text{(Raw Fuel)}}{C_{\alpha_i}H_{\beta_i}O_{\gamma_i}N_{\delta_i}S_{\varepsilon_i}A} \longrightarrow \underset{\text{(Char)}}{C_{\alpha}H_{\beta}O_{\gamma}N_{\delta}S_{\varepsilon}A} + \text{Volatiles } (CO + H_2 + CO_2 + CH_4 + H_2S + N_2 + \text{Tar}) \quad (1)$$

Since oxygen is rich in the pyrolysis zone, the burning of combustible volatiles (CO, H_2, CH_4, tar and hydrocarbons etc.) can be assumed complete. A large amount of heat is thus produced in the gas phase which heats the solid fuel rapidly to the pyrolysis temperature.

2.2 Combustion and Gasification Zone

In the Combustion and Gasification Zone, the devolatilized char reacts with the remaining oxygen to produce CO/CO_2, and with steam and CO_2 to produce CO and H_2. The combustible gases, CO and H_2, in turn react in the gas phase with oxygen to produce more heat. The following reactions are considered in this second zone.

(i) Char-Oxygen Reaction:

$$C_\alpha H_\beta O_\gamma N_\delta S_\varepsilon A + \left(\frac{\alpha}{\phi} - \frac{\gamma}{2} + \frac{\beta}{2} - \varepsilon\right)O_2 \longrightarrow$$

$$2\left(1 - \frac{1}{\phi}\right)\alpha\, CO + \left(\frac{2}{\phi} - 1\right)\alpha\, CO_2 + \left(\frac{\beta}{2} - \varepsilon\right)H_2O + \varepsilon H_2S + \frac{\delta}{2}N_2 + \text{Ash} \quad (2)$$

(ii) Char-Steam Reaction:

$$C_\alpha H_\beta O_\gamma N_\delta S_\varepsilon A + (\alpha - \gamma)H_2O \longrightarrow$$

$$\alpha\, CO + (\alpha-\gamma + \frac{\beta}{2} - \varepsilon)H_2 + \varepsilon H_2S + \frac{\delta}{2}N_2 + Ash \qquad (3)$$

(iii) Char-CO_2 Reaction:

$$C_\alpha H_\beta O_\gamma N_\delta S_\varepsilon A + \alpha CO_2 \longrightarrow$$

$$2\,\alpha\, CO + \frac{\gamma}{2} H_2O + (\frac{\beta}{2} - \varepsilon-\gamma\ )H_2 + \varepsilon H_2S + \frac{\delta}{2}N_2 + Ash \qquad (4)$$

(iv) $H_2 + \frac{1}{2}O_2 \rightarrow H_2O$ (5)

(v) $CO_2 + \frac{1}{2}O_2 \rightarrow CO_2$ (6)

2.3 Gasification Zone

The combustion gas flows into the Gasification Zone where further heterogeneous reactions occur along with the water-gas-shift reaction. Methane is produced by hydrogasification of char but is reduced by the methane-steam reforming reaction. Therefore, in the Gasification Zone, three more reactions occur in addition to the char-steam reaction and char-CO_2 reaction (Eq. 3 and Eq. 4):

(vi) Char-H_2 Reaction

$$C_\alpha H_\beta O_\gamma N_\delta S_\varepsilon A + (2\alpha + \gamma + \varepsilon - \frac{\beta}{2})H_2 \longrightarrow$$

$$\alpha\, CH_4 + \gamma\, H_2O + \varepsilon H_2S + \frac{\delta}{2}N_2 + Ash \qquad (7)$$

(vii) $CO + H_2O \rightleftharpoons CO + H_2$ (8)

(viii) $CH_4 + H_2O \rightleftharpoons CO + 3\,H_2$ (9)

The final products leaving the gasifier are mainly CO, H_2 and CO_2. Since volatiles are burned in the oxygen-rich zones, no tar appears in the product. H_2S and N_2, which originate from the sulfur and nitrogen respectively in the raw fuel, together with CH_4, constitute the minor species of the gas product.

III. Coal Gasification Reaction Kinetics

Major solid-gas reactions involved in coal gasification are pyrolysis, char-steam, char-carbon dioxide, char-oxygen and char-hydrogen reactions. Pyrolysis reaction which releases the moisture and volatile matter in the raw fuel, is usually the first to occur and the fastest among these reactions. In addition to major chemical changes, there is a substantial change in the physical characteristics of the fuel particle during the rapid stage of pyrolysis. The yields of volatiles and their composition depend not only upon the volatile matter content of the raw fuel but also on the temperature, pressure and rate of heating during pyrolysis. For temperatures below 1000°C, char-steam, char-carbon dioxide and char-hydrogen reactions are usually slow and take place according to the volumetric reactions. However, at temperatures above 1200°C, the rates of these reactions, perhaps except for that of the char-hydrogen reaction, are controlled by gas film diffusion and ash layer diffusion. In an entrained bed reactor, the operating temperatures are usually much higher than 1000°C, and therefore diffusion through the gas-film and ash layer is the controlling factor in the gasification. Since the particle loading in an entrained bed gasifier is small (less than 1% of reactor volume), particle collisions are unlikely to be frequent and the ash layer formed can be assumed to remain on the fuel particle during the reaction. It is thus reasonable to assume that the reaction rates may be estimated by the Unreacted-Core Shrinking Model [19] for an entrained-bed gasifier. The kinetics of each individual reaction are discussed in the following sections.

3.1 Pyrolysis

Coal, when heated to high temperatures, decomposes producing volatiles which consist of a mixture of combustible gases, carbon dioxide, water vapor and tar. The degree of coal devolatilization depends not only on the type of coal, but also on the operating conditions such as heating rate, temperature and pressure. Rates of coal pyrolysis in an inert atmosphere have been investigated by many researchers. Equations of Badzioch and Hawksley [3], Anthony and Howard [4] and Wen et al. [5] are based essentially on the concept that the rate of pyrolysis is proportional to the amount of volatile content remaining in the coal:

$$\frac{dV}{dt} = k(V^* - V) \qquad (10)$$

where

$$k = k_o \exp(-E/RT)$$

For Badzioch and Hawksley[3] and for Wen et al. [5], the activation

energy, E, is a constant. Following the idea of Pitt [6], Anthony and Howard [4] introduced Gaussian distribution of activation energy, E, with a mean value of E_o and a standard deviation of σ. Suuberg et al. [9] applied this model to simulate their experimental results of product distribution and kinetics of lignite pyrolysis. Since this model required a number of parameters which depend on coal type the model is difficult to adapt to modeling of coal gasification reactions. Russel et al. [21] recently proposed an elaborate model describing the combined effect of chemical reaction and mass transfer occurring in a single coal particle during hydropyrolysis or pyrolysis. The activation energy reported by Badzioch and Hawksley [3] for ten types of coal is 17.8 Kcal/mole while Anthony and Howard [4] reported a wide range from 2 to over 50 Kcal/mole which depends on coal type and operating conditions. Differences in equipment and experimental procedures are also reasons for such a discrepancy of the data reported. In this study, the activation energy, E, and the pre-exponential factor, k_o, are selected according to Badzioch and Hawksley [3]. Eq. (10) is re-written as:

$$\frac{dV}{dt} = 1.14 \times 10^5 \exp(-8900/T_s) \cdot (V^* - V) \qquad (11)$$

Badzioch and Hawksley's equation [Eq. (11)] predicts a higher pyrolysis rate than most other existing data which has been summarized by Anthony Howard [4]. However, in an entrained bed gasifier, all the volatiles produced in the pyrolysis stage will burn completely in the oxygen-rich zone. The accuracy of the pyrolysis rate expression will not have an important effect on the model's results. Thus, Eq. (11) is used to calculate the rate of pyrolysis in this study. Experimental studies [7] show that volatile yields increases significantly with corresponding decreases in operating pressure, increases in hydrogen partial pressure, and increases in the final temperature of the particle. The volatile yield also increases slightly with increasing rate of heating. Anthony et al. [4] were able to explain the pressure effect on the volatile yield by a mathematical model which considers the competition between diffusional escape and the secondary reactions of reactive volatile species during the pyrolysis process. Their expression is shown as follows:

$$V^* = V_{nr}^* + V_r^{**}/(1 + 0.56\, P_t) \qquad (12)$$

where V_{nr}^* is the potential ultimate yield of volatiles at very high pressure (greater than 100 atm), and V_r^{**} is the portion of volatile yield that exceeds V_{nr}^* at very low pressure (less than 0.001 atm.). However, V_{nr}^* and V_r^{**} are different for different types of coal and there is currently insufficient experimental data on these quantities available; at this time, most experimental data are available for only 1 atm. conditions. This expression can not be applied directly in a gasification model. In this study, linear interpolation of their data is made to account for the pressure effect;

$$V^* = V^*_{\text{(at 1 atm.)}} \cdot (1 - a \ln P_t) \qquad (13)$$

where a is calculated to be approximately 0.066 for bituminous coals. This expression can be used to estimate the total yield of volatiles, if the total pressure in the gasifier is between 0.1 atm. and 50 atms. However, the estimation of volatile product composition is difficult, since it depends more significantly on fuel type, operating conditions and solid residence time. Experiments have been done by Loison and Chauvin [8] and Suuberg et al. [9] to measure the product composition of pyrolysis for several types of coal. Suuberg et al. [9] correlated their experimental results by using a model with the distribution of activation energies. The data of Loison and Chauvin can be summarized and shown graphically in Figure 2. [8]. The yield of hydrogen is seen to be independent of coal rank, whereas those of all other volatile constituents increase with increasing proximate volatile matter contents. Based on information on the amount of hydrogen, the ratio of CO/CO_2 and H_2O/CO_2 obtained from Fig. 2, together with the material balance on elements, C, H, O, N, S, one can roughly estimate the product distribution for a pyrolysis process.

3.2 Volatile Combustion

Volatiles produced on pyrolysis burn with oxygen either immediately as the volatiles leave the particles or after the volatile jets break through a distance from the particle. Two hypotheses for the combustion during pyrolysis have been proposed regarding whether or not the burning occurs in the coal particles. Howard and Essenhigh [22] assumed that the burning of volatiles occurs both in the interior of the solid as well as within the laminar layer of gas surrounding the particles. Field et al. [10], on the other hand, assumed that because volatiles mix with oxygen at the particle surface and the burning rate is extremely fast, the overall rate is likely to be controlled by the boundary layer diffusion. Dobner et al. [15] argued that combustion of volatiles proceeds in the laminar layer outside of the particle and that oxygen cannot reach the interior of the particle until the combustion of volatiles outside of the particle is completed.

An alternative model is based on a common assumption that volatiles react rapidly with oxygen to form CO and H_2O with the subsequent CO oxidation as the rate determining step. According to Hottel et al. [23], the following equation can be used to calculate CO oxidation rate:

$$\frac{dC_{CO}}{dt} = A \cdot C_{CO} \cdot C_{O_2}^{0.3} \cdot C_{H_2O}^{0.5} \cdot \exp(-16{,}000/R_gT) \qquad (14)$$

where the concentration terms are expressed in g mole/cm^3 and the value of A ranges from 3×10^{10} to 18×10^{10}. At combustion temperature of about 1500°C, CO combustion rate is about 10^5 times greater than the subsequent burning rate of char and oxygen.

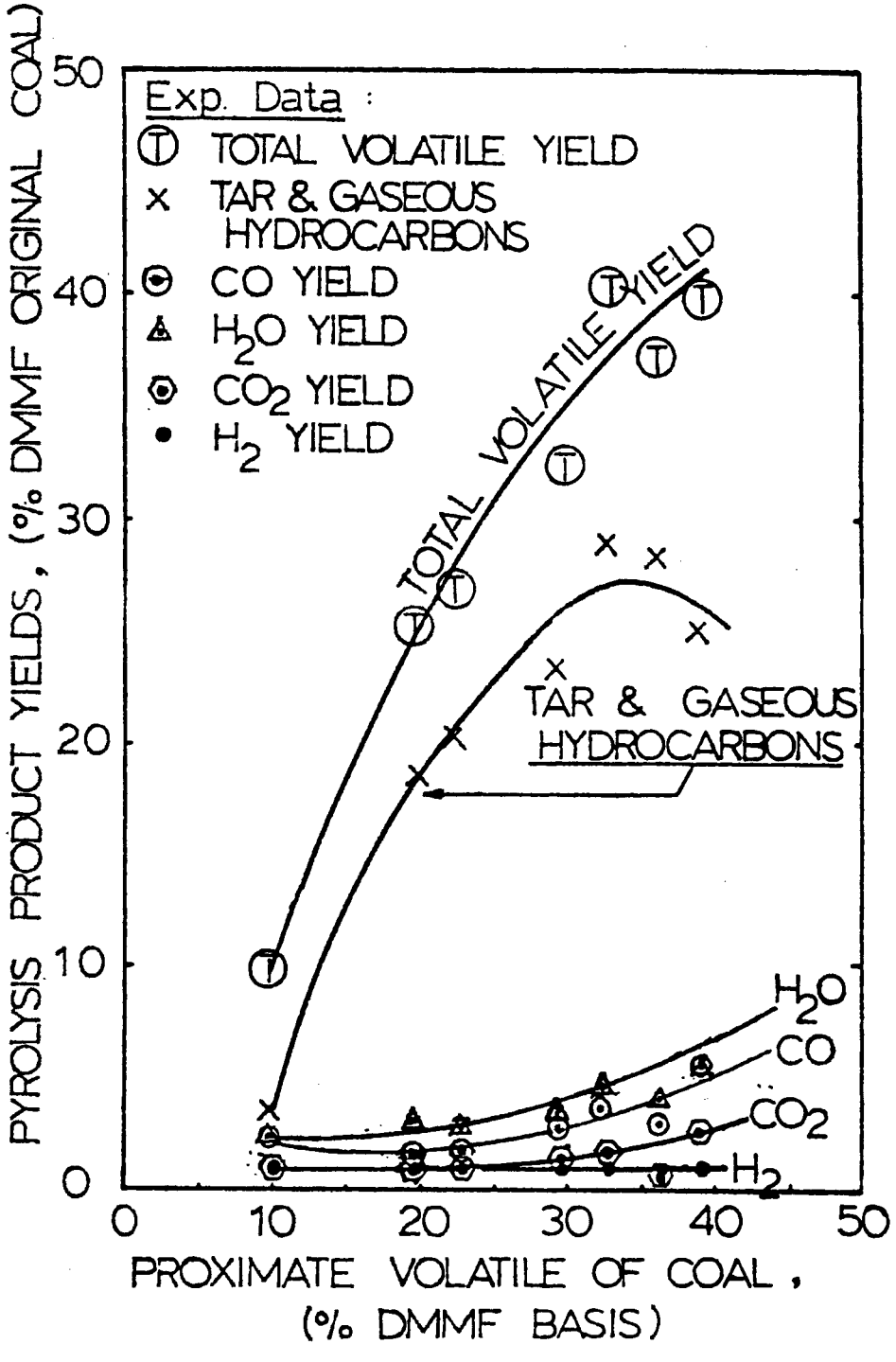

FIGURE 2. PRODUCT YIELDS OF COAL PYROLYSIS, SUMMARIZED FROM DATA OF LOISON AND CHAUVIN [8], AT ~10^3°C/SEC TO ~1050 °C.

In an entrained bed gasifier the burning of carbon monoxide can be assumed to be almost instantaneous. This is due to the following two facts: (1) the reaction temperature in the combustion zone is very high (> 1500°C); (2) both oxygen concentration and steam concentration are high in the combustion zone especially when operating at high pressures. In the model development, Eq. (5) and Eq. (6) are thus assumed complete as long as oxygen exists. Comparison has been made against the above assumption by using Eq. (14) to calculate CO combustion rate in the model. However, no significant difference in results has been found.

3.3 Char-Gas Reactions

The char formed as the result of the first stage reaction, namely pyrolysis and volatile combustions, is very different from its parent coal in size, shape and pore structure. The char-gas reactions are heterogeneous reactions and can be classified into two distinct modes of reactions, i.e., volumetric reaction and surface reaction. In the volumetric reaction, the gas diffuses into the interior of the particles and the reaction takes place throughout the interior of the particle. The intrinsic reaction rate for volumetric reaction is usually much slower than the diffusion rate and is usually the rate controlling step of the process. In the case of surface reaction, the reacting gas does not penetrate into the interior of the solid particles but is confined at the surface of the "shrinking core of unreacted solid" [11]. Generally, the surface reaction occurs when the chemical reaction is very fast, and diffusion is the rate controlling step.

In an entrained bed gasifier, most char-gas reactions can be considered as the surface reaction because of high operating temperatures (above 1000°C). Since the solid loading in an entrained bed gasifier is very small, the particle collisions are unlikely to be frequent and therefore the ash layer formed can be assumed to remain on the fuel particle during the reaction. The Unreacted-Core Shrinking Model [11] is applied in this study to estimate the heterogeneous solid-gas reaction rates. In this model the effect of both ash layer diffusion and gas film diffusion is considered in addition to chemical reaction effect. The overall rate, according to this model, can be expressed as follows:

$$\text{Rate} = \frac{1}{\frac{1}{K_{dg}} + \frac{1}{K_{dash}}\left(\frac{Y-1}{Y}\right) + \frac{1}{Y^2 k_s}} \cdot (P_i - P_i^*) \qquad (15)$$

where

$$Y = \frac{r_c}{R}$$

r_c is the radius of the unreacted-core

R is the radius of the whole particle including the ash layer

$(P_i - P_i^*)$ is the effective partial pressure of the gas taking into account the reverse reaction effect

k_{dg} is the gas film diffusion constant

k_s is the surface reaction constant

and k_{dash} is the ash diffusion constant.

The ash diffusion rate constant, k_{dash}, depends both on the gas diffusity and the voidage of the ash layer. Here, k_{dash} is roughly estimated by the following correlation [11]:

$$k_{dash} \cong k_{dg} \cdot \varepsilon^{2\sim3} \qquad (16)$$

where ε is the voidage of the ash layer.

Detailed descriptions of the kinetics for each individual solid-gas reaction are given in the following sections. A summary of the rate expressions used in the model development is given in Appendix 2.

3.4 Char-Oxygen Reaction

The mechanism of char-oxygen reaction is better understood than either pyrolysis or volatile combustion. Thring and Essenhigh [24] showed that the burning rate of the char-oxygen reaction is zero order with respect to oxygen concentration below 1200°K and is first order between 1200°K and 2200°K. The rate determining step in the combustion of char varies depending on the range of temperature, particle size and specific surface area of the char. Field [25] reported the burning rate of pulverized coal of various sizes and showed that for small particles (below 50 microns) the combustion is chemical reaction controlled while for large particles (above 100 microns) combustion is diffusion controlled. Mulcahy and Smith [26] reported that the burning rate at temperatures higher than 1200°K and for particles larger than 100 microns is determined by diffusion rate of oxygen to the surface.

Both carbon monoxide and carbon dioxide are formed as primary products of the surface reaction as shown in the following equation:

$$C^* + \frac{1}{\phi} O_2 \longrightarrow 2\left(1 - \frac{1}{\phi}\right) CO + \left(\frac{2}{\phi} - 1\right) CO_2 \qquad (17)$$

where C^* represents the carbon in the char and ϕ is the mechanism factor of the combustion reaction (moles of carbon consumed per mole of oxygen). ϕ takes a value of 2 when CO is the direct product of char-O_2 reaction and a value of 1 when CO_2 is the direct product. Arthur [27] presented an empirical correlation for CO to CO_2 ratio as follows:

$$\frac{CO}{CO_2} = 10^{3.4} \cdot \exp(-12400/RT), \text{ T in } ^\circ K \qquad (18)$$

It is apparent that CO is the dominant product at high temperature.

The burning mechanism of char and the product gas concentration distributions around the burning char are very complex, and many researchers have proposed different models [20]. When the combustion is controlled by diffusion alone, Borghi et al. [28] suggested that for large particles it is possible for the rate of the reaction $2\ CO + O_2 \rightarrow 2\ CO_2$ to be fast enough to consume all the oxygen before it reaches the carbon surface. The CO then is supplied by the reaction $CO_2 + C \rightarrow 2\ CO$. If the reaction is kinetically controlled, the atmosphere surrounding the particle will be approximately uniform, and CO_2 and O_2 will have equal opportunity to reach the surface. The $C + CO_2$ reaction then is too slow to compete with the oxidation by O_2.

Wicke and Wurzbache [29] measured the concentration profiles of CO, CO_2 and O_2 in the thin film surrounding a burning carbon rod and found evidence of the existence of a maximum in the concentration of CO_2. DeGraaf [30] and Kish [31] found a temperature maxima of gas surrounding the particle which is several hundred degrees above the solid surface temperature.

On the other hand, Avedesian and Davidson [32] suggested that O_2 and CO burn rapidly in a very thin reaction zone surrounding the particle. Carbon monoxide produced at the surface diffuses out toward the reaction zone while O_2 from the main stream diffuses in and burns in a diffusion flame to produce CO_2 as shown in Fig. 3. According to their model, no CO appears in the main stream when there is an abundant supply of O_2.

Essenhigh [33] presented a physical model as shown in Fig. 3. Gases diffuse through the boundary layer and penetrate into the porous solid. $C\text{-}CO_2$ and $C\text{-}CO_2$ reactions occur heterogeneously at all available surfaces, exterior and interior. In his model the CO/CO_2 ratio rises with temperature, and CO becomes the principal product at about 1000°C and above (Arthur [27]). The CO also reacts in the gas phase with oxygen to produce CO_2, partly in the particle pores and partly in the boundary layer of the char. As the oxygen concentration in the main stream is enriched, there is more CO burn-up inside the solid.

Caram and Amundson [34] suggested that large particles (> 2 mm) burn according to the double film theory [35] shown in Fig. 3, whereas small particles (< 100 microns) burn according to the single film model. In analyzing the homogeneous combustion of CO and the heterogeneous reaction of carbon with oxygen and with carbon dioxide according to double film models, they concluded that large particles (5 mm) tend to reach an upper steady state in which the particle is surrounded by a CO flame. For very small particles (< 50 microns) such a flame does

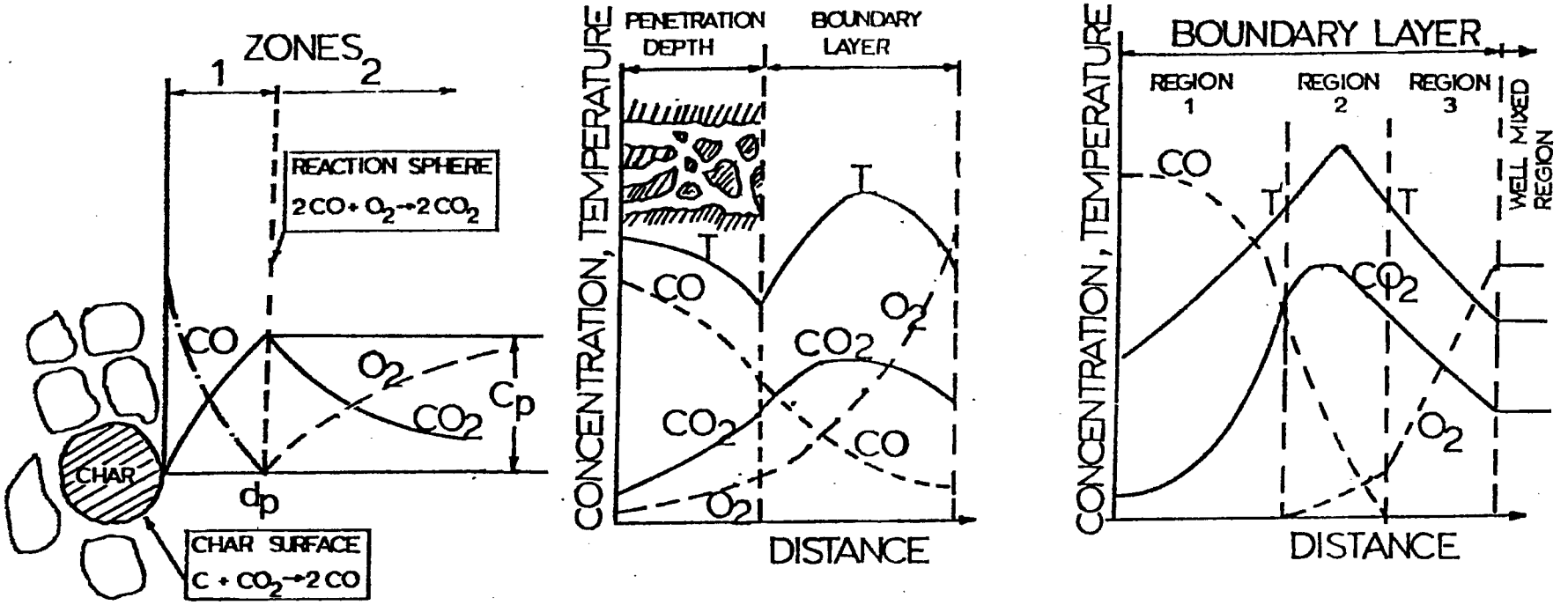

d_p : diameter of char or coke particle

C_p : oxygen concentration

T : temperature

MODEL 1
(Avedesian & Davidson [32])

MODEL 2
(Essenhigh [33])

MODEL 3
(Caram & Amundson [34])

FIGURE 3. TYPICAL PHYSICAL MODELS OF COAL-CHAR COMBUSTION [20]

not develop. Thus, it is evident that the char-oxygen reaction occurs in the interior surface of smaller particles at low temperatures because oxygen does not get consumed near the external surface while enough is supplied to the interior by the pore diffusion from the bulk phase.

The mechanism factor, ϕ, is thus a function of coal type, particle size and temperature. For large particle sizes, according to the double film model [34], CO_2 might be the only product gas in the char-oxygen reaction. Arthur's correlation [27] is applicable only for small particle sizes. Wen and Dutta [19] proposed a correlation for a rough estimation of the mechanism factor, ϕ, by a linear interporation between small particle sizes and large particle sizes. This correlation is shown below:

$$\phi = (2z + 2)/ (z + 2) \quad \text{for } d_p \leq 0.005 \text{ cm}$$

$$\phi = [(2z + 2) - z\,(d_p - 0.005)/0.095] /(z + 2) \text{ for}$$

$$0.005 \text{ cm} < d_p \leq 0.1 \text{ cm} \qquad (19)$$

and

$$\phi = 1.0 \text{ for } d_p > 0.1 \text{ cm}$$

where $z = 2500 \exp(-6249/T_m)$

and $T_m = (T_s + T_g) / 2$ in ^oK

The above equations become Arthur's correlation, [Eq. (18)], when the particle size is smaller than 50 microns.

The chemical reaction rate constant and the gas film diffusion constant given by Field et al. [10] is shown respectively as follows:

$$k_s = 8710 \exp(-17967/T_s) \quad \text{gm/cm}^2 \cdot \text{sec} \cdot \text{atm.} \qquad (20)$$

$$k_{dg} = \frac{0.292\ D}{d_p\ T_m} \qquad (21)$$

where D = diffusivity of oxygen in the gas film

$$= 4.26 \left(\frac{T_g}{1800}\right)^{1.75} \left(\frac{1}{p_t}\right) \qquad (22)$$

In spite of a great number of studies available on coal combustion rate, the understanding of the phenomenon is far from complete. In fact, the combustion rate data available up to now are very confusing even for relatively small particles. As shown in Fig. 4 [25, 26, 36, 37, 38], the rates of combustion seem to be affected by the types of coal but the quantitative effect of the temperature and

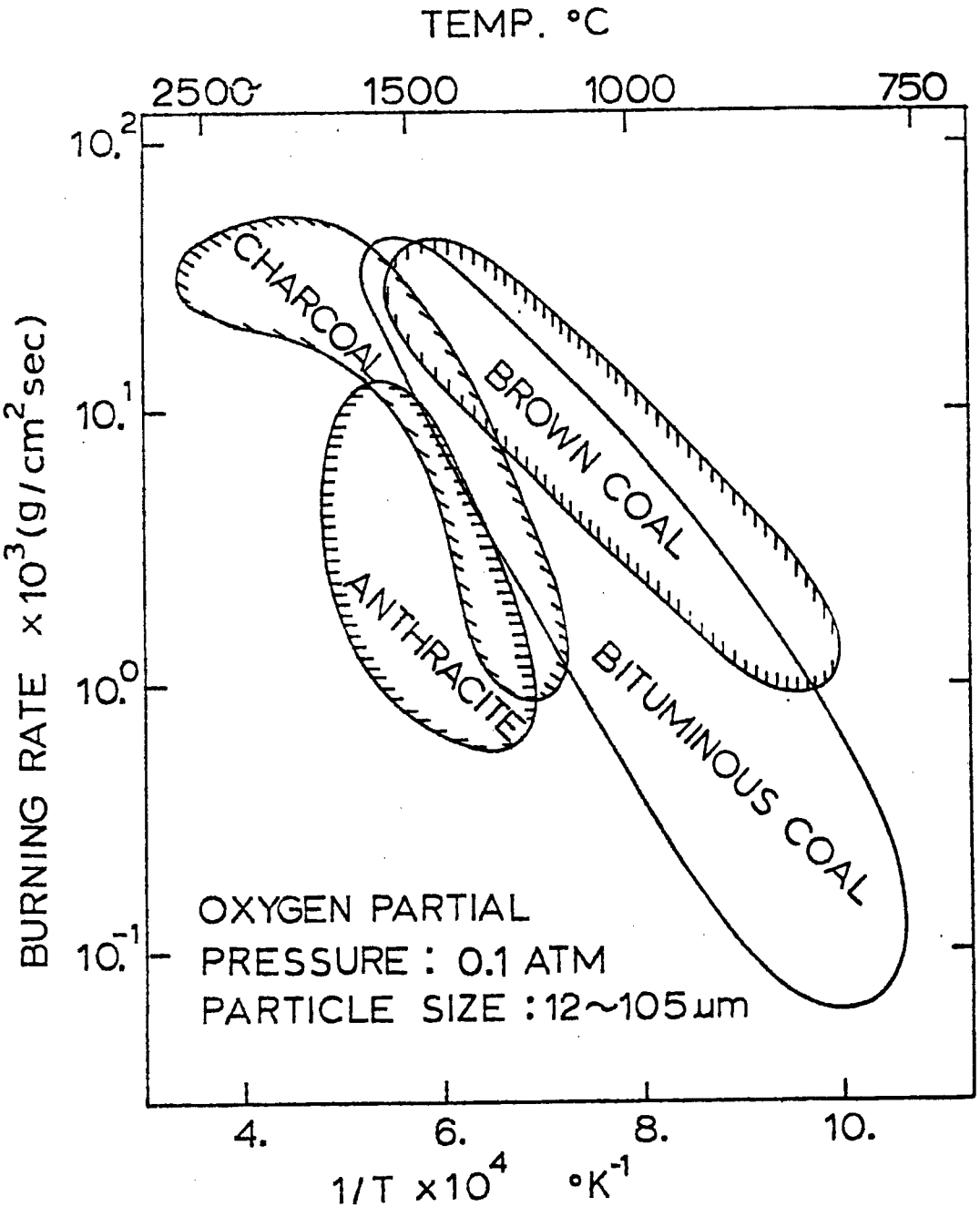

FIGURUE 4. COMBUSTION RATES FOR VARIOUS COALS NEAR CHEMICAL CONTROLLING REGIME [25, 26, 36, 37, 38, 20]

particle size as well as the rate determining factors are not yet clearly understood. This is primarily due to the difficulty in experimental evaluation of the particle temperature and the measurement of changes in physical properties of coal during the course of combustion.

By applying Eq. (16) - Eq. (19) in the Unreacted-Core Shrinking Model, the rate of char-oxygen reaction is shown graphically for d_p = 350 microns and p_t = 24 atms. in Fig. 10 in Appendix 2.

3.5 Char-Steam Reaction

Char-steam reaction is one of the most important reactions in industrial practice for generation of CO and H_2. Most of the earlier investigators, [39, 40] used Langmuir-type adsorption equations to express the rate of this reaction. This reaction is apparently controlled by chemical reaction between 1000°C and 1200°C for particles smaller than 500 microns and is affected by diffusion through the pore in the char above 1200°C [41, 42, 43].

While most literature treated the carbon-steam reaction as a volumetric reaction, Riede and Hanesian [44] found that the graphite-steam reaction is surface reaction controlling between 500°C and 900°C and the gas film diffusion becomes gradually important above 700°C. The data obtained by Gray and Kimber [45] of BCURA represents the only set of kinetic measurements made on the gasification of pulverized char at flame temperature. They estimated the surface reaction constant at 2300°K and 2800°K, from which the activation energy is calculated to be 42 Kcal/g mole. Based on the data of Gray and Kimber [45], Dobner [15] proposed a rate expression for both carbon-steam and carbon-carbon dioxide reaction in the temperature range of an entrained bed gasifier as shown below:

$$k_s = 247 \cdot \exp(-21060/T_s),\ g/cm^2 \cdot sec \cdot atm. \qquad (23)$$

Fig. 11 in Appendix 2 shows the calculated overall rate constants based on the above k_s and the Unreacted-Core Shrinking Model.

In the low temperature range, the apparent activation energy has been reported to vary from 35-45 Kcal/mole [16] to 60-80 Kcal/mole [42, 46, 47]. Fig. 5 shows the volumetric reaction constant, k_v, for various types of coal and char. Depending on the type of coal, the volumetric reaction rate constant, k_v, can vary almost three orders of magnitude at temperatures below 1200°C. Since adequate data are not available to estimate the reaction rate constants for the char-steam reaction and the char-CO_2 reaction at temperatures higher than 1200°C it is difficult to postulate the accuracy any proposed rate expression used in modeling an entrained bed gasifier.

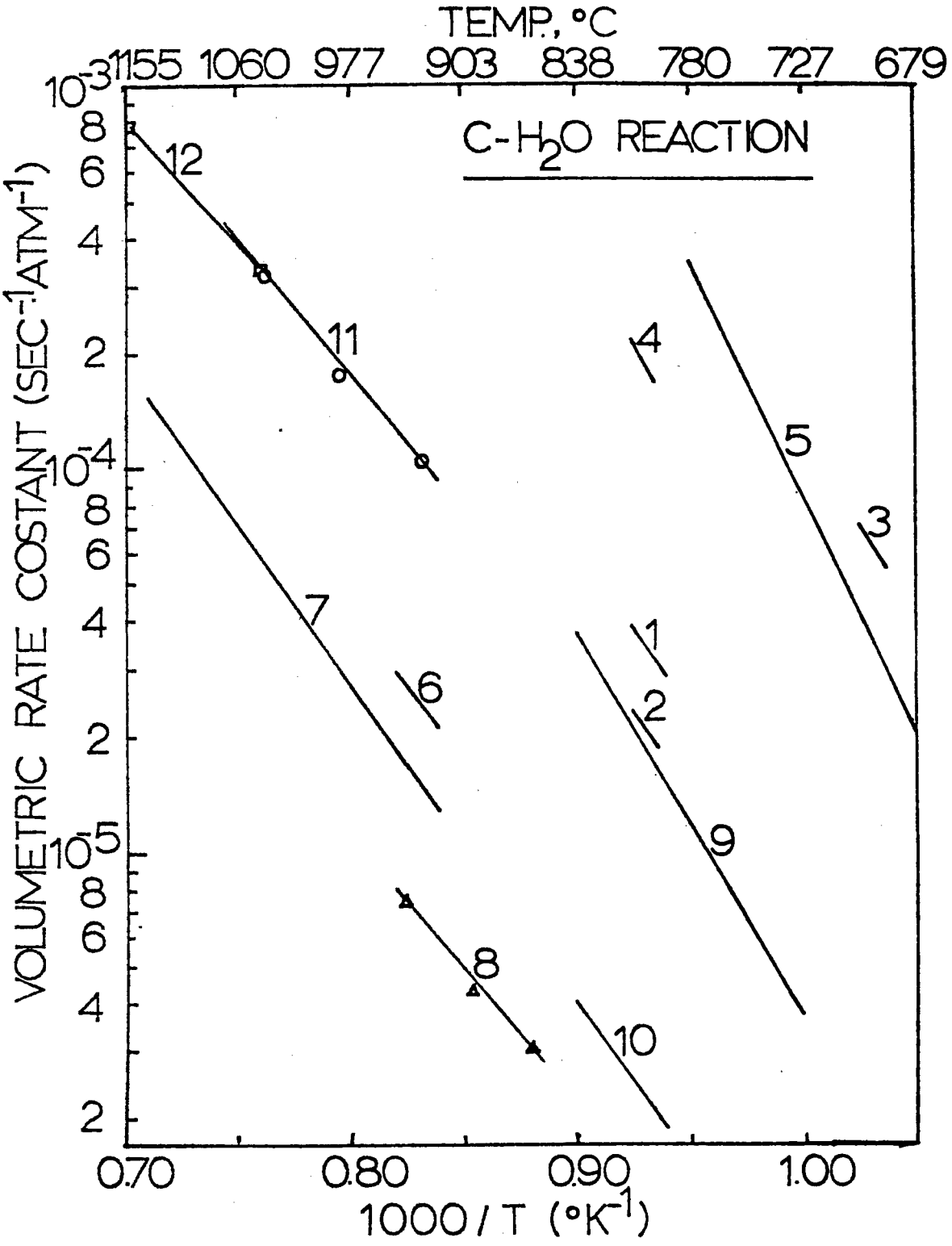

FIGURE 5. ARRHENIUS PLOT FOR THE REACTION OF STEAM WITH VARIOUS FORMS OF CARBON (SEE THE LEGEND IN TABLE II) [19]

TABLE II LEGEND TO FIGURE 5

Line	Investigators (Year)	Material	Total Pressure (Atms.)
1, 2	Jolly & Pohl (1953) [63]	Coke	1.0
3, 4	Gadsby et al. (1946) [40]	Nut char coal char	1.0
5	Long & Sykes (1948) [64]	Coconut shell charcoal	0.2 1.0
6	Feldkirchner & Linden (1963) [65]	Low temperature bituminous coal coal	104
7	Feldkirchner & Huebler (1965) [66]	Low temperature bituminous coal char	70
8	Johnstone et al. (1952) [67]	Cylindrical porous graphite rod	1.0
9, 10	Blackwood & McGrory (1958) [68]	Coconut carbon	1. 50.
11	Johnson (1974) [56]	Air-pretreated HVab Pittsburgh No. 8	35.0
12	Jensen (1975) [41]	Coal minerals from Kentucky No. 9	1.0

3.6 Char-Carbon Dioxide Reaction

The rate of char-CO_2 reaction is relatively slow and is comparable with that of char-steam reaction. Dutta et al. [48] measured the rate of char-CO_2 reaction and concluded that for particles smaller than 300 microns and when the temperature is lower than 1000°C, the reaction is controlled by the rate of chemical reaction and takes place nearly uniformly throughout the interior of the char particle. Yang and Steinberg [49] measured the rates of reaction between nuclear graphite and carbon dioxide at temperatures between 1200°C and 1600°C and concluded that the rates are controlled by both surface reaction and diffusion in this temperature range. Gray and Kimber [45] estimated the surface reaction rate constant at 2300°K and 2800°K for both char-steam and char-carbon dioxide reactions. Dobner [15] proposed the same rate expression for both char-steam and char-carbon dioxide reactions based on Gray and Kimber's data as shown in Eq. 24.

$$k_s = 247 \exp(-21060/T_s),\ g/cm^2 \cdot sec \cdot atm. \qquad (24)$$

Based on the Unreacted-Core Shrinking Model, the rate of char-CO_2 reaction is plotted for d_p = 350 microns and p_t = 24 atm. as shown in Fig. 12 in Appendix 2. In the low temperature range the reported volumetric reaction rate constant for char-carbon dioxide reaction also scatters widely as shown in Fig. 6 [19].

3.7 Char-Hydrogen Reaction

The reaction of char and hydrogen is quite exothermic and produces mainly methane. This reaction is very slow when hydrogen partial pressure is low and temperature is low. But at high hydrogen partial pressure and at temperatures above 700°C, the rate of this reaction becomes appreciable. The mechanism of this reaction is rather complicated and had been studied by a number of investigators [50, 51, 52, 53]. The initial phase of reaction between hydrogen and coal, or hydropyrolysis, is very rapid and has been discussed in detail by Russel et al. [21]. Depending on the operating condition, it is possible to convert more than 40% of coal during the first stage of hydropyrolysis. The reaction of hydrogen with the remaining char is much slower and takes place mostly on the solid surface. Wen and Huebler [54] proposed the following empirical equation for the rate of second stage hydrogasification (char-hydrogen reaction).

$$\frac{dx}{dt} = k_v (1-x) \left(P_{H_2} - \sqrt{P_{H_2} / K_{eq}}\right) \qquad (25)$$

where $x = \dfrac{X - f}{1 - f}$ and is the carbon conversion in the second stage, X is the carbon conversion and f is the fraction of carbon that can be converted in the first (pyrolysis) stage.

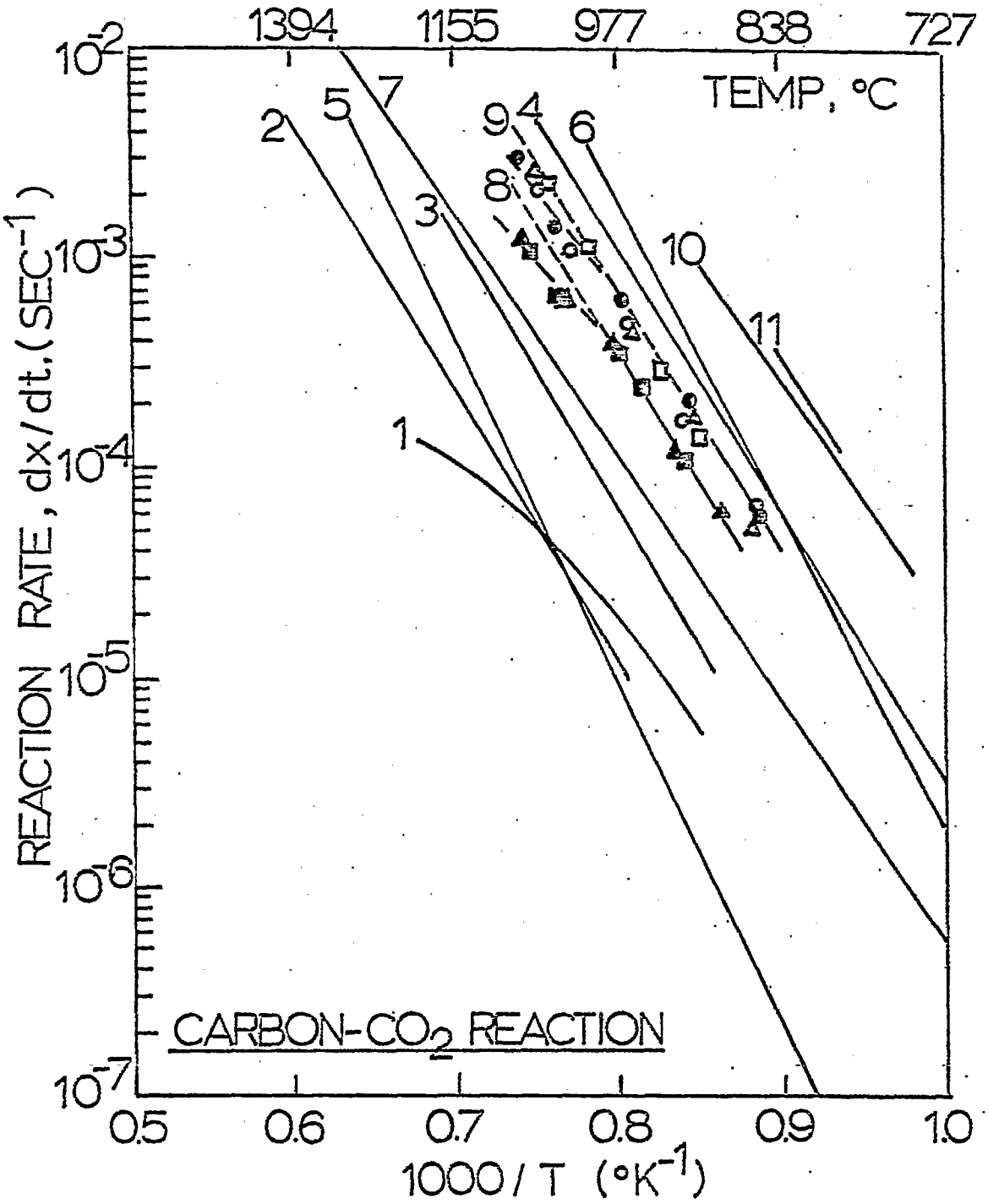

FIGURE 6. ARRHENIUS PLOTS FOR THE REACTION BETWEEN CO AND VARIOUS FORMS OF CARBON (SEE THE LEGEND IN TABLE III) [19]

TABLE III LEGEND TO FIGURE 6

Line No.	Investigators	Year	Type, Size and Shape of Carbon	Remarks
1	Yoshida and Kunii[69]	(1969)	Graphite Sphere, 1.5 cm. Dia.	Initial Rates
2	Ergun[70]	(1956)	Ceylon Graphite, -10+200 mesh	Initial Rate in a fluidized bed.
3	-do-		Activated Graphite, -10+200 mesh	-do-
4	-do-		Activated Carbon, -10+200 mesh	-do-
5	Turkdogan and Vinters[71]	(1969)	Electrode Graphite Particles, -10+40 mesh	Initial Rates
6	-do-		Coconut charcoal particles, -10+40 mesh	Initial Rates
7	Austin and Walker [72]	(1963)	Graphitized Carbon cylinder, 5.1 cm. long and 1.27 cm. dia.	Calculated initial Rates
8 & 9	Dutta et al.[48]	(1977)	o - Illinois Coal #6 ● - Synthane Char #122 ▵ - Hydrane Char #49 ▫ - IGT Char #HT155 ▲ - Hydrane Char #150 × - Pittsburgh HVab Coal all of size -35+60 mesh	Rates at 20% conversion level
10	Fuchs and Yovorsky [73]	(1975)	Hydrane Char from Pittsburgh Coal, -60+100 mesh	Average Rate in a fluidized bed at 16-32 atm. partial pressure of CO_2 with He as diluent
11	-do-		Synthane Char from Illinois Coal #6, -60+100 mesh	Average Rate in a fluidized bed at 32 atm. partial pressure of CO_2 with He as diluent

Fig. 7 [19] shows the reported volumetric reaction rate constant based on this expression. The apparent activation energy of this reaction is found to lie between 30 and 41 Kcal/mole. [53, 55, 56]

In order to simplify the calculation procedure, an approximate conversion from k_V to k_S is made so that the overall rate can be calculated by the Unreacted-Core Shrinking Model. Since the char-hydrogen reaction is mostly in the chemical reaction regime ($k_S < k_{dg}, k_{dash}$), based on the Unreacted-Core Shrinking Model, the rate can be expressed as follows:

$$\text{Rate} = k_{over} \cdot \left(\frac{6}{\rho_s \cdot d_p}\right) \cdot \text{Peff} \qquad (26)$$

where

$$k_{over} = \frac{1}{\frac{1}{k_{dg}} + \frac{1}{k_s Y^2} + \frac{1}{k_{dash}}\left(1 - \frac{1}{Y}\right)} \qquad (27)$$

$$\cong k_s Y^2$$

$$= k_s \left(\frac{r_c}{R}\right)^2 = k_s (1 - x)^{\frac{2}{3}}$$

$$x = \frac{X - f}{1 - f} \text{ as defined before,}$$

and

$$P_{eff} = P_{H_2} - \sqrt{P_{CH_4} / K_{eq}}$$

However, based on the volumetric rate expression;

$$\text{Rate} = k_V (1 - x) P_{eff} \qquad (28)$$

From Eq. (26), (27) and (28), k_S can be approximated from k_V by:

$$k_S = k_V (1 - x)^{\frac{1}{3}} \left(\frac{\rho_s R}{3}\right) \qquad (29)$$

In this way the rate constant can be calculated from the experimental data [19] as shown below:

$$k_S = 0.12 \exp(-17921 / T_S) \qquad (30)$$

Fig. 13 in Appendix 2 shows the overall reaction rate constant based on the above equation and the Unreacted-Core Shrinking Model.

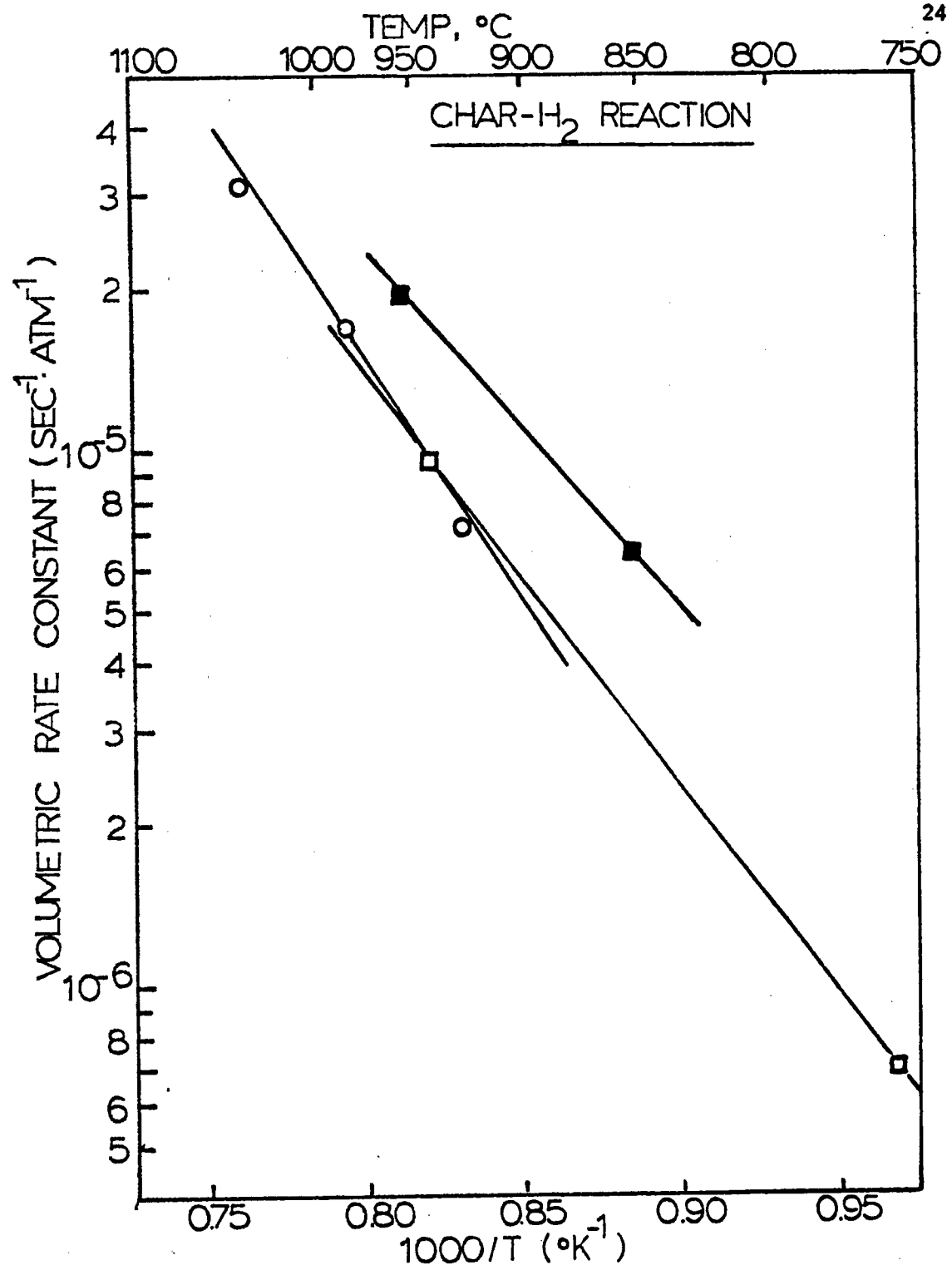

FIGURE 7. ARRHENIOUS PLOTS FOR CHAR HYDROGASIFICATION

- ■ Australian Yallourn coal char Birch et al.[55], pressure : 42 atm
- □ Concoal Montour No.10 Bitu. Coal Char, Pyrocioch and Linden[53], pressure 104 atm
- o Air-pretreated Pittsburgh No 8 coal char. Johnson[56], pressure : 35 atm.

3.8 Water-Gas Shift Reaction

The water-gas shift reaction is one of the most important reactions which determines the product distribution of a gasifier. This reaction is very fast especially in the presence of a catalyst. Most water-gas shift reactors employed an iron-base or chromium-base catalyst to produce hydrogen from CO and H_2O. Both first-order [17,57,58,59] and second order [60, 61] rate expressions have been proposed to explain the rate of reaction. Recently Singh and Saraf [17] proposed a first order rate equation taking into account the effect of temperature, pressure, age of catalyst, and H_2S content in the reacting gases on a catalyst (72% Fe_2O_3 - 8% Cr_2O_3). By certain modification this equation can be used to estimate the rate of water-gas shift reaction in a coal gasifier.

Water-gas shift reaction is found to occur very rapidly at the surface of char particles; the reaction is strongly catalyzed by the ash content of the char. Table IV lists the analysis of random samples of the ash from coal liquefaction residues used by Texaco pilot plant tests. A significant amount of Fe_2O_3 and other mineral materials that may act as the catalyst of water-gas shift reaction is found in coal ash.

By assuming a correction factor, F_w, which represents the reactivity of ash in the char as a catalyst, the rate of water-gas shift can be given by [17]:

$$\text{Rate} = F_w \cdot (2.877 \times 10^5) \cdot \frac{1}{P_t} \left(P_{CO} - \frac{P_{CO_2} P_{H_2}}{k_{eq} P_{H_2O}}\right) \cdot \exp\left(-\frac{27760}{1.987T}\right)$$

$$P_f \cdot R_a(T) \text{ g mole/sec} \cdot (\text{g ash}) \qquad (31)$$

where k_{eq} is the equilibrium constant of the water-gas shift reaction;

$P_f = P_t^{(0.5 - P_t/250)}$ is the pressure correcting factor, P_t is the total pressure in atm;

$R_a(T) = \exp\left(-8.91 + \frac{5553}{T}\right)$, is the temperature correcting factor;

F_w = correction factor taking into account the relative reactivity of ash to the iron-base catalyst.

In this study, F_w is selected to be 0.2.

3.9 Methane-Steam Reforming Reaction

The methane-steam reforming reaction is the reverse reaction of the methanation reaction and is believed to be catalyzed by the minerals present in the coal. The exact nature of the methane destruction is

TABLE IV

Typical Ash Analysis of H-Coal Liquefaction Residues [1]

Ash Composition (ASTM D-2795) Wt. Pct.	Illinois No. 6	Wyodak
SiO_2	46.90	31.40
Al_2O_3	19.30	15.80
Fe_2O_3	18.90	5.83
TiO_2	0.91	0.86
P_2O_5	0.15	1.63
CaO	4.33	23.83
MgO	1.16	5.79
Na_2O	1.29	2.26
K_2O	1.98	0.27
B_2O_3	0.15	0.13
SO_3	3.67	7.38
Unaccounted for	1.26	4.82
Ash Fusion (ASTM D-1857) Reducing Atmosphere		
IT	1077°C (1971°F)	1160°C (2120°F)
ST	1110°C (2030°F)	1188°C (2170°F)
HT	1176°C (2149°F)	1195°C (2183°F)
FT	1235°C (2255°F)	1210°C (2210°F)

not clear. Allen et al. [62] proposed a complicated model for nickle-catalyzed methane-steam reaction based on the assumption that the desorption of products is the controlling step. However, their rate expression consists of at least five parameters that depend on the operating temperature and the type of catalysts used. Zahradnik and Grace [18] proposed the following expression for Pittsburgh seam coal:

$$\frac{d\ C_{CH_4}}{dt} = - k\ C_{CH_4} \qquad (32)$$

where

$$k = 312 \exp (- 30{,}000/RT) \text{ in } sec^{-1} \text{ and } T \text{ in } {}^{o}K$$

The fraction of methane decomposed in a stirred tank reactor, y, can be calculated as

$$y = 1 - e^{- k \cdot \Delta t} \qquad (33)$$

where Δt is the residence time of gas in sec.

IV. Model Development

A successful development of an entrained bed gasification model will require a good understanding of both chemical kinetics and hydrodynamics. One of the reasons why the modeling of an entrained bed gasifier is difficult is that the degree of mixing of solid and gas flow varies along the bed and differs for each different geometry of the bed. Published techniques for analyzing the hydrodynamics in an entrained gasifier are currently at a primitive level. Complexity of the modeling is further compounded by the lack of experimental data on the complex structure changes of coal/char particles during reactions and on rates of gasification for various coals.

4.1 Hydrodynamics

In some of the gasifiers, the mixing depends on axial jets from injection nozzles whereas others develop a vortex field induced by tangential firing. In practice, turbulence and gas recirculation are produced by the introduction of fuel and oxidant into the combustion zone through high velocity jets. The combustion zone immediately following the inlet of an entrained-bed gasifier is similar to a utility boiler equipped with burners which produce a highly turbulent flow. Residence time data indicate that the immediate combustion zone behaves much like a stirred tank reactor, while directly adjacent to the burner zone the vortex pattern dissipates rapidly so that plug flow (with dispersion) can be assumed [10]. Kane and McCallister [12] recently analyzed the flow field of an entrained flow gasifier and determined the dimensionless groups which govern the scaling laws of the gasifier. Among the important dimensionless groups they identified are the swirl number, geometric scale ratio, Froude number and particle loading ratio. Existing models are not adequate to predict solid concentrations and gas velocity for such a complex flow system.

Because of the lack of data to estimate the degree of mixing in the entrained-bed gasifier, the concept that assumes the gas phase completely mixed at the entrance region followed by a region approximating plug flow and the solid phase plug flow throughout the reactor is adopted in this model development. Similar assumptions have been employed by Ubhayakar et al. [13] in their simulation of coal pyrolysis and gasification by MHD exhaust gas in an entrained bed reactor. By this assumption, the compartment-in-series approach [14], which selects a large compartment size (about 1/20 of the effective reactor length) for the mixing zone immediately following the inlet and smaller compartment sizes (about 1/100 of the effective reactor length each) for the following plug flow (with dispersion) zones, is employed for the gas phase in the model development. The purpose of this model is to obtain temperature and concentration profiles for both solid phase and gas phase along the reactor.

4.2 Heat and Mass Balances

The basic assumptions used in the model development are summarized below:

1. Gas phase is completely mixed in the pyrolysis and volatile combustion zone followed by a region approximating plug flow in the later section. This is accomplished by the compartment-in-series approach which employs a large first compartment and smaller size for each of the following compartments.

2. Solid phase is plug-flow throughout the reactor.

3. The gasifier is conceptually divided into three reaction zones: pyrolysis and volatile combustion zone, combustion and gasification zone, and the gasification zone.

4. This is a steady state process.

Based on the above assumptions, heat and mass balance equations can be set up for each compartment as shown below by referring to Figure 8.

Gas Phase

$$\Sigma(W_{g_i} C_{pg_i} T_g)_{z+\Delta z} - \Sigma(W_{g_i} C_{pg_i} T_g)_z = -(A_t \cdot a \cdot \Delta z)[\sigma F_{sg}(\varepsilon_g T_g^4 - \alpha_g \varepsilon_s T_s^4) + h_c(T_g - T_s)] + \sum_k (-\Delta H_k) \cdot A_t \cdot \Delta z - \underbrace{2\pi \cdot \sqrt{\frac{A_t}{\pi}} \cdot [\sigma F_{wg}(\varepsilon_g T_g^4 - \alpha_g \varepsilon_w T_w^4) + h_{cw}(T_g - T_w)] \cdot \Delta z}_{H_{loss.g-w}} \quad (34)$$

$$W_{g_i, z+\Delta z} - W_{g_i, z} = A_t \cdot \Delta z \cdot \sum_k \nu_{ik} \cdot r_k \quad (35)$$

Solid Phase

$$\frac{d(W_s C_{ps} T_s)}{dz} = a \cdot A_t \cdot [\sigma F_{sg}(\varepsilon_g T_g^4 - \alpha_g \varepsilon_s T_s^4) + h_c(T_g - T_s) + (a \cdot A_t \cdot) \sum_j (-\Delta H_j) \cdot \gamma_j - \underbrace{(1 - \alpha_g) \sigma F_{sw}(\varepsilon_s T_s^4 - \varepsilon_w T_w^4)}_{H_{loss.s-w}} \quad (36)$$

$$\frac{dW_s}{dz} = a A_t \sum_j r_j \quad (37)$$

where $a = \frac{W_s}{A_t v_s}\left(\frac{6}{\rho_s d_p}\right)$, is the contact area between gas and solid per unit volume of reactor (cm^2/cm^3), Δz is the compartment size (cm), and h_c is the convection and conduction heat transfer coefficient which can be obtained approximately by $h_c = 2K_g/d_p$. j and k are the

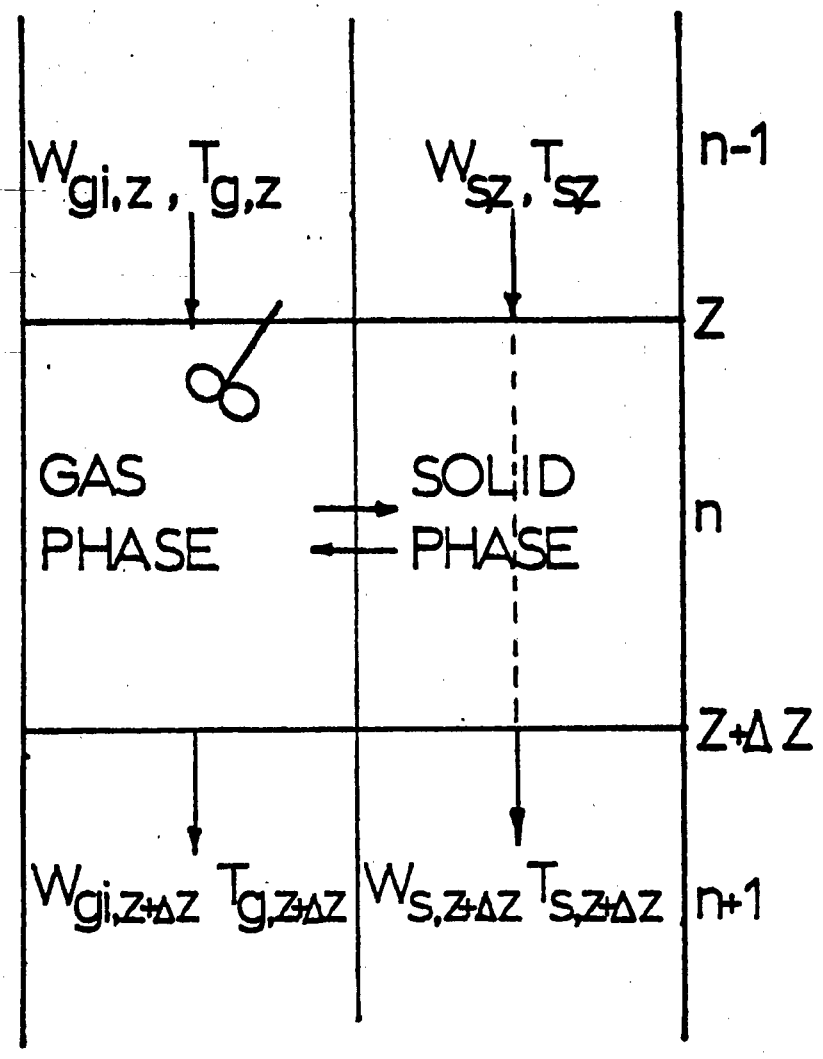

FIGURE 8. HEAT AND MASS BALANCES IN n-th COMPARTMENT

reactions in solid and gas phase respectively and are described in Appendix 1 for each reaction zone.

By substituting the relations: $a = \frac{W_s}{A_t v_s} \cdot (\frac{6}{\rho_s d_p})$, $dz = v_s d_t$, $\alpha_g = \varepsilon_g = \varepsilon$, $F_{sg} = F$, $\varepsilon_s = 1$, and $H_{loss,s-w} << a \cdot A_t \cdot [\sigma F_{sg}(\varepsilon_g T_g^4 - \alpha_g \varepsilon_s T_s^4) + h_c (T_g - T_s)]$, into Equation (36) the following equation is obtained.

$$\frac{dT_s}{dt} = \frac{6}{\rho_s C_{ps} d_p} [eF\sigma(T_g^4 - T_s^4) + h_c(T_g - T_s) + \sum_j (-\Delta H_j) r_j] \qquad (38)$$

By modifying Equation (36) and adding to Equation (34), the following heat balance equation can be obtained:

$$(\sum_i W_{g_i} C_{pg_i} T_g + W_s C_{ps} T_s)_{z+\Delta z} - (\sum_i W_{g_i} C_{pg_i} T_g + W_s C_{ps} T_s)_z$$

$$= \sum_j a(-\Delta H_j) r_j (A_t \Delta z) + \sum_k (-\Delta H_k) r_k (A_t \Delta z) - H_{loss,g-w} \qquad (39)$$

The above equation can also be obtained from a total heat balance on both solid phase and gas phase in each compartment:

(Total enthalpy output) - (Total enthalpy input)

= (Total heat generated by reactions) - (Heat loss through the reactor wall) (40)

Experimental data on heat exchange between the gas and the reactor wall are difficult to obtain. In this study, the following assumptions are made in order to account for the heat loss:

(1) In the combustion zones, 30% of the total heat generated by reactions is transferred from gas phase to the reactor wall, which is about 7%-10% of the heating value of the raw fuel.

(2) In the zones following the combustion zones where oxygen is exhausted, the rate of heat exchange per unit area of reactor wall between the gas and the reactor wall is calculated by $U_o(T_g - T_w)$. The value of U_o is selected to be about 25 BTU/hr ft^2°F which is within the reported range of the overall heat transfer coefficient for a gas heat exchanger [75, 76]. Since no measurement of the wall temperature has been reported, a linear correlation of the wall temperature is assumed for the simulation. For example, in all of the runs with coal liquefaction residues, the reactor wall temperature is assumed to be $T_w = 2100 - 600\ (Z/L_t)$ in °K.

Since solid loading in the entrained gasifier is generally less than 1% of the reactor volume, the fuel particles can be assumed to be completely surrounded by the gas. Therefore, the viewing factor, F, for

radiation heat transfer between gas and fuel particles can be assumed to be 1.0. However, determination of emissivity, e, of the gas mixture is difficult. It is a function of the partial pressure of each gaseous component, temperature and reactor geometry. McAdams [75] presented a method for a rough estimation of gas emissivity. The emissivity of the gas mass in the reactor is a function of the product P_iL (atm-ft), where P_i is the partial pressure of the radiating constituent and L is the mean beam length. If more than one radiating constituent is present, the emissivities are additive, although a small correction must be made for the interference of radiation between different types of molecules. At an operating pressure of 24 atm., the summation of the product $\sum_i P_i L$, is in the order of 100 atm-ft for Texaco's pilot plant gasifier. This is beyond the range of the experimental data of Evans [77] and McAdams [75]. By extrapolating their data, however, the emissivity of the gas mixture is selected to be 0.9 for the Texaco entrained bed gasifier.

The solid residence time, Δt, in each compartment can be obtained by momentum balance. Since the solid particle size employed in an entrained bed system is generally very small, it is assumed that Stoke's Law applies for solid flow in this system. The solid entraining velocity can be calculated by the following formula:

a) Downflow:

$$v_s = v_{si}\, e^{-b\Delta t} + (v_g + v_t)(1 - e^{-b\Delta t}) \qquad (41)$$

b) Upflow:

$$v_s = v_{si}\, e^{-b\Delta t} + (v_g - v_t)(1 - e^{-b\Delta t}) \qquad (42)$$

where

$$b = \frac{18\mu}{\rho_s d_p^{\,2}}$$

$$v_t = \frac{(\rho_s - \rho_g) d_p^{\,2} g}{18\,\mu}$$

v_{si} = initial solid velocity (cm/sec)

and Δt = solid residence time in this compartment (sec).

The solid residence time, Δt, is related to the compartment size, Δz, as shown below:

$$\Delta z = \int_o^{\Delta t} v_s \, dt \qquad (43)$$

The above three equations can be solved simultaneously by applying the Newton-Raphson method to obtain the solid residence time, Δt, in each compartment.

The simplest way to solve the above equations for each compartment is listed below:

1) Assume a T_g value for this compartment which has been assumed to be completely mixed for the gas phase.

2) Obtain the solid temperature profile from Eq. (38) by Runge-Kutta-Gill method.

3) Do material balances

4) Check total heat balance by Eq. (40). If the total heat balance meets the required error criteria, start the calculations of the next compartment. If the total heat balance does not meet, use root-search methods such as Regula-Falsi or Wegstein method to help searching for a better value of T_g and repeat the procedure again.

Figure 9 shows the computer flow diagram of the calculation procedures. The computer program simulating the Texaco Pilot Plant Entrained-Bed Gasifier is shown in the Appendix 8.

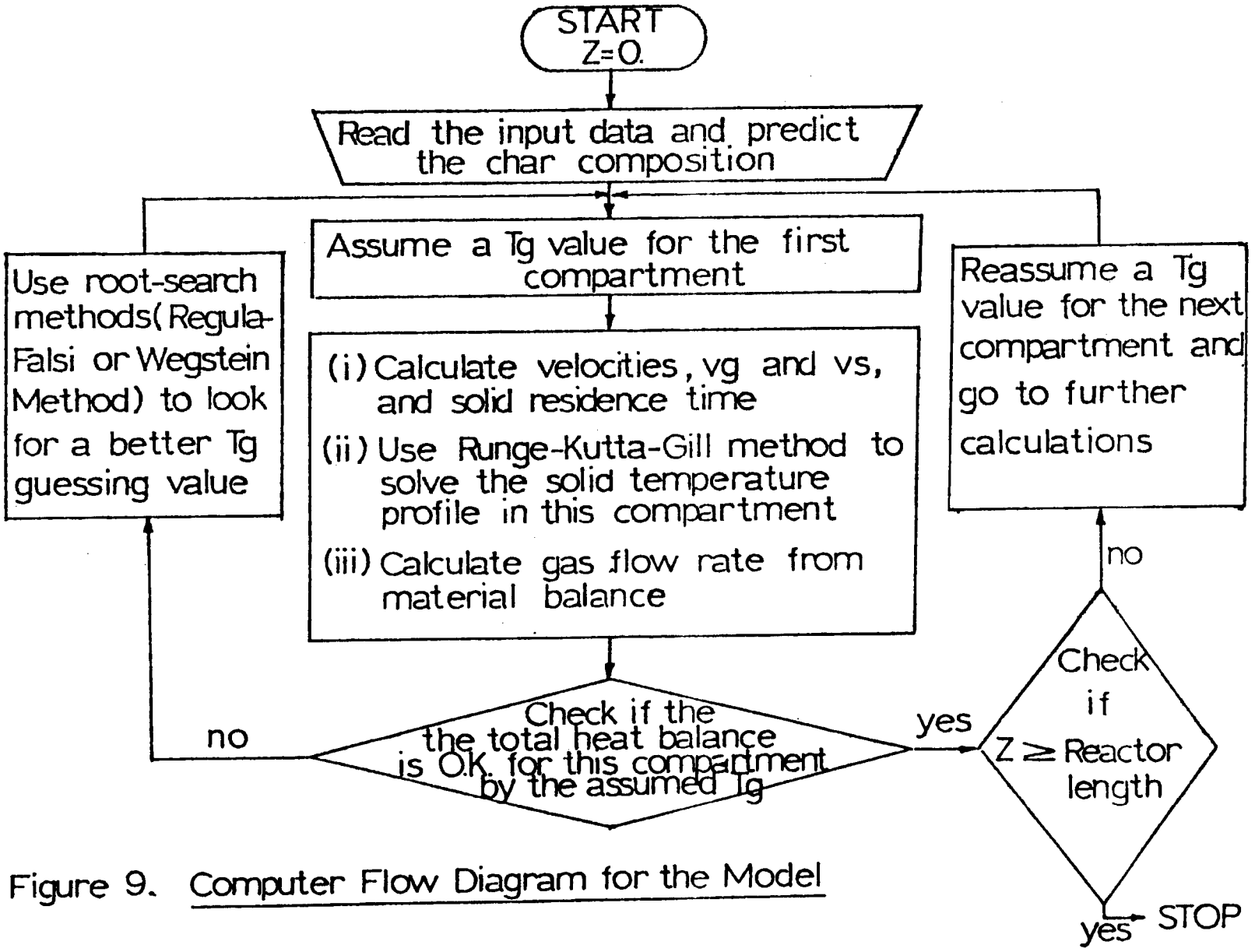

Figure 9. Computer Flow Diagram for the Model

V. Results and Discussion

Comparison of the computed results based on the model with the experimental data of the Texaco Downflow Entrained Bed Pilot Plant has been made for 27 runs using coal liquefaction residues and two runs using coal-water slurries as feedstock (see Appendix 6). Good agreement between the computed and the experimental data in the major product (CO, H_2 and CO_2) gas distribution is seen. Temperature and concentration profiles obtained by the proposed model for seven typical runs are shown in Appendix 5. [Fig. 14(A) - Fig. 20(B)].

Parameter studies are made to provide a better understanding of the reactor performance for various operating conditions utilizing the model. These are shown in Appendix 7.

Fig. 21 shows the effect of oxygen/fuel ratio on carbon conversion at various steam/fuel ratios feeding the H-coal residue from Illinois No. 6 coal into the Texaco Pilot Plant Gasifier. Fig. 22 shows the effect of steam/fuel ratio on carbon conversion at various oxygen/fuel ratios using coal liquefaction residue as feedstock. In coal liquefaction residue runs, it is found that the oxygen/fuel ratio more significantly affects carbon conversion than does the steam/fuel ratio. In a short residence-time device like an entrained bed gasifier, the oxygen/fuel ratio is critical to the conversion since the heat produced from combustion reactions supports the endothermic gasification reactions. However, it is also seen that for the Texaco Pilot Plant Gasifier, there is no need to exceed the oxygen/fuel ratio beyond 0.9 in coal liquefaction residue runs. To obtain 98-99% conversion, an oxygen/fuel ratio between 0.8 and 0.9 is required for this gasifier. Texaco [1,2] operated at oxygen/fuel ratio between 0.768-0.94 and obtained 91-99.7% carbon conversions for their coal liquefaction residue runs. Interestingly, the model shows an optimal steam/fuel ratio to exist at a fixed oxygen/fuel ratio using coal liquefaction residues as feedstock. Although increasing the steam/fuel ratio promotes the char-steam reaction, the optimal steam/fuel ratio exists because of the following two disadvantages: (1) the char-steam reaction is highly endothermic and would lower the reaction temperature which in turn will lower the gasification rate; (2) a large amount of steam can carry a large quantity of sensible heat from the reaction system and reduce the reaction temperature. Depending on the oxygen/fuel ratio this optimal steam/fuel ratio ranges from about 0.3 to 0.6 for the Texaco Pilot Plant Gasifier using coal liquefaction residues as feedstock. Texaco operated at steam/fuel ratio between 0.241 and 0.429 for the first two sets of pilot plant tests using H-coal residue from Illinois No. 6 coal and from Wyodak coal [1]. However, they obtained high carbon conversions (99%) for later tests [2] using smaller oxygen/fuel ratio (0.77-0.79) and higher steam/fuel ratio (0.3-0.5).

Fig. 31 shows the effect of water/coal ratio on carbon conversion at various oxygen/coal ratios for coal-water slurry runs. It is found that the water/coal ratio has much more significant effects on carbon conversion in coal-water slurry runs than does the steam/fuel ratio in coal liquefaction residue runs. Within the testing range of water/coal ratio from 0.4 to 0.8, no optimum feeding ratio of water/coal has been found operating at fixed oxygen/coal ratios. As the water/coal ratio is decreased, the carbon conversion increases. This is due to the latent heat of evaporation when water is used in the system. The latent heat of the feeding water absorbs a large amount of heat in the reactor and lowers the reaction temperature. The heat required to support the endothermic gasification reaction therefore becomes the most important factor in determination of carbon conversion in the coal-water slurry runs. On the other hand, in liquefaction residue runs, both the reaction temperature and steam concentration are of similar importance in determining the carbon conversion. These two factors compete with each other, thus resulting in an optimum steam/fuel ratio at fixed oxygen/fuel ratios for systems feeding steam.

Although the steam/fuel ratio does not significantly affect the carbon conversion in coal liquefaction residue runs, it does affect the gas product distribution as shown in Fig. 27-Fig. 30. The oxygen/fuel ratio, on the contrary, does not have a significant effect on the gas product distribution is shown in Fig. 23-Fig. 26. As the steam/fuel ratio increases, the fraction of CO in the product gas decreases while those of H_2 and CO_2 increase. However, increasing the oxygen/fuel ratio at fixed steam/fuel ratios eventually shows a reduction in the fraction of hydrogen in the product gases (see Fig. 23-26). As the oxygen/fuel ratio increases the concentration of CO increases while the concentration of CO_2 first decreases and then increases. These concentration variations are due to the competition between char-oxygen, char-CO_2, char-steam, and water-gas shift reactions. The water-gas shift reaction is found to be very close to the equilibrium state at the outlet of the reactor in almost all cases.

Fig. 32-Fig. 36 show the effect of pressure on the carbon conversion and product gas distribution. Increasing the pressure will increase the carbon conversion especially at high steam/fuel ratios and for oxygen/fuel ratios smaller than 0.8. For oxygen/fuel ratios larger than 0.8 the pressure effect becomes insignificant. The effect of pressure on the product gas distribution is small as shown in Fig. 34. Increasing the pressure will slightly increase CO and H_2 concentrations while decreasing the CO_2 concentration in the product gas at oxygen/fuel ratios less than 0.8.

The fuel particle size or droplet size has a significant effect on the carbon conversion as shown in Fig. 37. This effect is easily understood since fuel residence time and the specific contact area for solid-

gas reactions are closely related to the particle size. Large particles have greater terminal velocities and thus travel at higher particle velocities and shorter residence time than small particles in the reactor as shown in Fig. 37.—On the other hand, the specific contact area between reacting gases and the fuel particle is inversely proportional to the particle size. These two effects combine to give lower conversion for large particles compared to small particles.

In simulating Texaco's pilot plant operation, however, the fuel particle size and the initial particle velocity are not known after being sprayed from the nozzle in the reactor. In this study, a trial-and-error procedure has been used to estimate this information. An initial partial velocity of 300 cm/sec was selected for the simulation. The fuel particle size was selected to be around 350 μm for most of the cases except that 400 μm was used for cases with Wyodak coal liquefaction residue. It was reported [1] that Wyodak coal residue is much more viscous than the Illinois No. 6 coal residue. Under these assumptions, the fuel residence time in the pilot plant reactor is calculated to be between five to eight seconds.

VI. Conclusion and Recommendation

The Texaco Downflow Entrained-Bed Gasifier has demonstrated the ability to gasify coal liquefaction residues, light oil and coal-water slurries into synthesis gas. This process can provide the required hydrogen or synthesis gas for coal liquefaction processes or for fuels and chemical feedstocks. This study provides an insight into the importance of the operating parameters on the reactor performance and furnishes a procedure for gasifier scale-up.

In this study a mathematical model was developed to simulate the performance of entrained bed gasifiers. A major effort has been focused on simulating the experimental results from Texaco Downflow Entrained-Bed Pilot Plant Gasifier using coal liquefaction residues and coal-water slurries as feedstock. Good agreement has been obtained between the computational results from the model and the experimental data from Texaco's pilot plant tests. This model provides the temperature and concentration profiles for both solid and gas within the reactor.

In order to better understand the operation of the entrained gasifier, the model is used to simulate the performance under various operating conditions. The following conclusions are obtained:

(1) An increase in the oxygen/fuel ratio significantly increases the carbon conversion. In order to obtain 99% carbon conversion in Texaco's pilot plant gasifier, an oxygen/fuel ratio of at least 0.8 but no more than 0.9 is required when using H-coal residue from Illinois No. 6 coal.

(2) For a given oxygen/fuel ratio, there is an optimal ratio of steam/fuel which maximizes the carbon conversion for systems utilizing steam rather than water. Such an optimum condition is more pronounced when the oxygen/fuel ratio is low.

(3) An increase in the steam/fuel ratio increases the H_2 and CO_2 concentration but decreases the CO concentration in the product gas.

(4) The product gas distribution is relatively insensitive to oxygen/fuel ratio. However, increasing the oxygen/fuel ratio slightly decreases the hydrogen concentration while it increases the CO concentration in the product gas.

(5) An increase in the operating pressure in an entrained bed gasifier can increase the carbon conversion. This effect is particularly significant at high steam/fuel ratios and when oxygen/fuel ratios are below 0.8.

(6) Fuel particle (or droplet) size has an important effect on the carbon conversion. Small particles give high carbon conversions for a given mass feed rate.

Although the proposed model can provide some insight into the mixing of gas and solid, additional information is needed regarding the geometry of the feeding zone and the hydrodynamics associated with the zone. Experimental data on temperature and concentration profiles for different types of coals are also needed to verify and refine the entrained gasifier model developed.

VII. Notation

a	the contact area between solid and gas per unit volume of reactor, $a = \frac{W_s}{A_t v_s}\left(\frac{6}{\rho_s d_p}\right)$, (cm^2/cm^3)
A_t	the cross-sectional area of the reactor, (cm^2)
C_{pg}, C_{ps}	specific heats of gas and solid respectively, (cal/g^oK)
d_p	the particle size, (cm)
e	emissivity of gas
h_c	the convection heat transfer coefficient between gas and solid, $(cal/cm^{2o}K)$
$H_{loss,g-w}$	the heat exchange between gas and reactor wall, (cal/cm)
K_g	thermal conductivity of gas, (cal/cm^oK)
r_j	the reaction rate of j-th solid phase reaction, $(g/cm^2 sec)$
r_k	the reaction rate of k-th gas-involved reaction, $(g/cm^3 sec)$
T_g, T_s	temperatures of gas and solid respectively, (^oK)
v_g, v_s	velocities of gas and solid respectively, (cm/sec)
W_s, W_{g_i}	flow rate of solid and the i-th component gas respectively, (g/sec)
ρ_s, ρ_g	densities of solid and gas respectively, (g/cm^3)
μ	gas viscosity, (poise)
ν_{ik}	the stoichiometric parameter for the i-th component gas in the k-th reaction
dt	differential solid residence time (sec)
dz	differential reactor length, $dz - v_s\, dt$, (cm)
X_c	carbon conversion, %
L_t	total effective reactor length, (cm)

R	outside radius of an unreacted-core-shrinking particle, (cm)
r_c	radius of the unreacted core of an unreacted-core-shrinking particle, (cm)
Y	ratio of r_c/R in an unreacted-core-shrinking particle, (dimensionless)
Z	distance from the top of the reactor, (cm)

Subscripts:

i	gaseous component
j,k	reactions in solid and gas phase respectively, see definition in Appendix 1

VIII. Literature Cited

1. Robin, A. M., "Hydrogen Production from Coal Liquefaction Residues", EPRI Rpt., EPRI-AF-233, Dec. 1976.

2. Robin, A. M., "Gasification of Residual Materials from Coal Liquefaction", D.O.E. Quarterly Report, FE-2274-11, October 1977.

3. Badzioch, S. and P. B. W. Hawksley, Ind. Eng. Chem., Process Des. Dev., 9, 521 (1970).

4. Anthony, D. B. and J. B. Howard, AIChE J., 22, 625 (1976).

5. Wen, C. Y., R. C. Bailie, C. Y. Lin, and W. S. O'Brien, "Coal Gasification", Adv. Chem. Ser., 131, 9 (1974).

6. Pitt, G. J., Fuel, 41, 267 (1962).

7. Anthony, D. B., J. B. Howard, H. C. Hottel and H. P. Meissner, Fuel, 55, 121 (1976).

8. Loison, R. and R. Chauvin, Chim. Ind., 91, 269 (1964).

9. Suuberg, E. M., W. A. Peters, and J. B. Howard, Ind. Eng. Chem., Process Des. Dev., 17, 37 (1978).

10. Field, M. A., D. W. Gill, B. B. Morgan and P. B. W. Hawksley, "Combustion of Pulverized Coal", BCURA, Leatherhead, 1967.

11. Wen, C. Y., Ind. Eng. Chem., 60, 34 (1968).

12. Kane, R. S. and R. A. McCallister, AIChE J., 24, 55 (1978).

13. Ubhayaker, S. K., D. B. Stickler and R. E. Gannon, Fuel, 56, 281 (1977).

14. Wen, C. Y. and L. T. Fan, "Models for Flow Systems with Emphasis on Chemical Reactor Modeling", Chap. 7.

15. Dobner, S., "Modeling of Entrained Bed Gasification: The Issues", EPRI, Palo Alto, CA, Jan. 15, 1976.

16. Wen, C. Y., "Optimization of Coal Gasification Processes", R&D Report No. 66, 1972.

17. Singh, C. P. P. and D. N. Saraf, Ind. Eng. Chem. Proc. Des. Dev., Vol. 16, No. 3, 1977, P. 313-319.

18. Zahradnik, R. L. and R. J. Grace, Adv. Chem. Ser., 131, 126 (1974).

19. Wen, C. Y. and S . Dutta, "Rate of Coal Pyrolysis and Gasification Reaction", chapter of the monograph "Coal Conversion Technology", edited by Wen and Lee, Addison Wesley Publishing Co., to be published, 1978.

20. Wen, C. Y. and S. Tone, "Coal Conversion Reaction Engineering" Chemical Reaction Engineering Reviews-Houston ACS Symposium Series 72, Ed. D. Luss and V. W. Weekman, Jr., 1978.

21. Russel,W. B., D. A. Saville and M. I. Greene, 70th AIChE Annual Meeting, New York, No. 10f, Nov. 1977

22. Howard, J. B. and R. H. Essenhigh, Ind. Eng. Chem., Process Des. Dev., 6, 74, (1967)

23. Hottel, H. C., G. C. Williams, N. M. Nerheim and G. R. Schneider, 10th Intern. Symp. on Combustion, 111-121, (1965)

24. Thring, M. W. and R. H. Essenhigh, "Chemistry of Coal Utilization-Supplementary Volume", Lowry, H. H., Ed., Chap. 17, John Wiley and Sons, New York, 1963.

25. Field, M. A., Combust. Flame, 13, 237 (1969)

26. Mulcahy, M. F. R. and I. W. Smith, Rev. Pure and Appl. Chem., 19, 81, (1969)

27. Arthur, J. R., Trans. Faraday Soc., 47, 164 (1951)

28. Borghi, G., A. F. Sorofim and J. M. Beer, 70th AIChE Annual Meeting, New York, No. 34C, Nov. 14-17, (1977)

29. Wicke, E. and G. Wurzbacher, Int. J. Heat Mass Transfer, 5, 277 (1962)

30. DeGraaf, J. G. A., Brennst-Warme-Kraft, 17, 227 (1965)

31. Kish, D., Ber. Bunsengas Phys. Chem. 71, 60 (1967)

32. Avedesian, M. M. and J. F. Davidson, Trans. Instn. Chem. Engrs., 51, 121 (1973)

33. Essenhigh, R. H., "Combustion of Coal" in Coal Conversion Technology ed. by E. S. Lee and C. Y. Wen, Addison-Wesley Publishing Co., in print, 1977.

34. Caram, H. S. and N. R. Amundson, Ind. Eng. Chem., 16, 171 (1977)

35. Burke, S. P. and T. E. W. Schuman, Proc. 3rd Int. Conf. Bituminous Coal, 2, 485 (1931)

36. Field, M. A., Combust. Flame, 14, 237 (1970)

37. Sergent, G. D. and I. W. Smith, Fuel, 52, 52 (1973)

38. Hamor, R. J., I. W. Smith and R. J. Tyler, Combust. Flame, 21, 153 (1973)

39. Walker, P. L., Jr., F. Rusinko, Jr., and L. G. Austin, Adv. Catalysis, 11, 133 (1959)

40. Gadsby, J., C. N. Hinshelwood and K. W. Sykes, Proc. Royal Soc. (London), A 187, 129 (1946)

41. Jensen, G. A., Ind. Eng. Chem., Process Des. Dev., 14, 314 (1975)

42. Klei, H. E., J. Sahagian and D. W. Sundstrom, Ind. Eng. Chem., Process Des. Dev., 14, 470 (1975)

43. Kayembe, N. and A. H. Pulsifer, Fuel, 55, 211 (1976)

44. Riede, B. E. and D. Hanesian, Ind. Eng. Chem., Process Des. Dev., 14 (1), 70 (1975)

45. Gray M. D. and G. M. Kimber, Nature, 214, 797 (1967)

46. Rossberg, M., Z. Elektrochem, 60, 952 (1956)

47. Montet, G. L. and G. E. Myers, Carbon, 6, 627 (1968)

48. Dutta, S., C. Y. Wen and R. J. Belt, Ind. Eng. Chem., Process Des. Dev., 16, 20 (1977)

49. Yang, R. T. and Mayer Steinberg, Ind. Eng. Chem., Fundam., 16 (2), 235 (1977)

50. Zielke, C. W. and E. Gorin, Ind. Eng. Chem., 47, 820 (1955)

51. Hiteshue, R. W., R. B. Anderson and M. D. Schlesingler, Ind. Eng. Chem., 49, 2008 (1957)

52. Hiteshue, R. W., R. B. Anderson and M. D. Schlesingler, Ind. Eng. Chem., 52, 577 (1960)

53. Pyrocioch, E. J. and H. R. Linden, Ind. Eng. Chem., 52, 290 (1960)

54. Wen, C. Y. and J. Huebler, Ind. Eng. Chem., Process Des. Dev., 4, 142, (1965)

55. Birch, T. J., K. R. Hall and R. W. Urie, J. Inst. Fuel, 33, 422 (1960)

56. Johnson, J. L., "Coal Gasification", Adv. Chem. Ser., 131, 145 (1974)

57. Atwood, K., M. R. Arnold, E. G. Appel, Ind. Eng. Chem., 42, 1600 (1950)

58. Laupichler, F. G., Ind. Eng. Chem., 30, 578 (1938)

59. Mars, P., Chem. Eng. Sci., 14, 375 (1961)

60. Moe, J. M., Chem. Eng. Prog., 58(3), 33 (1962)

61. Padovani, C., and A. Lotteri, J. Soc. Chem. Ind., 56, 391T (1937)

62. Allen, D. W., E. R. Gerhard and M. R. Likins, Jr., Ind. Eng. Chem., Process Des. Dev., 14(3), 256 (1975)

63. Jolly, L. J. and A. Pohl, J. Inst. Fuel, 26, 33 (1953)

64. Long, F. J. and K. W. Sykes, Proc. Royal Soc. (London), A193, 377 (1948)

65. Feldkirchner, H. L. and H. R. Linden, Ind. Eng. Chem. Process Des. Dev., 2, 153 (1963)

66. Feldkirchner, H. L. and J. Huebler, Ind. Eng. Chem. Process Des. Dev., 4, 134 (1965)

67. Johnstone, H. F., C. Y. Chen and D. S. Scott, Ind. Eng. Chem., 44, 1564 (1952)

68. Blackwood, J. D. and F. McGroy, Australia J. of Chem., 11, 16 (1958)

69. Yoshida, K. and D. Kunii, J. Chem. Eng. (Japan), 2, 170, (1969)

70. Ergun, S., J. Phy. Chem., 60, 480 (1956)

71. Turkdogan, E. T. and J. V. Vinters, Carbon, 7, 101 (1969)

72. Austin, L. G. and P. L. Walker, Jr., AIChE J., 9, 303 (1963)

73. Fuchs, W. E. and P. M. Yovorsky, Preprint 170th National ACS Meeting, Division Fuel Chem., 20(3), 115 (1975)

74. Bisset, L. A., "An Engineering Assessment of Entrainment Gasification", MERC/RI-78/2, Morgantown Energy Research Center, April 1978.

75. McAdams, W. H., "Heat Transmission", 3rd ed., McGraw-Hill Book Co. Inc., (1954)

76. Ludwig, E. E., "Applied Process Design for Chemical and Petrochemical Plants", Volume III, (1965)

77. Evans, F. L., Jr., "Equipment Desing Handbook for Refineries and Chemical Plants", Volume 2, Gulf Publishing, Houston, Texas, p.9, (1971)

Appendix 1

Reaction species in each zone:

The definition of reaction number for j and k used in Eq. (1)-Eq. (6) is given below:

(I) Reactions in the solid phase:

j	name of reaction
1	pyrolysis, Eq. (5)
2	char-oxygen reaction, Eq. (6)
3	char-steam reaction, Eq. (7)
4	char-carbon dioxide, Eq. (8)
5	char-hydrogen reaction, Eq. (11)
6	water-gas-shift reaction (catalyzed by the mineral materials in char), (12)
7	methane-steam reforming reaction (catalyzed by the mineral materials in char), Eq. (13)

(II) Reactions in the gas phase

k	name of reaction
1	$H_2 + 1/2 \cdot O_2 \rightarrow H_2O$
2	$CO + 1/2 \cdot O_2 \rightarrow CO_2$
3	$CH_4 + 2\ O_2 \rightarrow CO_2 + 2\ H_2O$
4	$C_6H_6 + 15/2 \cdot O_2 \rightarrow 6\ CO_2 + 3\ H_2O$
5	$CO + H_2O \rightleftarrows CO_2 + H_2$
6	$CH_4 + H_2O \rightleftarrows CO + 3\ H_2$

* The first four k's reactions are assumed to be simultaneous and, therefore, the reaction rates are controlled by the formation of H_2, CO, CH_4 and C_6H_6 in solid-involved reactions.

Specific reactions in the three conceptual zones:

Name of the reaction zone	J	k
Pyrolysis and Volatile Combustion Zone	1	1,2,3,4
Combustion and Gasification Zone	2,3,4	1,2,3
Gasification Zone	3,4,5,6,7	5,6

Appendix 2

Rate Expressions

(I) Surface Reaction Type: Unreacted-Core Shrinking Model [11]

$$\text{Rate} = \frac{1}{\frac{1}{k_{diff}} + \frac{1}{k_S Y^2} + \frac{1}{k_{dash}}\left(\frac{1}{Y} - 1\right)} \left(P_i - P_i^*\right) \qquad g/cm^2 atm\ sec$$

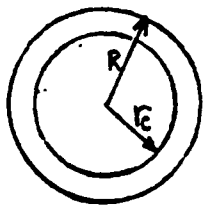

where

$$Y = \frac{r_c}{R} = \left(\frac{1 - x}{1 - f}\right)^{1/3}$$

f = conversion when pyrolysis is finished, based on original d.m.m.f coal

x = conversion at any time after pyrolysis is completed, based on original d.m.m.f coal

k_{diff} = gas film diffusion constant, $g/cm^2 atm\ sec$

k_S = ash film diffusion constant, $g/cm^2 atm\ sec$

k_{dash} = ash film diffusion constant, $g/cm^2 atm\ sec$

$\doteq k_{diff}\ (\varepsilon^{2.5})$

ε = voidage in the ash layer

P_i = partial pressure of i-component gas

$P_i - P_i^*$ = effective partial pressure of i-component taking account of the reverse reaction effect

(i) Char-O_2 Reaction, $\left[C + \frac{1}{\phi} O_2 \rightarrow 2\left(1 - \frac{1}{\phi}\right)CO + \left(\frac{2}{\phi} - 1\right)CO_2\right]$ [10]

$k_S = 8710 \cdot \exp(-17967/T_S)$, T_S in °K

$$k_{diff} = 0.292\ \phi\ \left(\frac{4.26}{T_g}\right)\left(\frac{T_g}{1800}\right)^{1.75}/(P_t\ d_p)$$

ϕ = the mechanism factor based on the stoichiometric relation of CO and CO_2, ϕ can be roughly estimated by the following equations: [19

$\phi = (2Z + 2)/(Z + 2)$ for $d_p \leq 0.005$ cm

$$\phi = [(2Z + 2) - Z(d_p - 0.005)/0.095]/(Z + 2)$$

for $0.005\ cm \leq d_p \leq 0.1\ cm$

and

$$\phi = 1.0 \text{ for } d_p > 0.1\ cm$$

where

$$Z = [CO]/[CO_2] = 2500 \exp(-6249/T)$$

d_p in cm and $T = (T_S + T_g)/2$ in °K

$$P_i - P_i^* = P_{O_2}$$

(ii) Char-Steam Reaction, (for temperature greater than 1100°C) [15]

$$k_S = 247 \exp(-21060/T_S)$$

$$k_{diff} = 10 \times 10^{-4} \left(\frac{T}{2000}\right)^{0.75}/(P_t\ d_p)$$

$$k_{eq} = \exp[17.644 - 30260/(1.8 \cdot T_S)]$$

$$P_i - P_i^* = P_{H_2O} - \frac{P_{H_2}\ P_{CO}}{k_{eq}}$$

(iii) Char-CO_2 Reaction, (for temperature greater than 1100°C) [16]

$$k_S = 247 \exp(-21060/T_S)$$

$$k_{diff} = 7.45 \times 10^{-4} \left(\frac{T}{2000}\right)^{0.75}/(P_t\ d_p)$$

$$P_i - P_i^* = P_{CO_2}$$

(iv) Char-Hydrogen Reaction

This reaction is still in chemical reaction regime even at high temperature (1600°K), because it has low intrinsic reaction rate but high diffusion characteristics. For the simplicity of calculation, the same expression as that of the Unreacted-Core Shrinking Model is used by changing K_v into K_s according to experimental conditions as follows:

$$k_S = k_v \left(\frac{1-x}{1-x_p}\right)^{1/3} \left(\frac{\rho_s d_p}{6}\right)$$

$$k_S = 0.12 \exp(-17921/T_S) \cdot g/cm^2 atm\ sec \qquad [16]$$

$$k_{diff} = 1.33 \times 10^{-3} \left(\frac{T}{2000}\right)^{0.75}/(d_p\ P_t)$$

$$k_{eq} = \frac{0.175}{34713} \exp\ [18400/(1.8\ T_S)]$$

$$P_i - P_i^* = P_{H_2} - \sqrt{P_{CH_4}/K_{eq}}$$

(II) Catalytic Reactions

(i) Water-Gas-Shift Reaction [17]

$$\text{Rate} = F_w(2.77 \times 10^5)(x_{CO} - x_{CO}^*)\exp\left(-\frac{27760}{1.987\ T}\right)P_t^{(0.5-P_t/250)}$$

$$\exp\left(-8.91 + \frac{5553}{T}\right) \qquad g\ mole/[sec(g\ ash)]$$

The adjustable parameter, F_w, which represents the relative catalytic reactivity of ash to that of iron-base catalyst, is selected to be 0.2 in the model development.

$$X_{CO} = P_{CO}/P_t$$

$$X_{CO}^* = \frac{1}{P_t}\left[\frac{P_{CO_2} P_{H_2}}{k_{eq} P_{H_2O}}\right]$$

$$k_{eq} = \exp\ (-3.6893 + 7234/(1.8\ T)]$$

P_t is the total pressure

(ii) Methane-Steam Reforming Reaction [18]

$$\text{Rate} = 312 \exp\ [-30{,}000/(1.987\ T)] \qquad 1/sec$$

Fig. 10-Fig. 13 show the calculated overall rate constants for char-oxygen, char-steam, char-carbon dioxide and char-hydrogen reactions respectively.

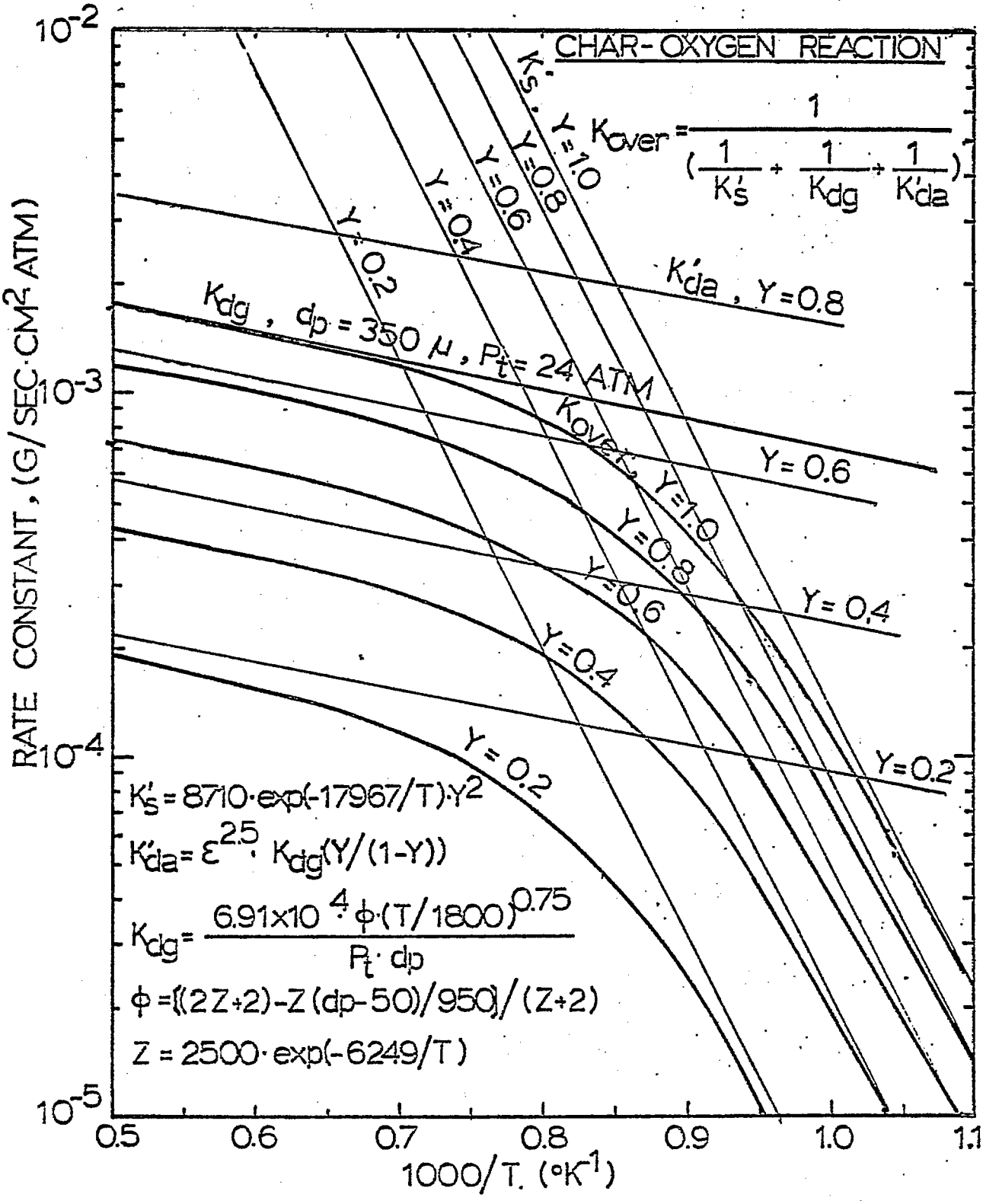

FIGURE 10. CALCULATED OVERALL CONSTANTS FOR CHAR-OXYGEN REACTION BASED ON THE UNREACTED-CORE SHRINKING MODEL

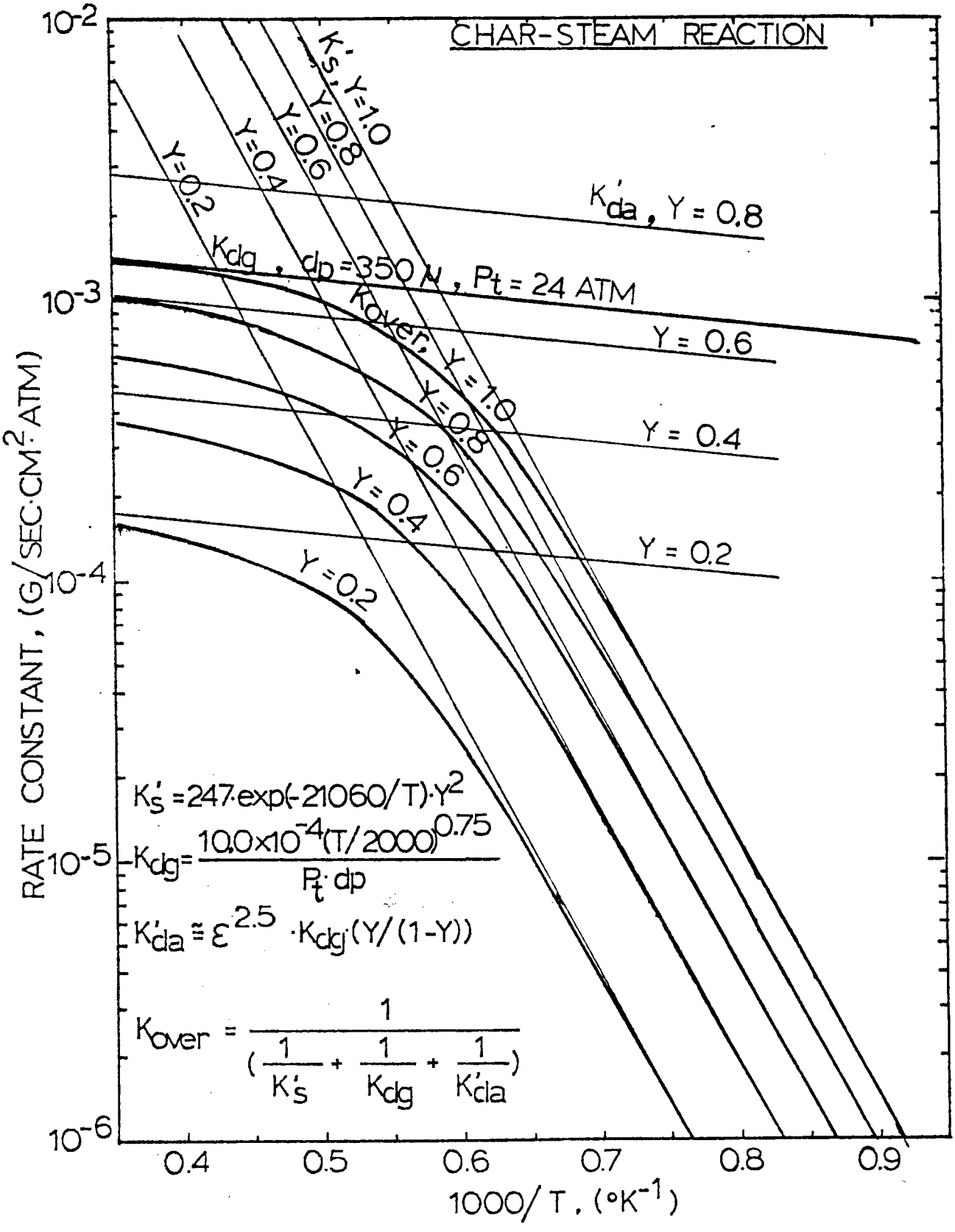

FIGURE 11. CALCULATED OVERALL CONSTANTS FOR CHAR-STEAM REACTION BASED ON THE UNREACTED-CORE SHRINKING MODEL

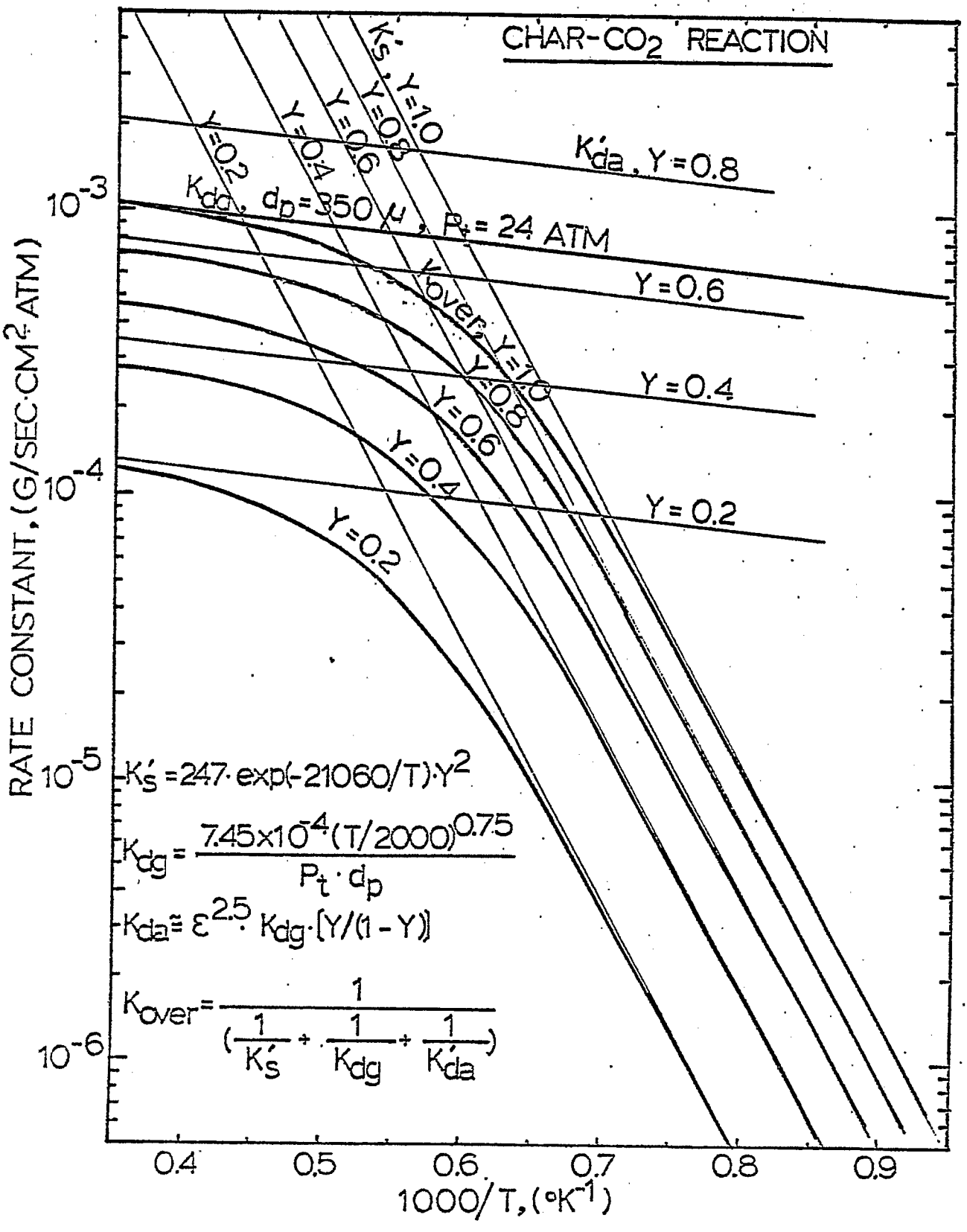

FIGURE 12. CALCULATED OVERALL CONSTANTS FOR CHAR-CARBON DIOXIDE REACTION BASED ON THE UNREACTED-CORE SHRINKING MODEL

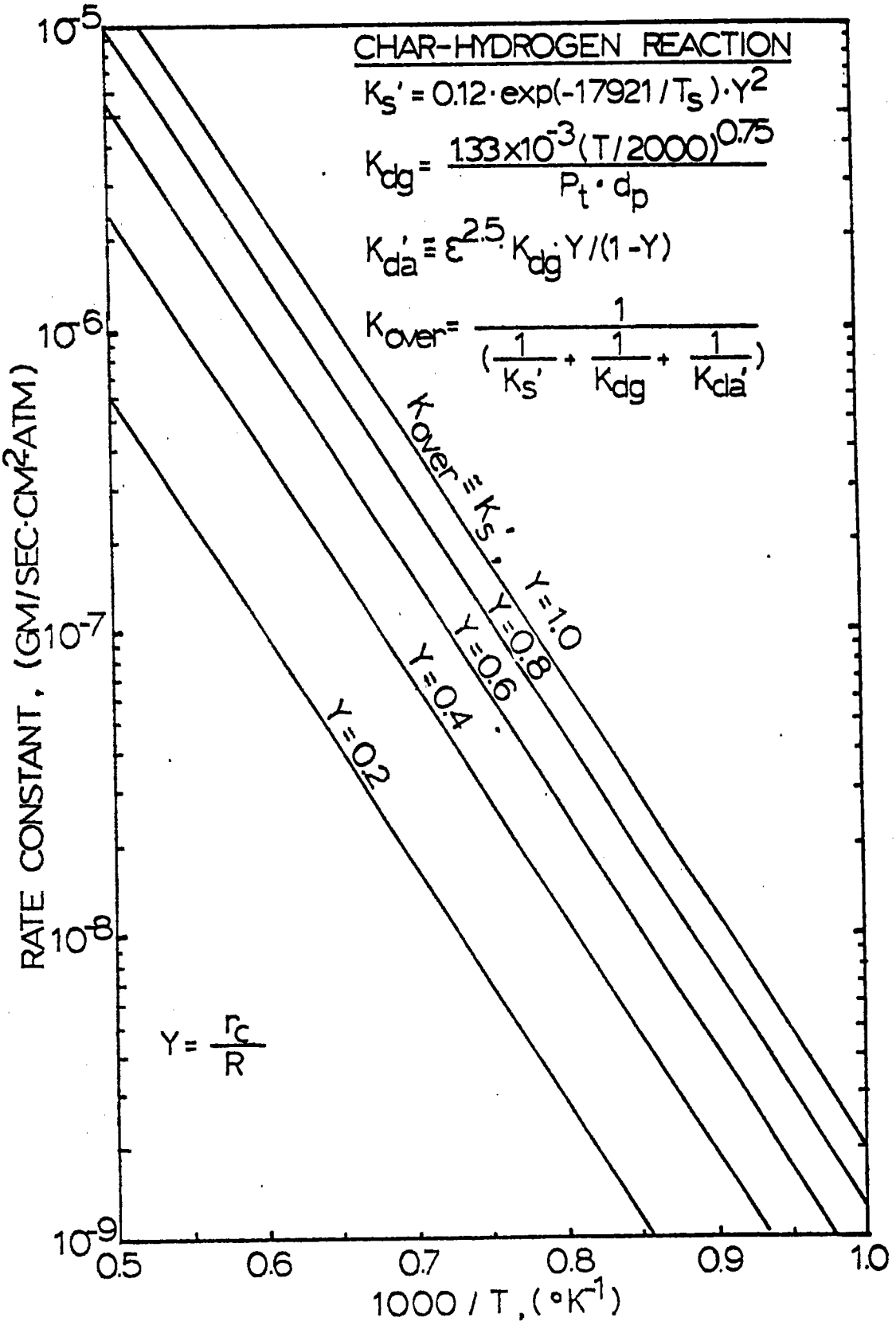

FIGURE 13. CALCULATED OVERALL CONSTANTS FOR CHAR-HYDROGEN REACTION BASED ON THE UNREACTED-CORE SHRINKING MODEL

Appendix 3: Typical ultimate analysis for the feedstock used in Texaco's pilot plant tests. [1,2]

Feedstock Source and Run Number	Dry Fuel Analysis (wt. %)						
	C	H	N	S	O	Ash	Cl
H-Coal residue from Illinois No. 6 coal for Run I-1 [1]	74.05	6.25	0.71	1.77	1.32	15.53	0.37
H-coal residue from Illinois No. 6 coal for Run I-2 [1]	73.04	5.82	0.73	1.37	1.70	16.83	0.48
H-coal residue from Wyodak coal for Run W-1 [1]	78.37	5.79	0.92	0.07	3.70	11.05	0.08
SRC II Vacuum Flash Drum Bottoms [2]	64.90	3.65	1.25	2.96	1.70	25.54	-
Exxon DSP Vacuum Tower Bottoms [2]	70.74	4.67	1.18	2.74	3.95	16.72	-
Western Coal used in Coal-Water Slurry Runs	74.56	5.31	0.99	0.46	11.47	7.20	-
Eastern Coal used in Coal-Water Slurry Runs	72.72	5.03	1.40	2.99	9.13	8.73	-

Appendix 4: Operating conditions for seven typical runs of Texaco's pilot plant tests.

Feedstock Source (Run Number)	Feed Rate			Feed Temperature (°K)		
	Fuel Rate (g/sec)	$\frac{H_2O}{Fuel}$	$\frac{O_2}{Fuel}$	Fuel	Steam	Oxygen
H-coal residue from Illinois No. 6 coal (Run I-1) [1]	76.66	0.241	0.866	505.22	696.67	298
H-coal residue from Illinois No. 6 coal (Run I-2) [1]	81.18	0.314	0.7682	496.33	676.33	298
H-coal residue from Illinois No. 6 coal (Run W-1) [1]	86.0	0.318	0.90	513.55	692.44	298
SRC II Vacuum Flash Drum Bottoms [2]	126.11	0.30	0.77	505.22	696.67	298
Exxon DSP Vacuum Tower Bottoms [2]	126.11	0.50	0.79	505.22	696.67	298
Western Coal used in coal-water slurry runs [74]	186.78	0.52	0.91	400	400	600
Eastern Coal used in coal-water slurry runs [74]	133.5	0.79	0.87	400	400	600

Appendix 5: Typical Temperature and Concentration Profiles in the Texaco Downflow Entrained-Bed Gasifier

Comparison of the computational results from the proposed model and the experimental results from the Texaco Pilot Plant Entrained-Bed Gasifier has been carried on for twenty-nine frun as shown in Appendix 6. Temperature and concentration profiles calculated from the model for five typical runs are shown in the following figures. The fuel analysis and operating conditions for these typical runs are shown respectively in Appendix 3 and 4.

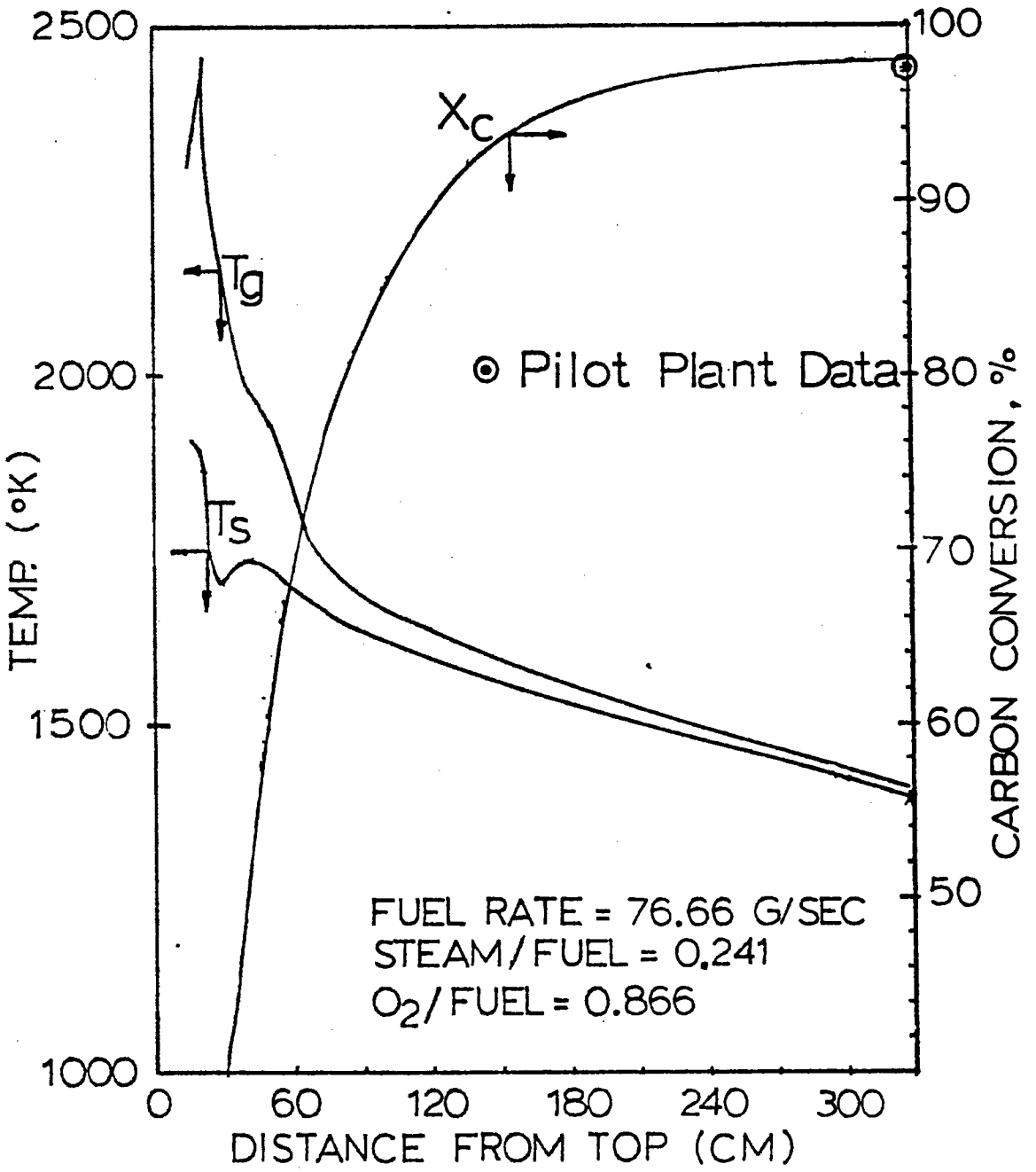

FIGURE 14(A) CALCULATED TEMPERATURE PROFILES AND CARBON CONVERSION PROFILE IN TEXACO PILOT PLANT GASIFIER FOR I-1 RUN.

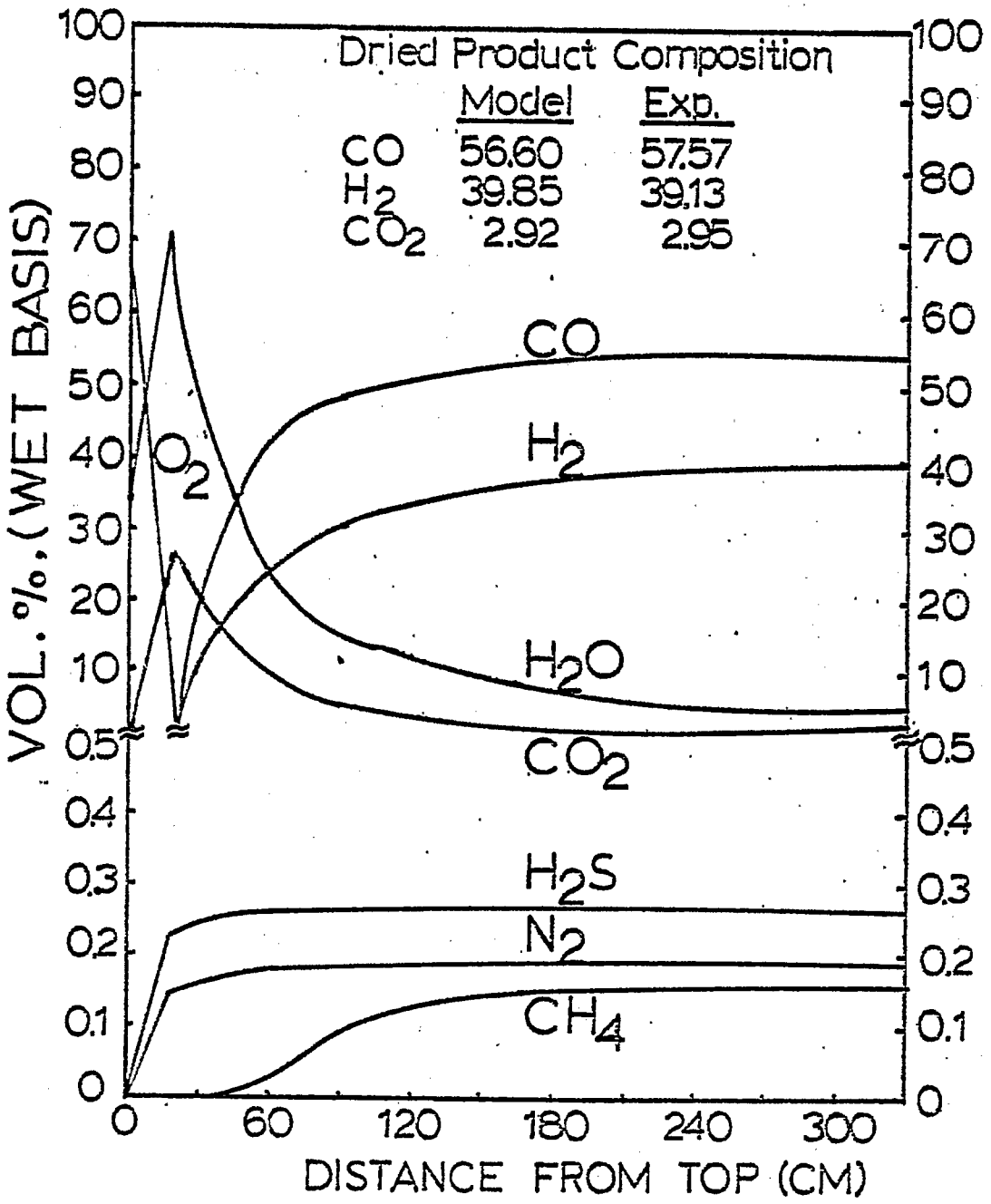

FIGURE:14(B) CALCULATED PRODUCT GAS COMPOSITION PROFILES (WET BASIS) IN TEXACO PILOT PLANT GASIFIER FOR I-1 RUN

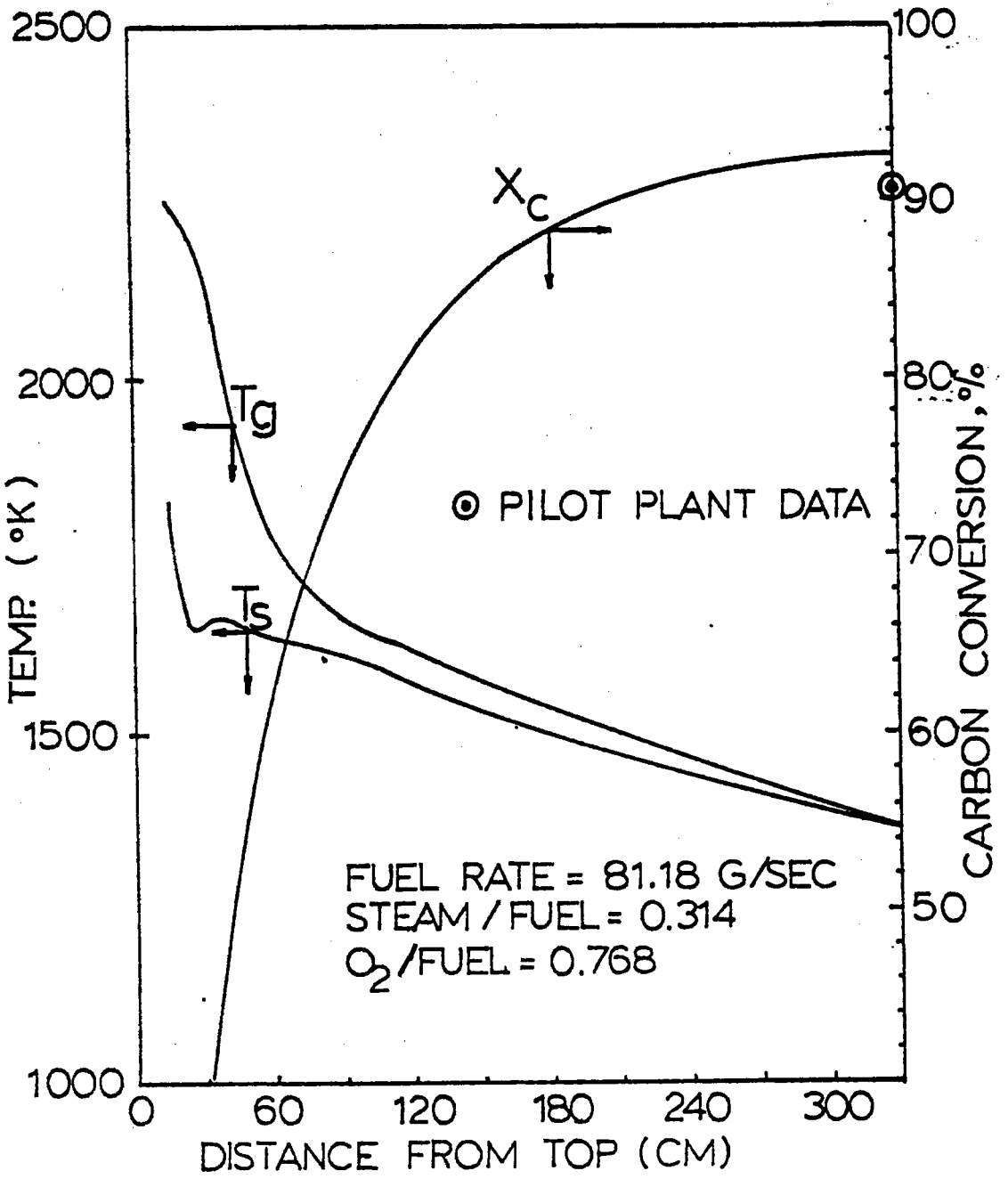

FIGURE 15(A) CALCULATED TEMPERATURE PROFILES AND CARBON CONVERSION PROFILE IN TEXACO PILOT PLANT GASIFIER FOR I-2 RUN

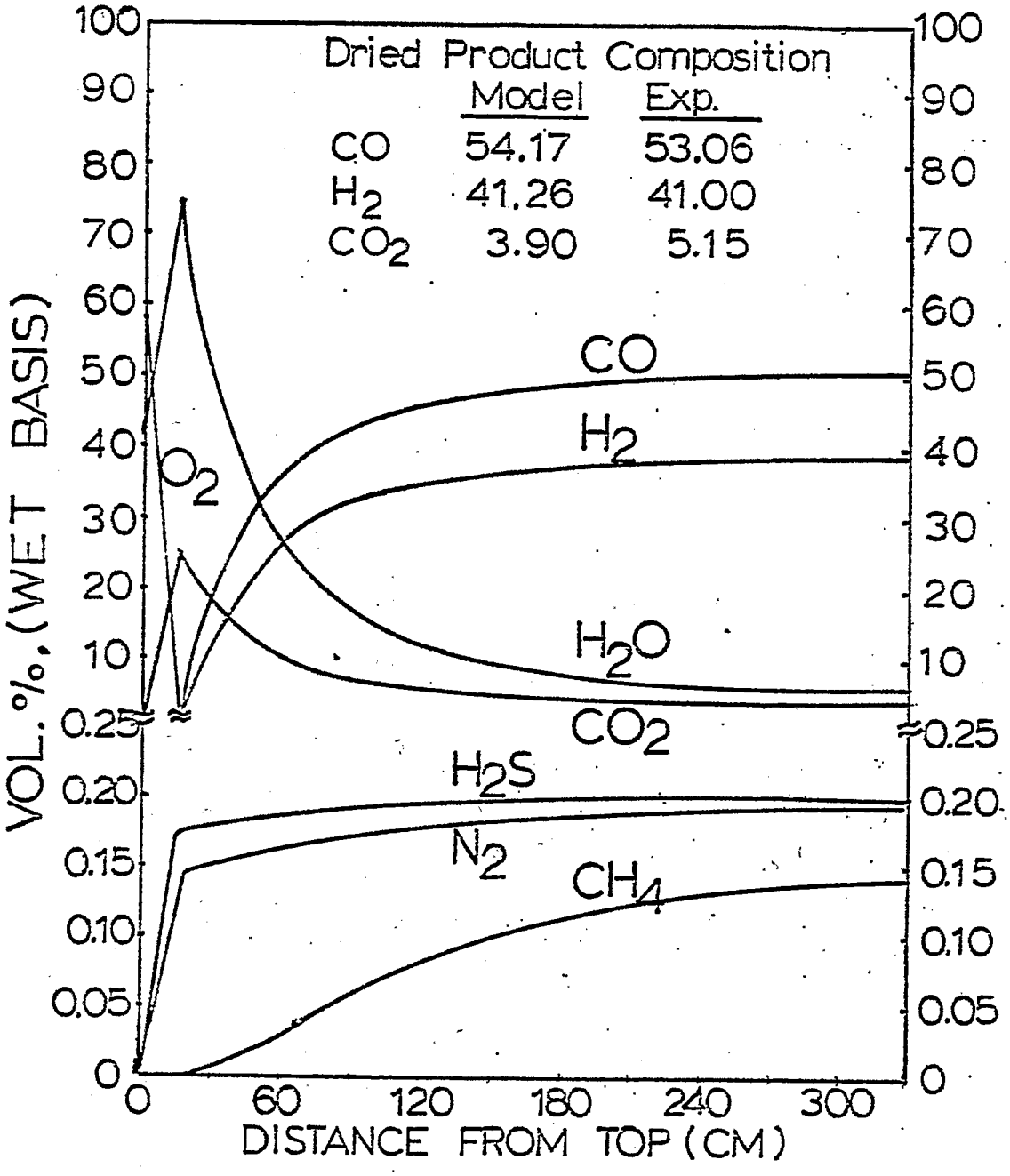

FIGURE 15(B) CALCULATED PRODUCT GAS COMPOSITION PROFILES (WET BASIS) IN TEXACO PILOT PLANT GASIFIER FOR I-2 RUN

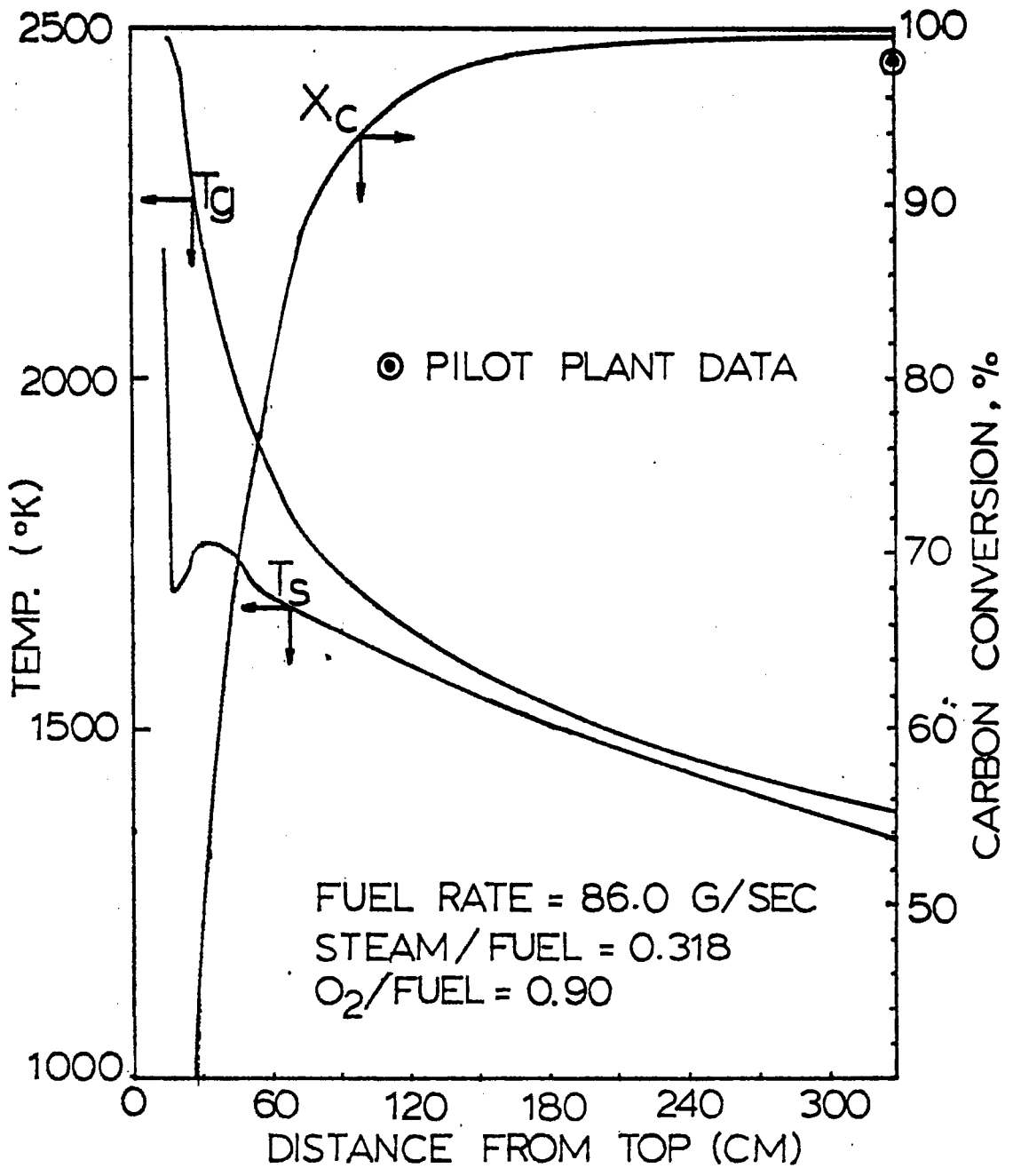

FIGURE 16(A) CALCULATED TEMPERATURE PROFILES AND CARBON CONVERSION PROFILE IN TEXACO PILOT PLANT GASIFIER FOR W-1 RUN

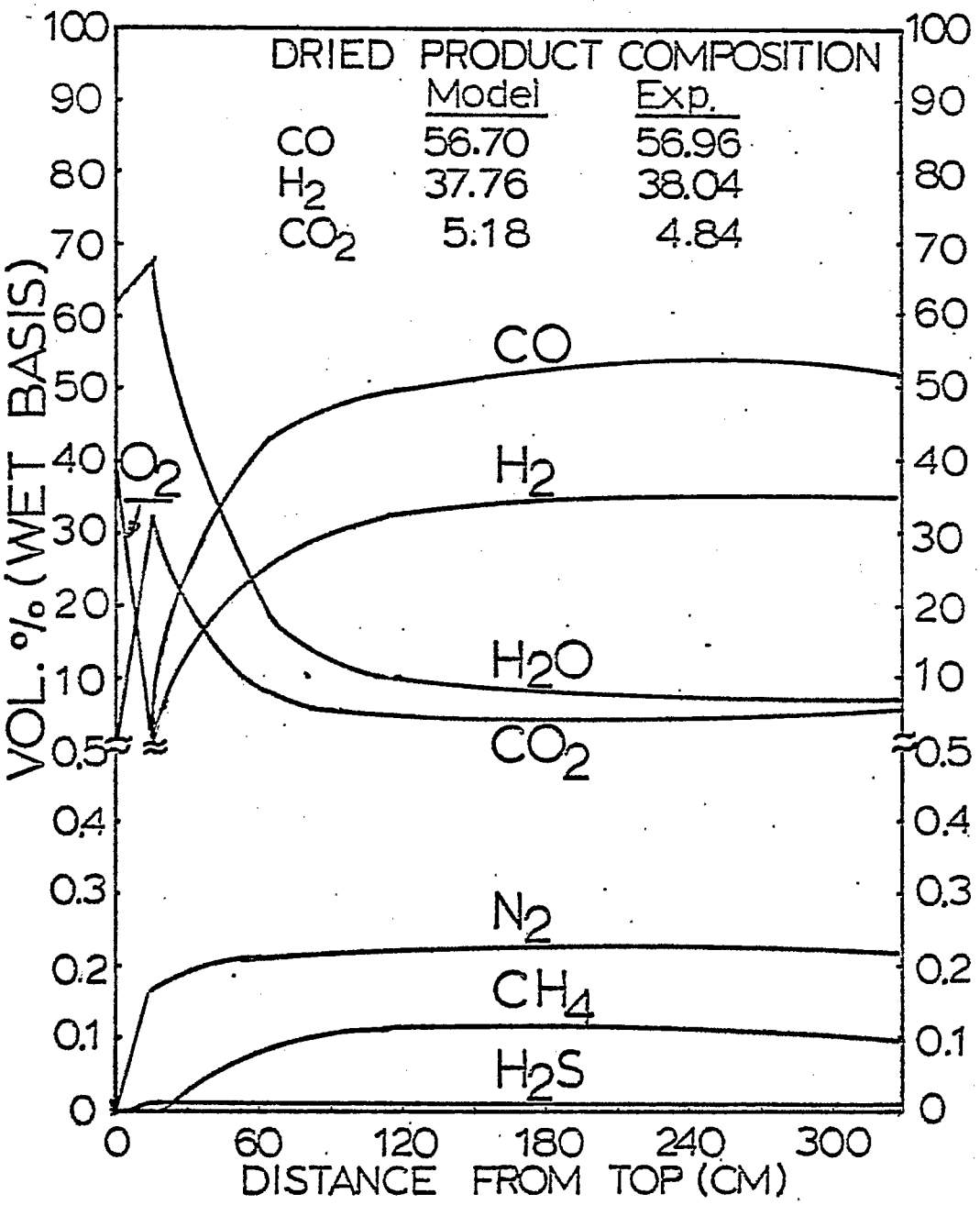

FIGURE 16(B) CALCULATED PRODUCT GAS COMPOSITION PROFILES (WET BASIS) IN TEXACO PILOT PLANT GASIFIER FOR W-1 RUN

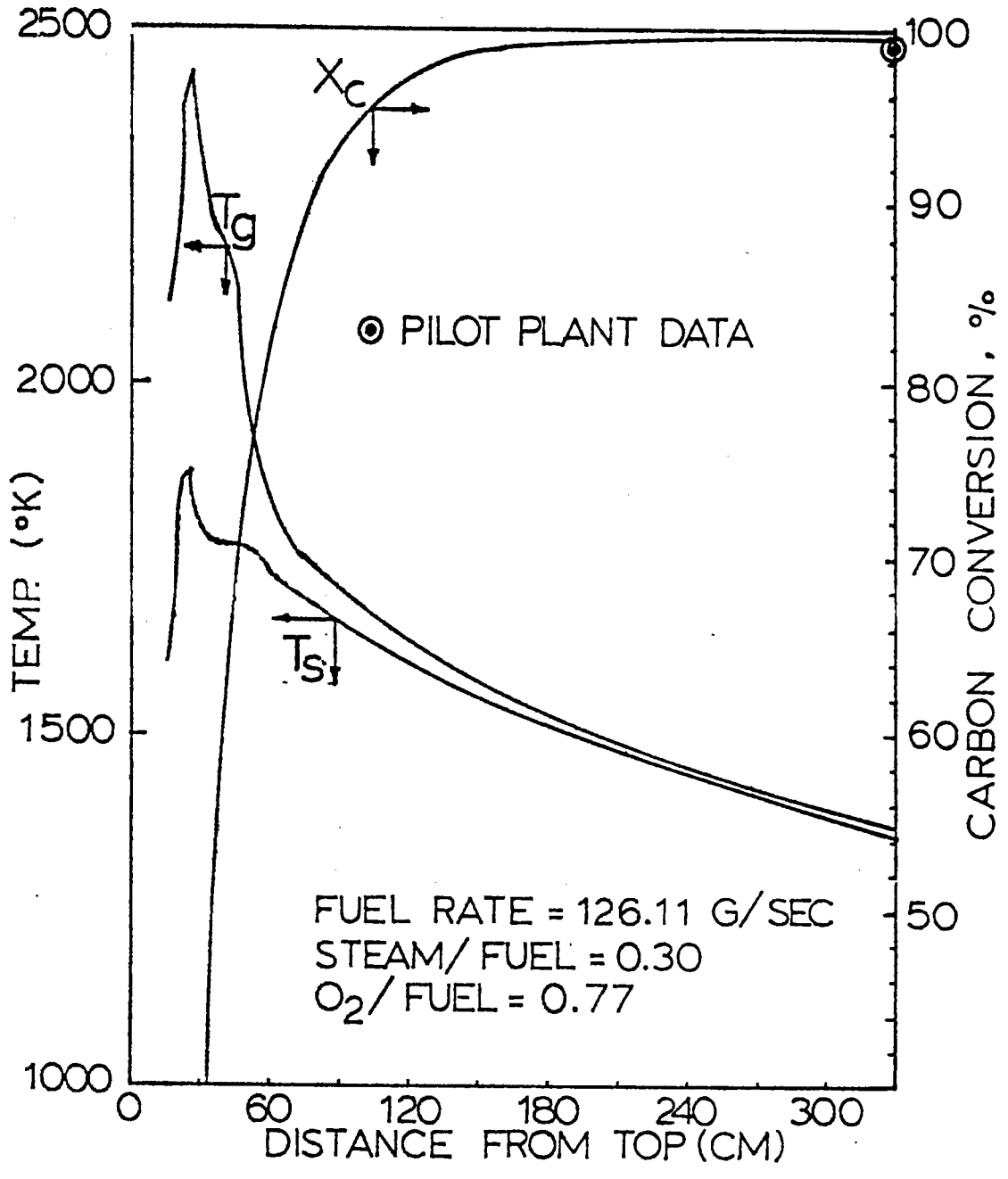

FIGURE 17(A) CALCULATED TEMPERATURE PROFILES AND CARBON CONVERSION PROFILE IN TEXACO PILOT PLANT GASIFIER USING SRC II VACUUM FLASH DRUM BOTTOMS AS FEEDSTOCK

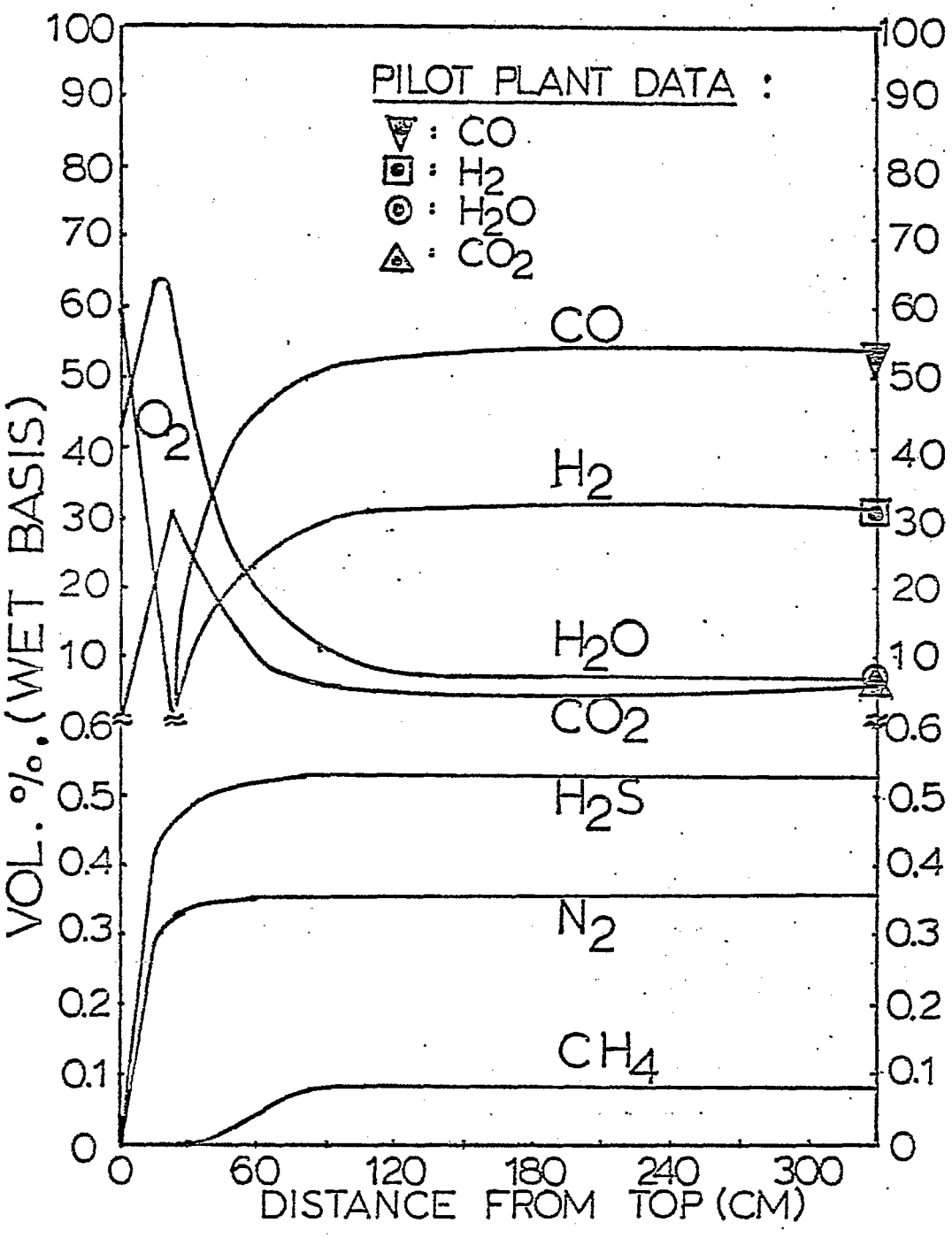

FIGURE 17(B) CALCULATED PRODUCT GAS COMPOSITION PROFILES (WET BASIS) IN TEXACO PILOT PLANT GASIFIER USING SRC II VACUUM FLASH DRUM BOTTOMS AS FEEDSTOCK

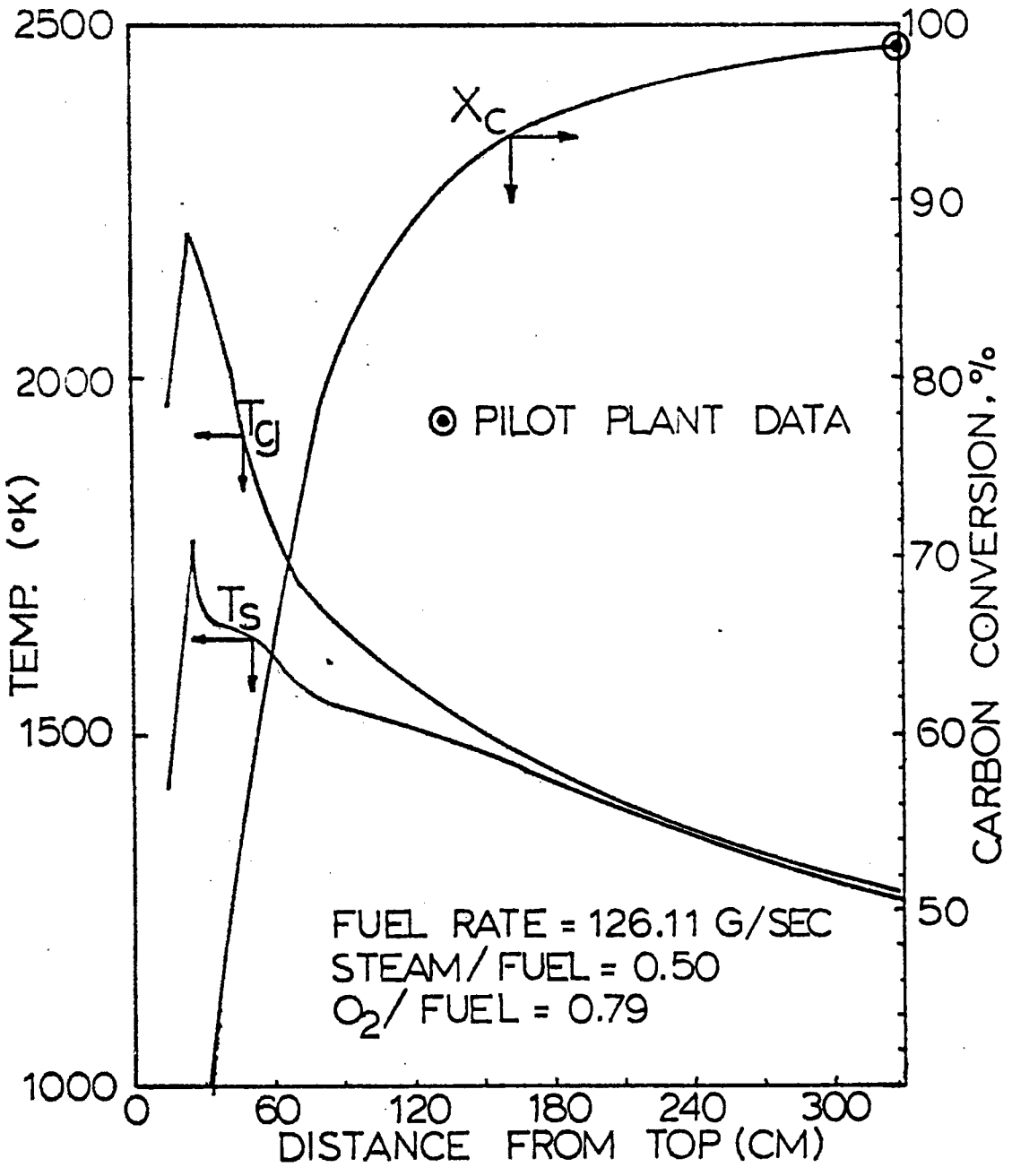

FIGURE 18(A) CALCULATED TEMPERATURE PROFILES AND CARBON CONVERSION PROFILE IN TEXACO PILOT PLANT GASIFIER USING EXXON DSP VACUUM TOWER BOTTOMS AS FEEDSTOCK.

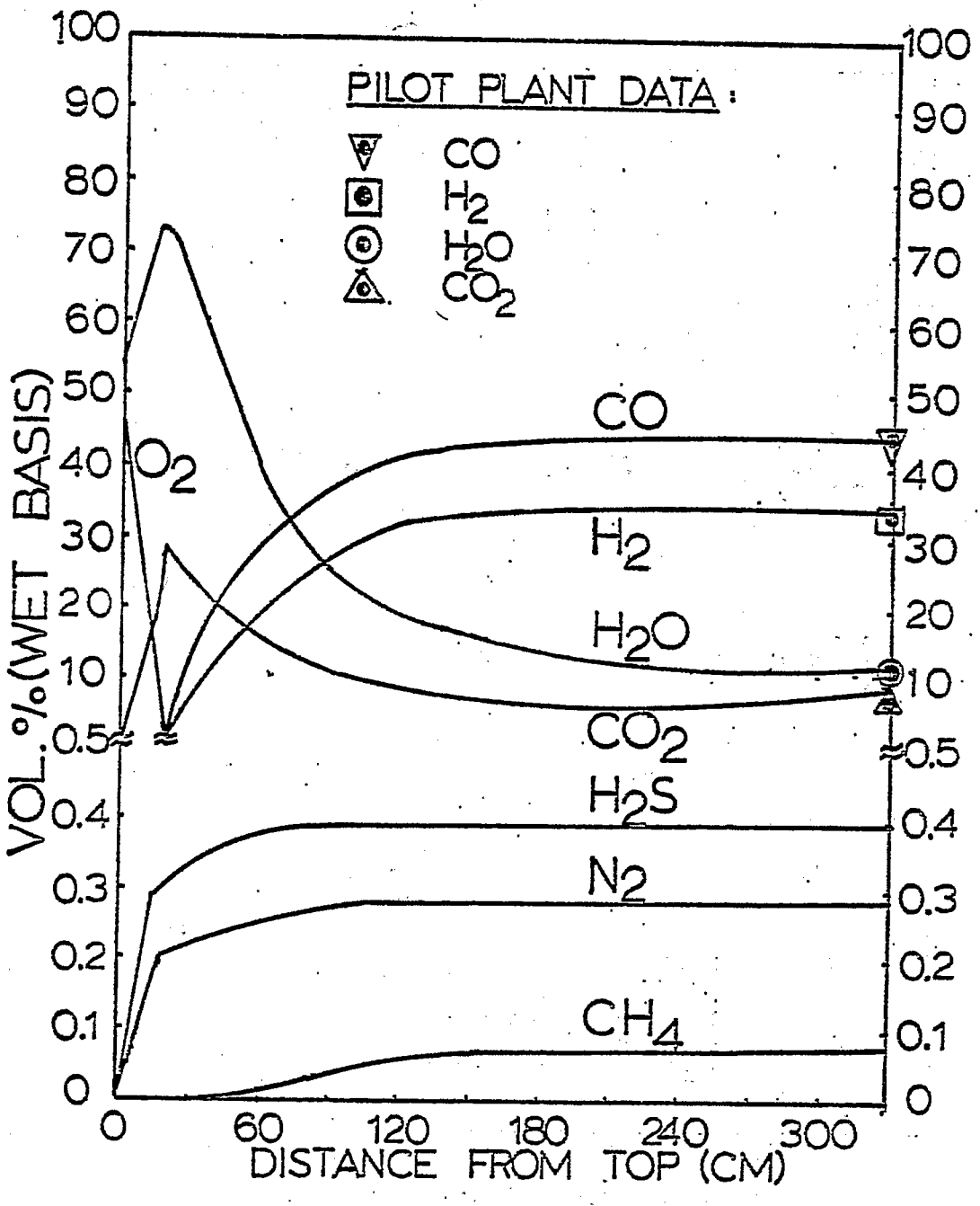

FIGURE 18(B) CALCULATED PRODUCT GAS COMPOSITION PROFILES (WET BASIS) IN TEXACO PILOT PLANT GASIFIER USING EXXON DSP VACUUM TOWER BOTTOMS AS FEEDSTOCK

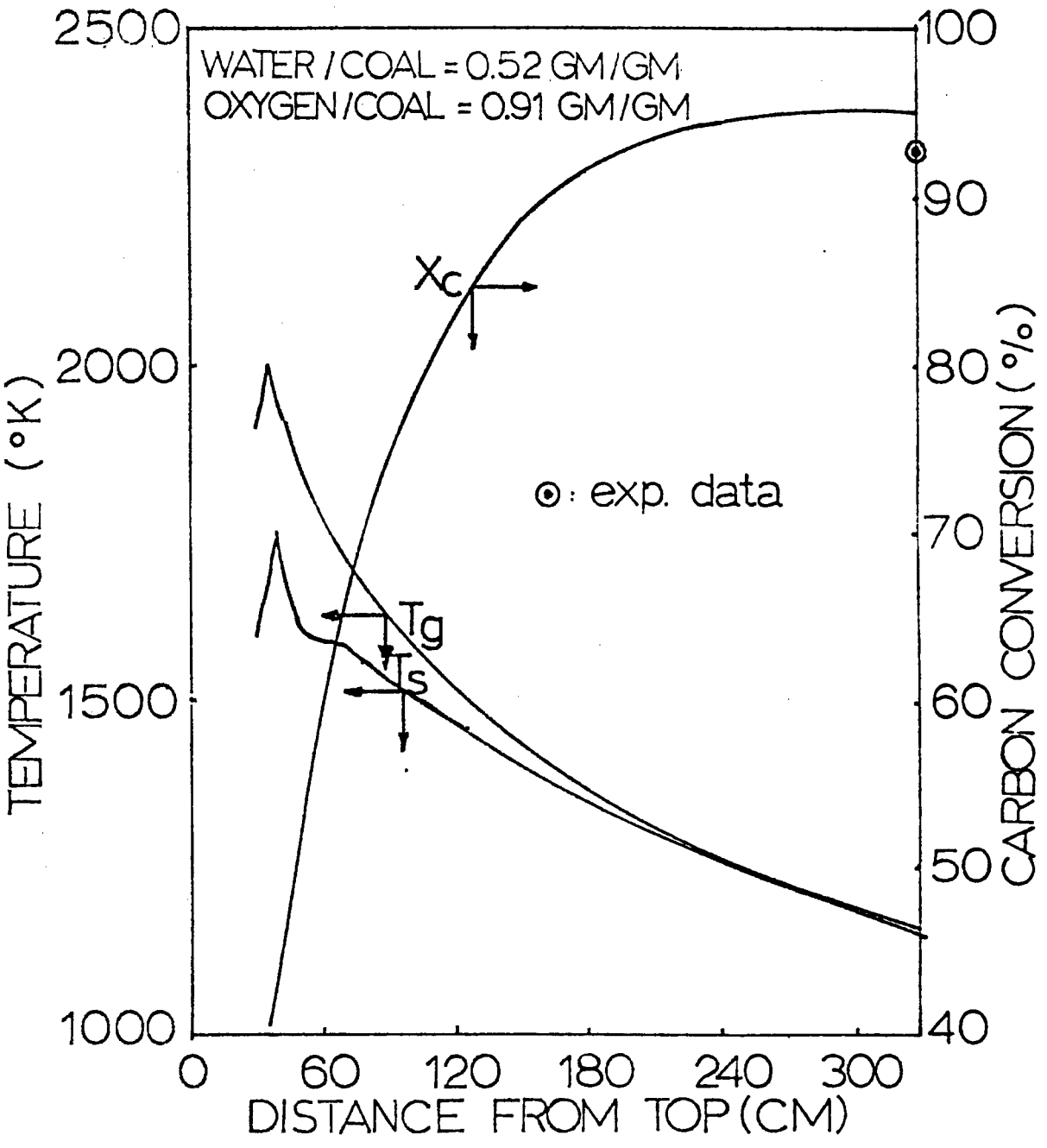

FIGURE 19(A) CALCULATED TEMPERATURE AND CARBON CONVERSION PROFILES IN TEXACO's PILOT PLANT GASIFIER USING WESTERN COAL AS FEEDSTOCK IN COAL-WATER SLURRY RUNS.

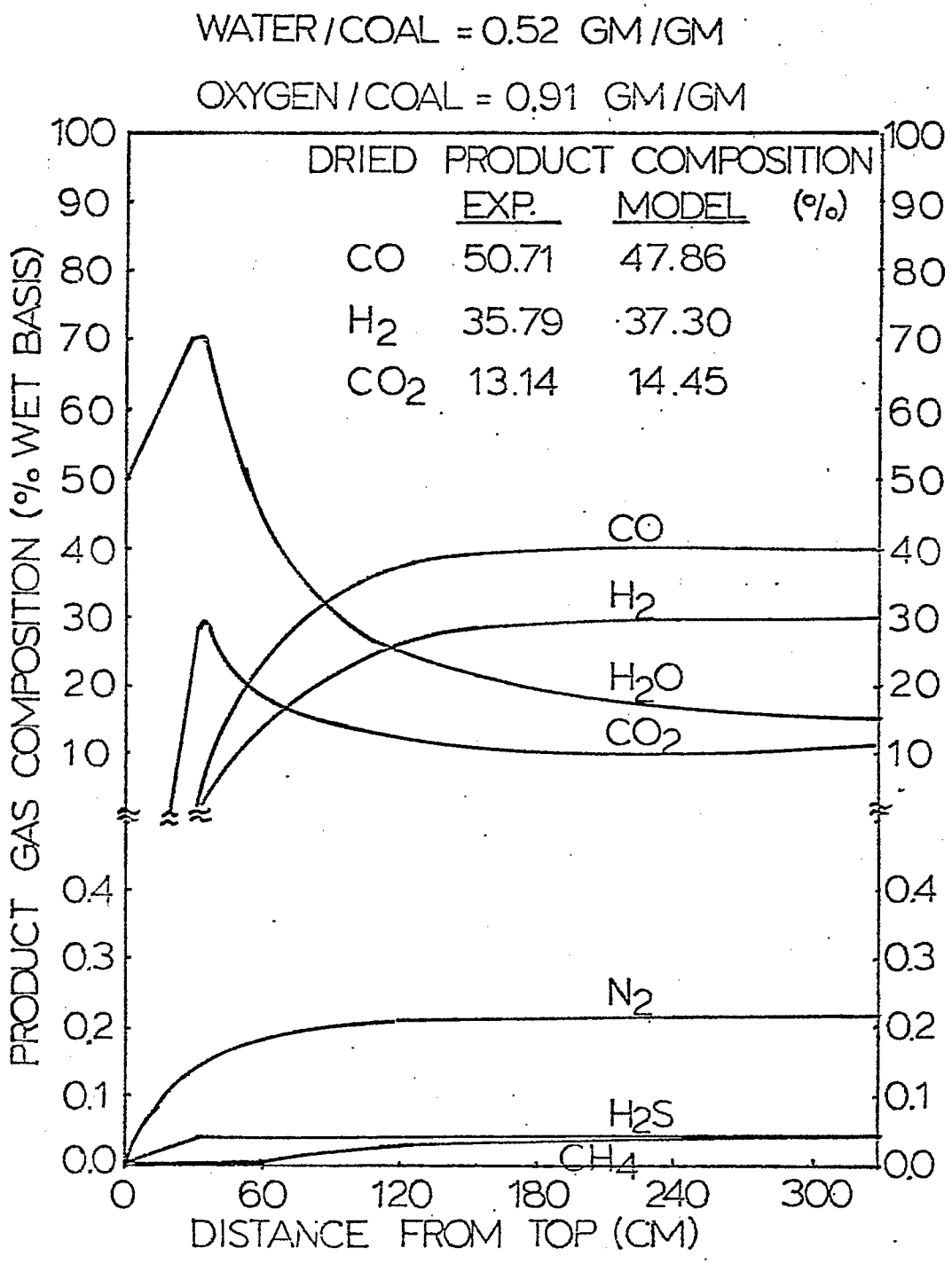

FIGURE 19(B) CALCULATED PRODUCT GAS COMPOSITION PROFILES IN TEXACO's PILOT PLANT GASIFIER USING WESTERN COAL AS FEEDSTOCK IN COAL-WATER SLURRY RUNS.

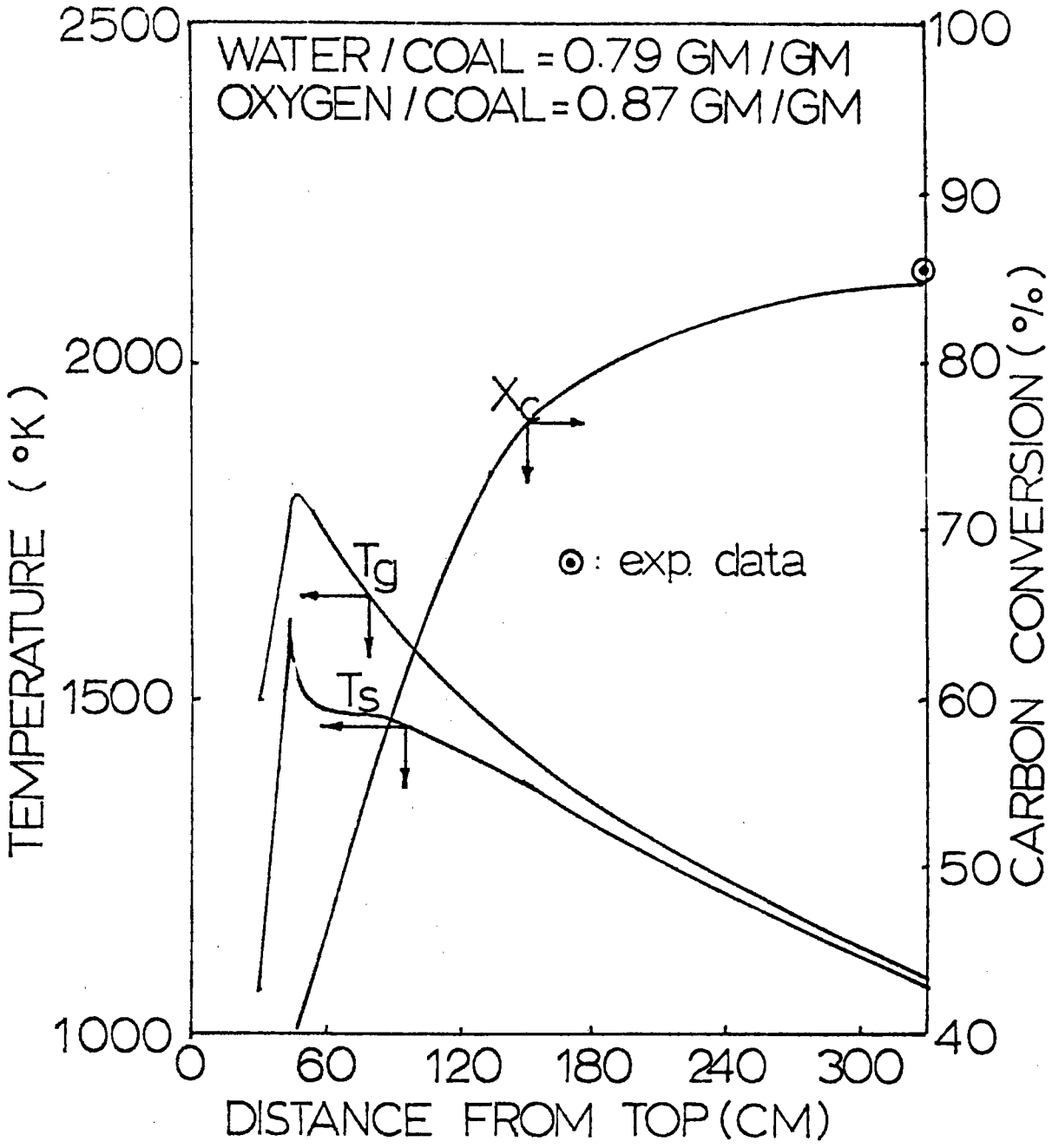

FIGURE 20(A) CALCULATED TEMPERATURE AND CARBON CONVERSION PROFILES IN TEXACO's PILOT PLANT GASIFIER USING EASTERN COAL AS FEEDSTOCK IN COAL-WATER SLURRY RUNS

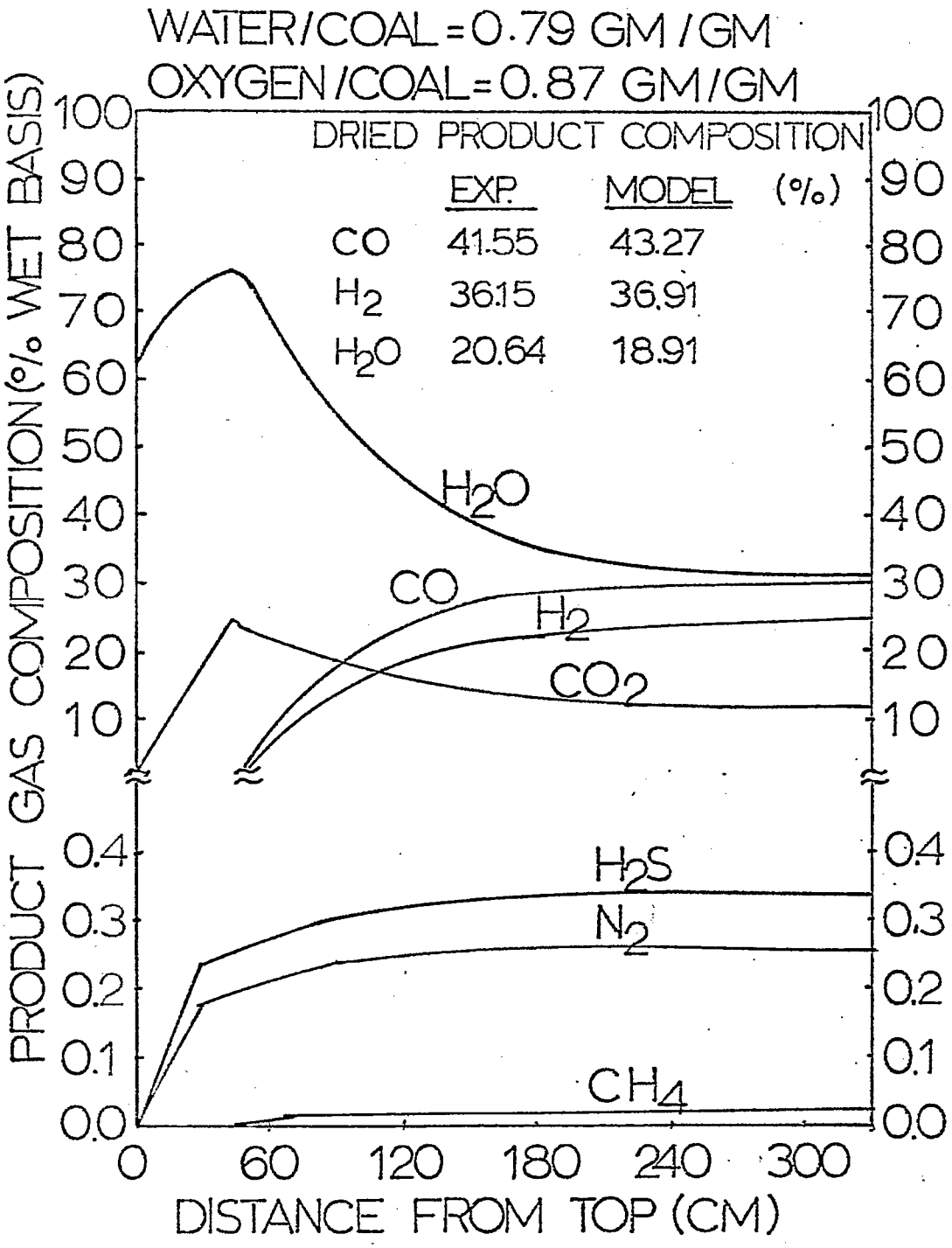

FIGURE 20(B) CALCULATED PRODUCT GAS COMPOSITION PROFILES IN TEXACO's PILOT PLANT GASIFIER USING EASTERN COAL AS FEEDSTOCK IN COAL-WATER SLURRY RUNS

Appendix 6 Comparison of computational results from the model with experimental results from Texaco Entrained Bed Pilot Plant Gasifier.

(A) Using H-Coal residues from Illinois No. 6 coal as feedstock: [1]

Run No.	Input Condition: Fuel Rate (g/sec)	Input Condition: O_2/Fuel	Input Condition: Steam/Fuel	Dry Product gas Source	CO Flow Rate g/sec (Vol. %)	H_2 Flow Rate g/sec (Vol. %)	CO_2 Flow Rate g/sec (Vol. %)	CH_4 Flow Rate g/sec (Vol. %)	H_2S Flow Rate g/sec (Vol. %)	N_2 Flow Rate g/sec (Vol. %)	Carbon Conversion %
I-1	76.66	0.866	0.241	Exp.	123.77 (57.57)	6.01 (39.13)	9.985 (2.95)	0.15 (0.12)	0.133 (0.06)	0.53 (0.12)	98.64
				Model	123.94 (56.60)	6.23 (39.84)	10.04 (2.92)	0.20 (0.16)	0.726 (0.27)	0.454 (0.208)	98.88
I-2	81.18	0.768	0.314	Exp.	112.52 (53.06)	6.211 (41.00)	17.2 (5.15)	0.56 (0.46)	0.59 (0.21)	0.1513 (0.07)	90.66
				Model	119.78 (54.11)	6.54 (41.39)	13.54 (3.89)	0.242 (0.193)	0.57 (0.212)	0.451 (0.204)	93.29
I-3	82.202	0.813	0.309	Exp.	121.5 (54.66)	6.24 (39.31)	19.26 (5.51)	0.114 (0.08)	0.67 (0.26)	0.133 (0.11)	98.28
				Model	126.4 (55.89)	6.36 (39.39)	14.56 (4.10)	0.17 (0.131)	0.77 (0.28)	0.496 (0.22)	99.75
I-4A	79.456	0.807	0.323	Exp.	116.0 (55.70)	5.78 (38.90)	16.74 (5.11)	0.15 (0.12)	0.32 (0.11)	0.0124 (0.00)	97.24
				Model	119.96 (55.18)	6.16 (39.69)	15.73 (4.60)	0.148 (0.12)	0.526 (0.20)	0.437 (0.201)	99.76
I-4B	81.846	0.797	0.310	Exp.	119.54 (54.90)	6.107 (39.26)	18.14 (5.30)	0.185 (0.14)	0.70 (0.23)	0.24 (0.11)	97.34
				Model	125.09 (55.71)	6.36 (39.68)	14.37 (4.07)	0.170 (0.132)	0.538 (0.197)	0.449 (0.20)	99.75
I-5A	71.64	0.8263	0.352	Exp.	103.32 (54.02)	5.30 (38.78)	19.972 (6.64)	0.0852 (0.07)	0.57 (0.21)	0.428 (0.22)	98.875
				Model	106.37 (54.89)	5.39 (38.98)	16.824 (5.525)	0.112 (0.101)	0.68 (0.29)	0.421 (0.217)	99.77
I-5B	65.0	0.817	0.392	Exp.	92.3 (52.48)	5.007 (39.85)	19.987 (7.22)	0.086 (0.08)	0.73 (0.31)	0.0034 (0.00)	98.868
				Model	95.45 (53.56)	5.08 (39.92)	16.58 (5.92)	0.100 (0.098)	0.62 (0.29)	0.386 (0.217)	99.75
I-5C	56.264	0.832	0.429	Exp.	81.853 (51.39)	4.53 (39.83)	20.61 (8.23)	0.0434 (0.04)	0.8035 (0.41)	0.0734 (0.04)	98.885
				Model	81.186 (52.75)	4.38 (39.84)	16.461 (6.81)	0.074 (0.084)	0.546 (0.29)	0.335 (0.218)	99.76

Run No.	Input Condition: Fuel Rate (g/sec)	Input Condition: O_2/Fuel	Input Condition: Steam/Fuel	Dry Product gas Source	CO Flow Rate g/sec (Vol. %)	H_2 Flow Rate g/sec (Vol. %)	CO_2 Flow Rate g/sec (Vol. %)	CH_4 Flow Rate g/sec (Vol. %)	H_2S Flow Rate g/sec (Vol. %)	N_2 Flow Rate g/sec (Vol. %)	Carbon Conversion %
I-6	87.73	0.774	0.291	Exp.	125.2 (55.03)	6.41 (39.43)	17.93 (5.01)	0.27 (0.20)	0.3 (0.10)	0.391 (0.17)	97.122
				Model	129.34 (55.85)	6.54 (39.52)	14.35 (3.94)	0.187 (0.142)	0.89 (0.32)	0.53 (0.23)	97.898
I-7A	90.974	0.7757	0.282	Exp.	130.3 (55.33)	6.67 (39.62)	17.1 (4.62)	0.27 (0.20)	0.292 (0.08)	0.213 (0.09)	96.826
				Model	133.58 (55.63)	6.85 (39.96)	14.20 (3.764)	0.202 (0.147)	0.798 (0.274)	0.555 (0.231)	97.735
I-7B	95.392	0.782	0.267	Exp.	139.75 (55.87)	6.975 (39.03)	17.3 (4.40)	0.197 (0.13)	0.866 (0.26)	0.640 (0.25)	96.992
				Model	141.11 (56.223)	7.08 (39.50)	14.29 (3.622)	0.22 (0.153)	0.829 (0.272)	0.583 (0.232)	96.735
I-8A	92.13	0.797	0.247	Exp.	140.7 (57.38)	6.732 (38.43)	14.27 (3.70)	0.13 (0.09)	0.91 (0.30)	0.102 (0.04)	98.641
				Model	140.09 (57.39)	6.735 (38.63)	12.77 (3.54)	0.213 (0.15)	0.797 (0.27)	0.562 (0.230)	97.744
I-8B	95.07	0.8016	0.239	Exp.	145.8 (57.67)	6.913 (38.28)	14.4 (3.62)	0.058 (0.03)	0.80 (0.25)	0.204 (0.08)	98.663
				Model	143.8 (57.56)	7.853 (38.37)	13.43 (3.42)	0.22 (0.152)	0.82 (0.27)	0.576 (0.23)	97.233
I-8C	92.86	0.800	0.246	Exp.	141.073 (57.02)	6.785 (38.39)	15.28 (3.93)	0.071 (0.04)	1.18 (0.37)	0.46 (0.18)	98.605
				Model	141.709 (57.46)	6.43 (38.58)	12.81 (3.31)	0.213 (0.15)	0.81 (0.27)	0.57 (0.23)	98.229
I-9	87.79	0.787	0.268	Exp.	125.4 (57.49)	5.966 (38.29)	12.89 (3.76)	0.096 (0.07)	0.80 (0.26)	0.148 (0.06)	97.45
				Model	131.20 (56.70)	6.43 (38.885)	13.88 (3.83)	0.189 (0.143)	0.65 (0.23)	0.529 (0.23)	97.60
I-10	129.77	0.8346	0.276	Exp.	201.16 (55.18)	10.22 (39.24)	26.92 (4.69)	0.15 (0.26)	0.58 (0.10)	1.73 (0.47)	99.158
				Model	195.918 (55.42)	9.99 (39.56)	24.76 (4.46)	0.284 (0.140)	0.94 (0.22)	0.672 (0.190)	96.01
I-11	132.79	0.8484	0.279	Exp.	204.16 (54.79)	10.57 (39.72)	29.96 (5.11)	0.193 (0.09)	0.68 (0.12)	0.42 (0.11)	99.187
				Model	199.72 (54.95)	10.30 (39.69)	27.50 (4.82)	0.278 (0.134)	0.977 (0.22)	0.697 (0.19)	96.57

(B) Using H-coal residues from Wyodak coal as feedstock: [1]

Run No.	Input Condition: Fuel Rate (g/sec)	Input Condition: O_2/Fuel	Input Condition: Steam/Fuel	Dry Product gas Source	CO Flow Rate g/sec (Vol. %)	H_2 Flow Rate g/sec (Vol. %)	CO_2 Flow Rate g/sec (Vol. %)	CH_4 Flow Rate g/sec (Vol. %)	H_2S Flow Rate g/sec (Vol. %)	N_2 Flow Rate g/sec (Vol. %)	Carbon Conversion %
W-1	86.0	0.90	0.318	Exp.	143.2 (56.96)	6.8325 (38.04)	19.15 (4.84)	0.0517 (0.03)	0.00 (0.00)	0.19 (0.07)	98.98
				Model	144.1 (56.85)	6.88 (38.00)	17.98 (4.51)	0.58 (0.401)	0.032 (0.010)	0.57 (0.224)	99.75
W-2	87.231	0.859	0.286	Exp.	146.25 (57.67)	6.865 (37.90)	17.1 (4.29)	0.0898 (0.06)	0.0325 (0.00)	0.078 (0.03)	99.17
				Model	148.44 (58.65)	6.741 (37.30)	13.40 (3.37)	0.656 (0.453)	0.028 (0.009)	0.547 (0.216)	99.65
W-3A	128.49	0.844	0.253	Exp.	212.71 (57.80)	9.85 37.47)	25.66 (4.43)	0.22 (0.10)	0.00 (0.00)	0.553 (0.15)	99.393
				Model	212.77 (59.20)	9.45 (36.81)	19.51 (3.454)	0.558 (0.272)	0.088 (0.020)	0.91 (0.251)	97.90
W-3B	128.67	0.86	0.264	Exp.	208.2 (56.02)	10.05 (37.02)	34.016 (5.82)	0.129 (0.06)	0.103 (0.01)	0.68 (0.18)	99.395
				Model	214.8 (58.97)	10.85 (36.86)	21.38 (3.75)	0.303 (0.146)	0.089 (0.020)	0.96 (0.262)	98.85
W-4	125.66	0.857	0.273	Exp.	211.44 (57.61)	10.06 (37.77)	23.77 (4.12)	0.28 (0.13)	0.00 (0.00)	1.20 (0.32)	98.765
				Model	210.58 (58.46)	9.56 (37.16)	20.22 (3.57)	4.215 (0.59)	0.0066 (0.002)	0.769 (0.213	98.215
W-5	129.826	0.854	0.263	Exp.	215.34 (57.00)	10.343 (38.32)	25.45 (4.28)	0.34 (0.15)	0.032 (0.00)	0.734 (0.19)	98.211
				Model	214.78 (57.95)	10.08 (37.56)	21.09 (3.62)	1.32 (0.625)	0.0615 (0.014)	0.837 (0.227)	97.66
W-6	132.82	0.855	0.318	Exp.	215.07 (54.91)	10.97 (39.20)	33.84 (5.49)	0.41 (0.18)	0.00 (0.00)	0.706 (0.18)	97.900
				Model	217.46 (56.17)	10.60 (38.34)	27.65 (4.55)	1.60 (0.762)	0.042 (0.009)	0.837 (0.236)	98.283
W-7	135.64	0.94	0.310	Exp.	220.02 (54.24)	11.00 (37.98)	48.576 (7.62)	0.00 (0.00)	0.00 (0.00)	0.477 (0.11)	99.676
				Model	228.74 (57.23)	10.56 (37.01)	31.12 (5.43)	0.234 (0.105)	0.0072 (0.001)	0.917 (0.229)	99.628

(C) Using SRC II Vaccum Flash Drum Bottoms as Feedstock: [2]

Input Condition			Wet Product Gas / Source	CO	H_2	CO_2	H_2O	CH_4	H_2S	N_2	Carbon Conversion %
Fuel Rate (g/sec)	$\frac{O_2}{Fuel}$	$\frac{Steam}{Fuel}$		Flow Rate g/sec (Vol. %)	Flow Rate g/sec (Vol. %)	Flow Rate g/sec (Vol. %)	Flow Rate g/sec (Vol. %)	Flow Rate g/sec (Vol. %)	Flow Rate g/sec (Vol. %)	Flow Rate g/sec (Vol. %)	
126.11	0.77	0.30	Exp.	167.584 (53.5)	6.936 (31.0)	32.98 (6.7)	14.50 (7.2)	0.00 (0.00)	4.1 (1.04)	1.566 (0.50)	99
			Model	171.48 (54.01)	7.178 (31.65)	29.54 (5.9)	15.19 (7.44)	0.151 (0.083)	2.016 (0.52)	1.146 (0.361)	99.77

(D) Using Exxon DSP Vaccum Tower Bottoms as feedstock: [2]

126.11	0.79	0.50	Exp.	176.98 (45.6)	9.37 (33.8)	45.87 (7.52)	29.69 (11.9)	0.00 (0.00)	3.81 (0.78)	1.475 (0.38)	99
			Model	175.36 (44.87)	9.57 (34.99)	47.82 (7.74)	29.14 (11.6)	0.173 (0.077)	1.857 (0.39)	1.089 (0.279)	99.00

(E) Coal-Water Slurry Runs:

Coal Type	Input Conditions			Dry Product Gas / Source	CO	H_2	CO_2	CH_4	H_2S	N_2	Carbon Conversion %
	Coal Rate (g/sec)	$\frac{O_2}{Coal}$	$\frac{Water}{Coal}$		Vol. %	Vol. %	Vol. %	Vol. %	Vol. %	Vol. %	
Western	186.78	0.91	0.51	Exp.	50.71	35.79	13.14	0.09	0.03	0.24	92.7
				Model	47.86	37.30	14.45	0.055	0.074	0.26	94.87
Eastern	133.5	0.87	0.79	Exp.	41.55	36.15	20.64	0.40	0.85	0.38	85.8
				Model	43.27	36.91	18.91	0.036	0.50	0.373	84.66

Appendix 7. Parameter studies of the reactor performance at various operation conditions.

Figure 19-Figure 28 show the effects of feeding ratios, oxygen/fuel and steam/fuel, on the carbon conversion and the major product gas composition in the Texaco Downflow Entrained Bed Pilot Plant Gasifier.

Figure 29-Figure 33 show the effects of total pressure on the carbon conversion and the major product gas composition in the Texaco Downflow Entrained Bed Pilot Plant Gasifier.

Figure 34 shows the effects of fuel particle size on the fuel residence time and the carbon conversion in the Texaco Downflow Entrained Bed Pilot Plant Gasifier.

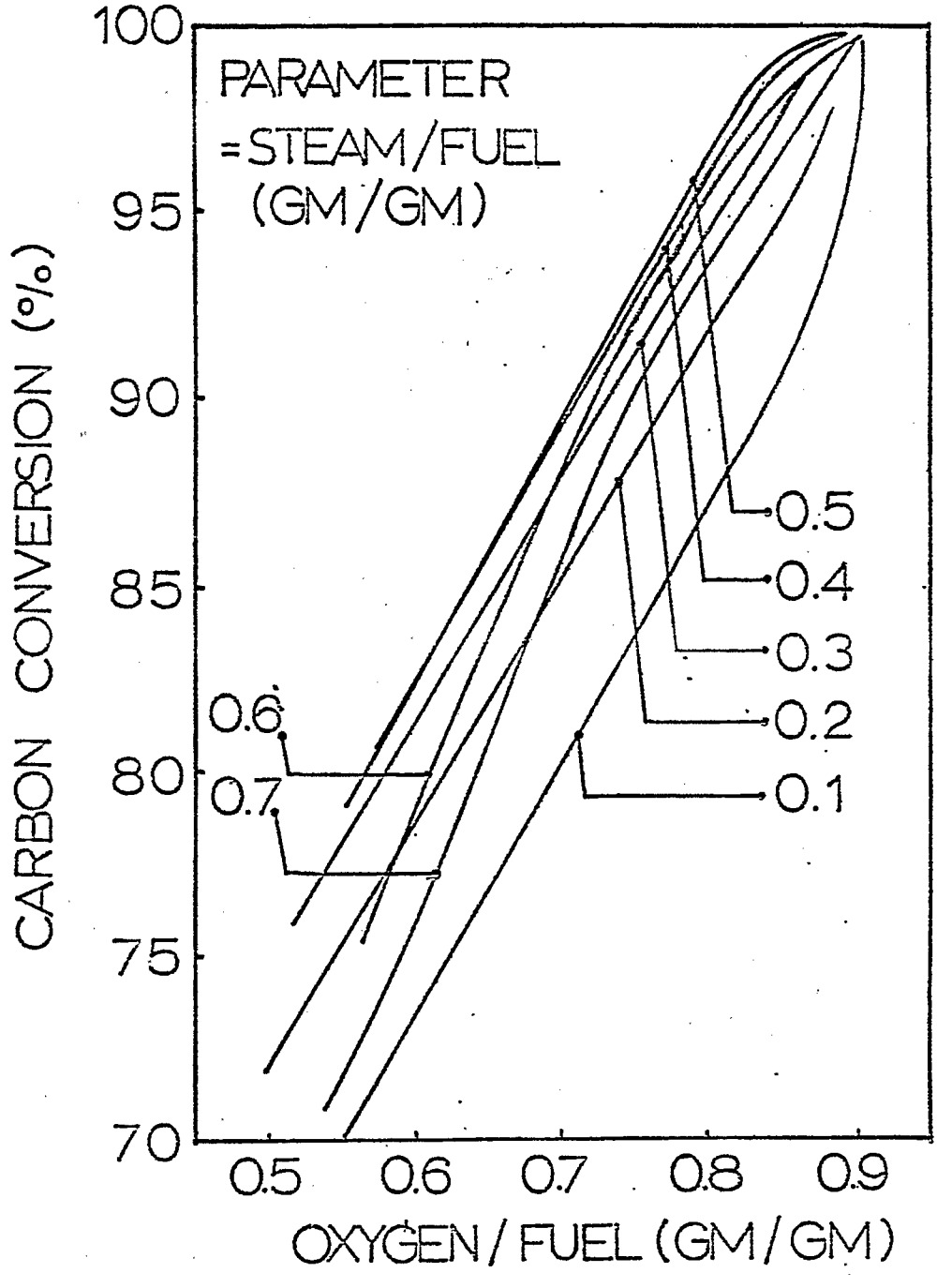

FIGURE 21. EFFECT OF OXYGEN/FUEL RATIO ON THE CARBON CONVERSION AT VARIOUS STEAM/FUEL RATIOS FEEDING THE H-COAL RESIDUE FROM ILLINOIS NO. 6 COAL IN THE TEXACO PILOT PLANT GASIFIER

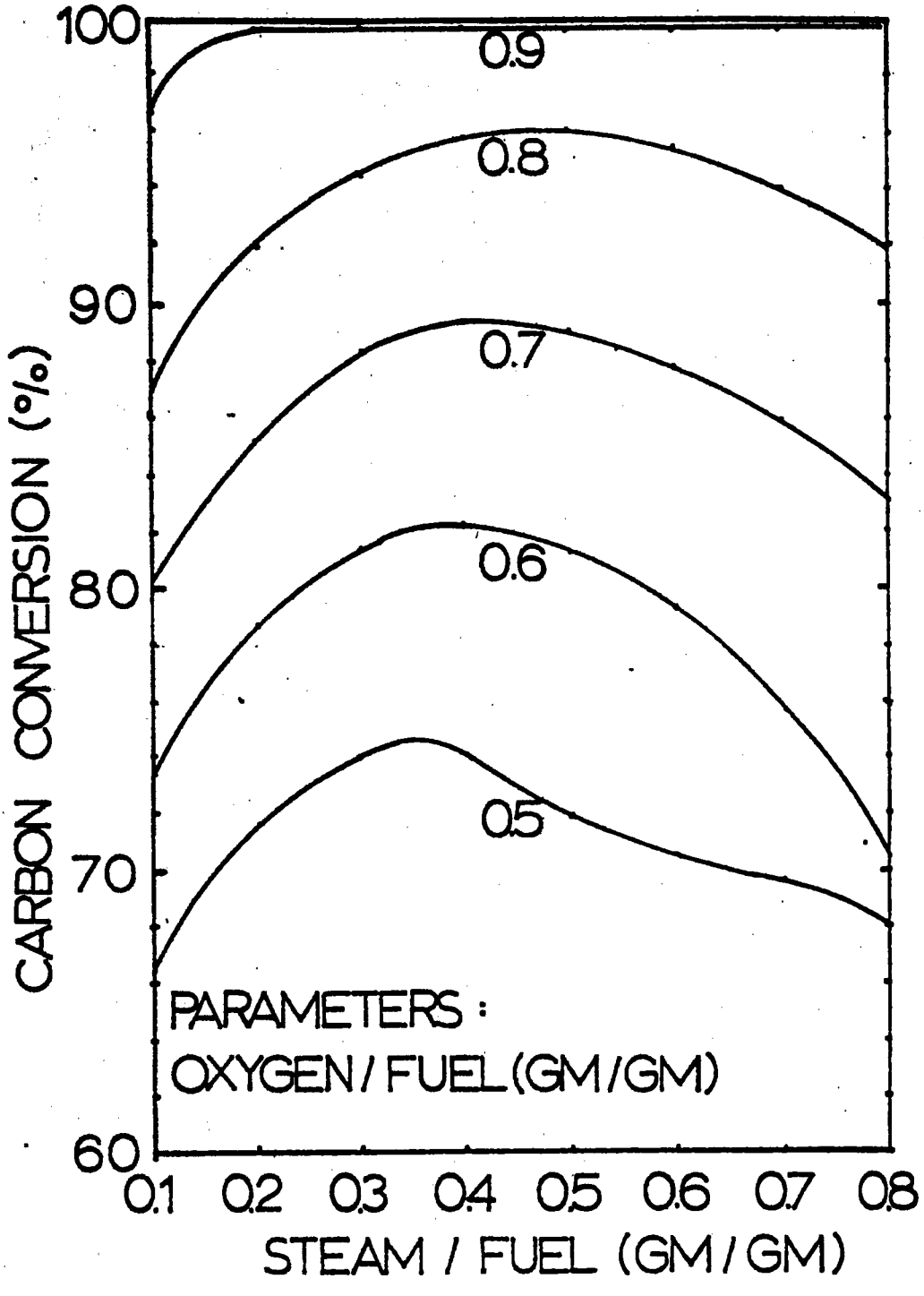

FIGURE 22 EFFECT OF STEAM/FUEL RATIO ON THE CARBON CONVERSION AT VARIOUS OXYGEN/FUEL RATIOS FEEDING THE H-COAL RESIDUE FROM ILLINOIS NO. 6 COAL IN THE TEXACO PILOT PLANT GASIFIER

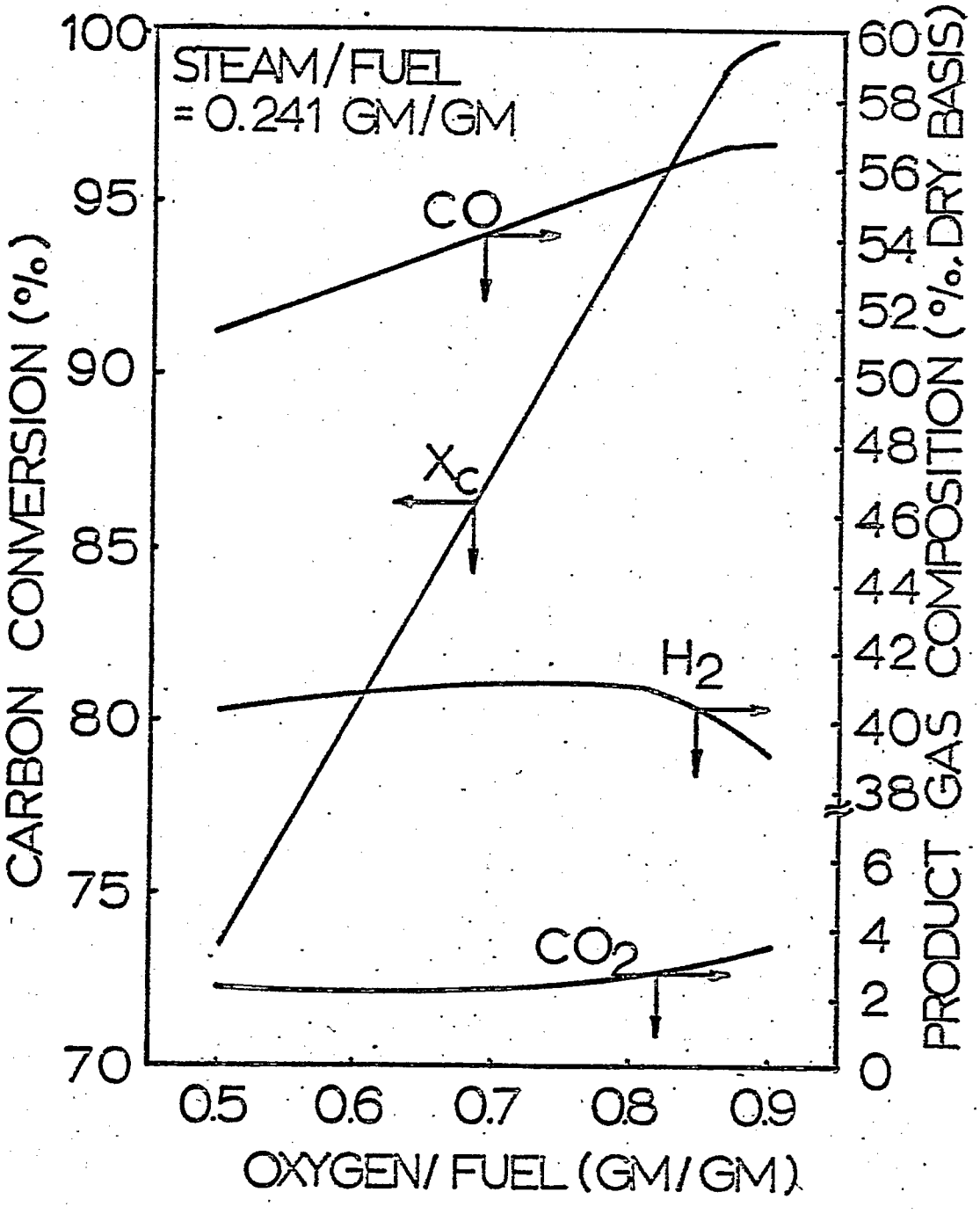

FIGURE 23. EFFECTS OF OXYGEN/FUEL RATIO ON THE CARBON CONVERSION AND THE MAJOR PRODUCT GAS COMPOSITION AT STEAM/FUEL = 0.241 GM/GM (I-1 RUN) FEEDING H-COAL RESIDUE FROM ILLINOIS NO. 6 COAL IN THE TEXACO PILOT PLANT GASIFIER

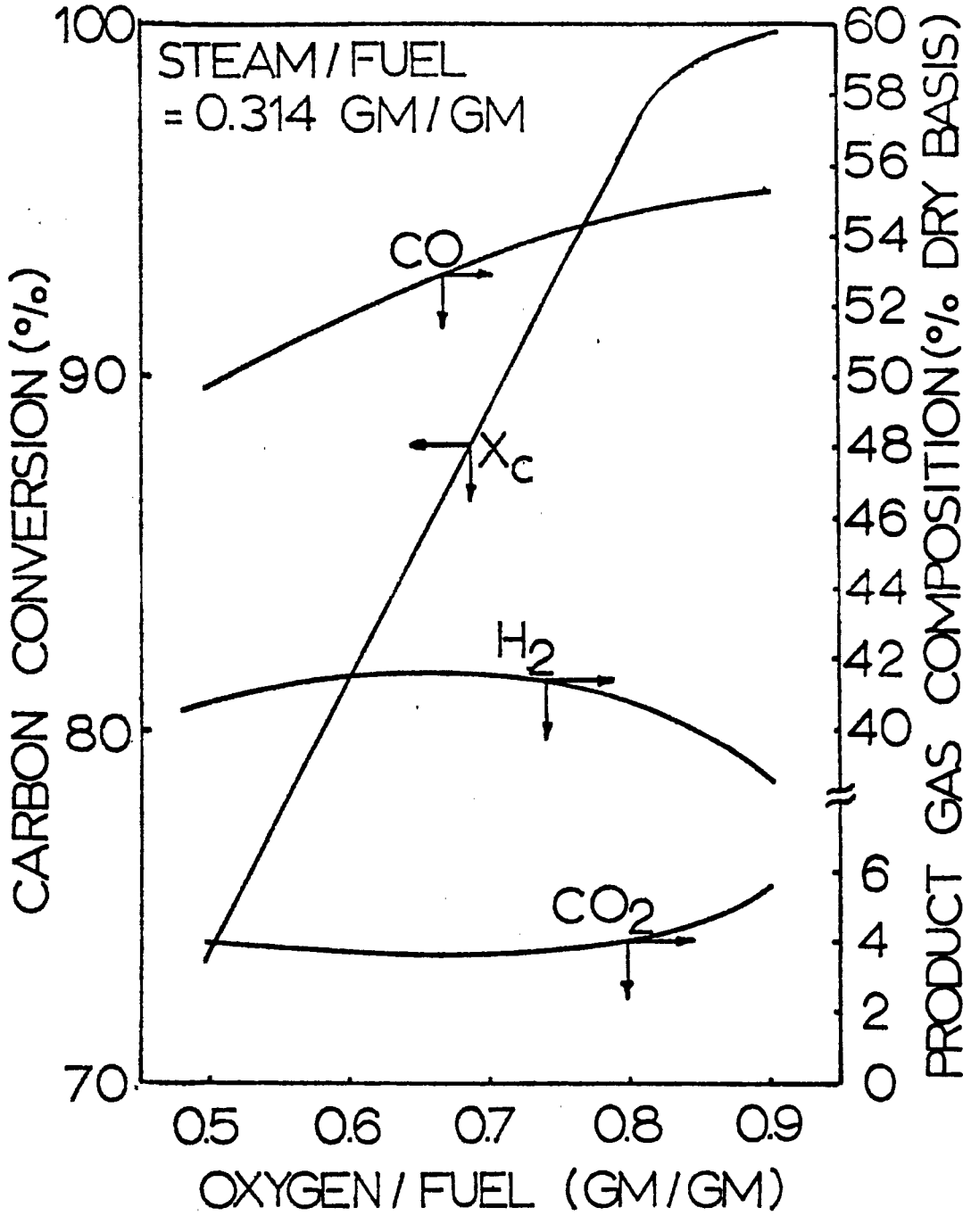

FIGURE 24 EFFECTS OF OXYGEN/FUEL RATIO ON THE CARBON CONVERSION AND THE MAJOR PRODUCT GAS COMPOSITION AT STEAM/FUEL = 0.314 GM/GM (I-2 RUN) FEEDING H-COAL RESIDUE FROM ILLINOIS NO. 6 COAL IN THE TEXACO PILOT PLANT GASIFIER.

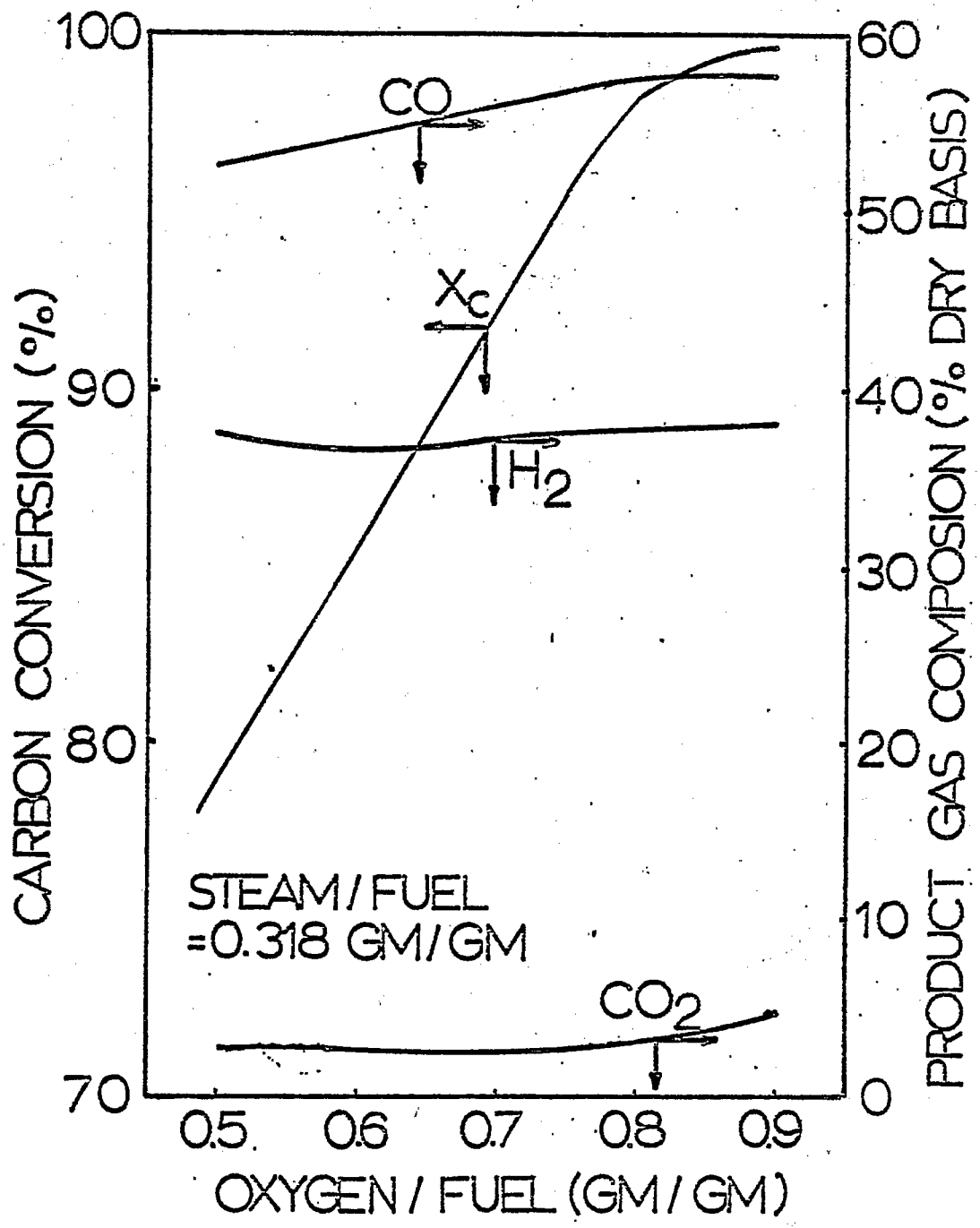

FIGURE 25 EFFECTS OF OXYGEN/FUEL RATIO ON THE CARBON CONVERSION AND THE MAJOR PRODUCT GAS COMPOSITION AT STEAM/FUEL = 0.318 GM/GM (W-1 RUN) FEEDING H-COAL RESIDUE FROM WYODAK COAL IN THE TEXACO PILOT PLANT GASIFIER

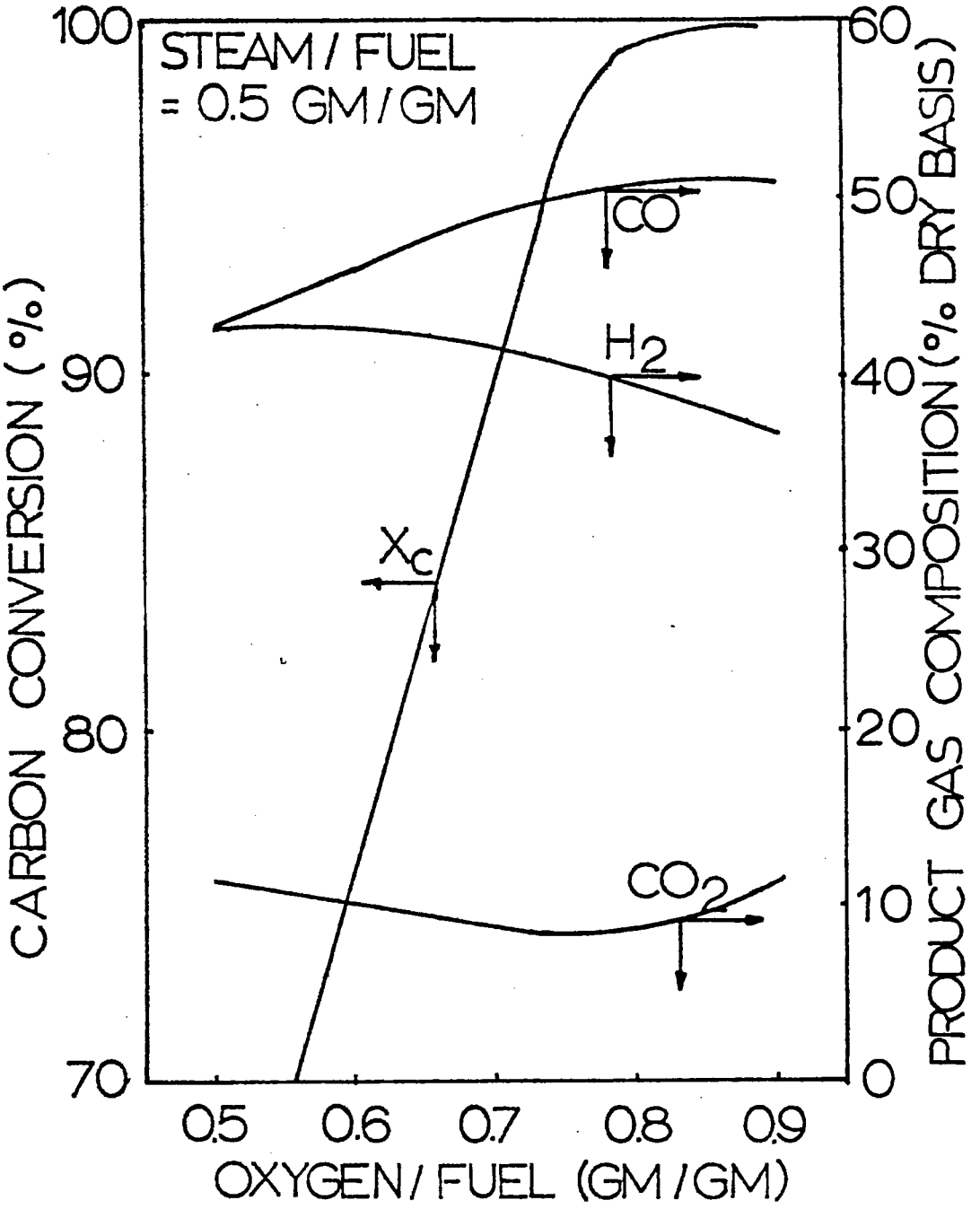

FIGURE 26 EFFECTS OF OXYGEN/FUEL RATIO ON THE CARBON CONVERSION AND THE MAJOR PRODUCT GAS COMPOSITION AT STEAM/FUEL = 0.5 GM/GM FEEDING COAL RESIDUES FROM EXXON DSP VACCUM TOWER BOTTOMS IN THE TEXACO PILOT PLANT GASIFIER

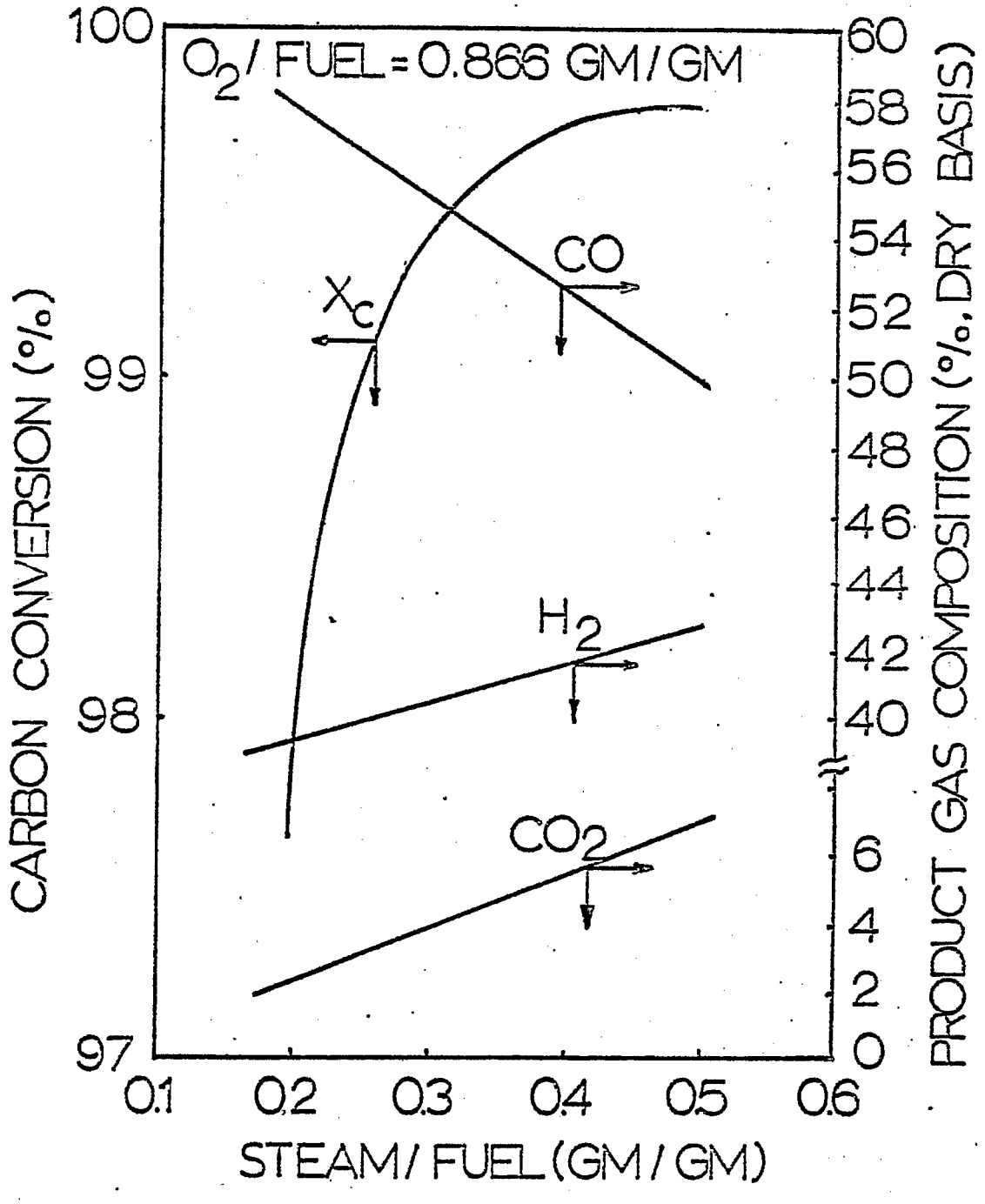

FIGURE 27 EFFECTS OF STEAM/FUEL RATIO ON THE CARBON CONVERSION AND THE MAJOR PRODUCT GAS COMPOSITION AT OXYGEN/FUEL = 0.866 GM/GM (I-7 RUN) FEEDING H-COAL RESIDUE FROM ILLINOIS NO. 6 COAL IN THE TEXACO PILOT PLANT GASIFIER

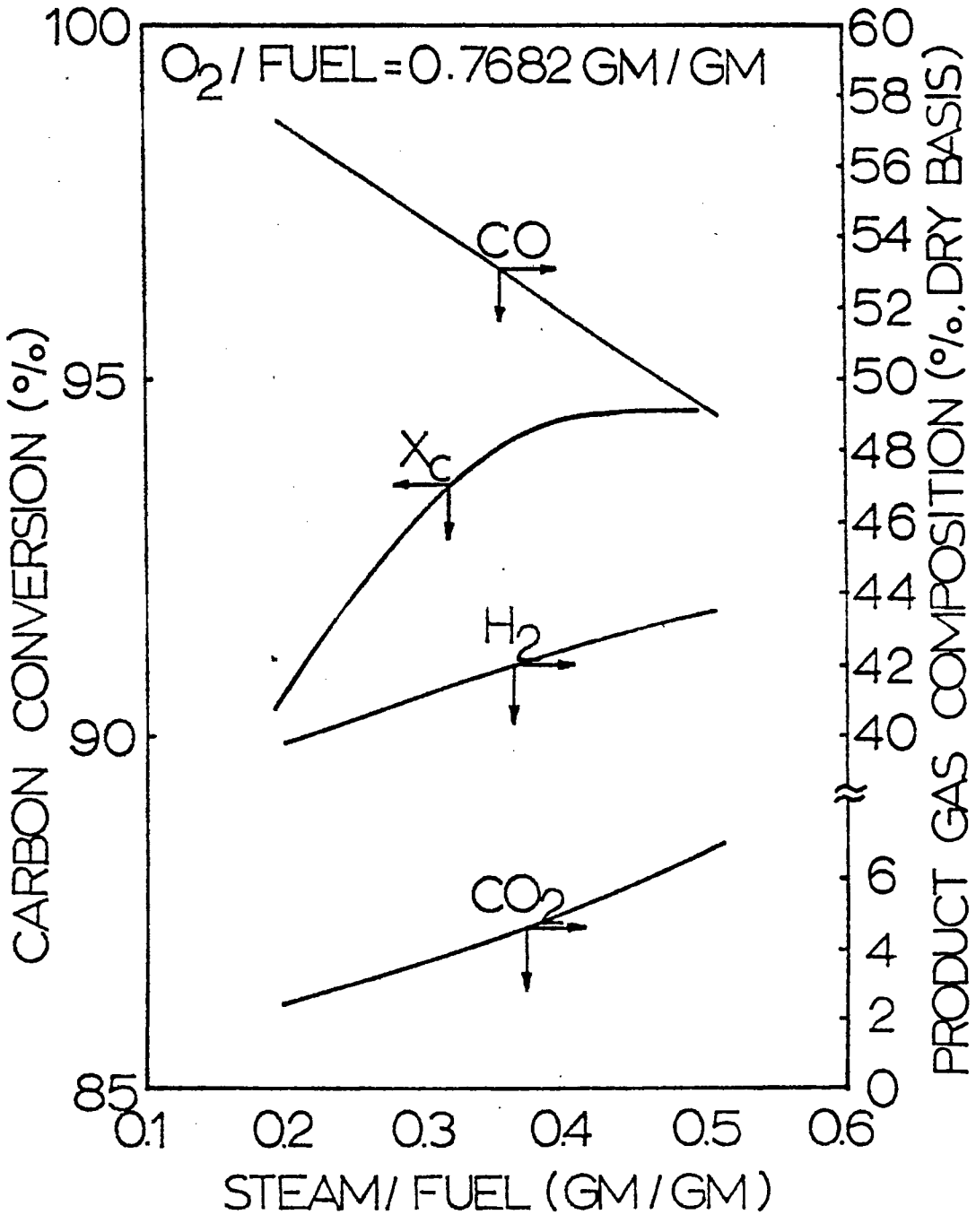

FIGURE 28 EFFECTS OF STEAM/FUEL RATIO ON THE CARBON CONVERSION AND THE MAJOR PRODUCT GAS COMPOSITION AT OXYGEN/FUEL = 0.7682 GM/GM (I-2 RUN) FEEDING H-COAL RESIDUE FROM ILLINOIS NO. 6 COAL IN THE TEXACO PILOT PLANT GASIFIER

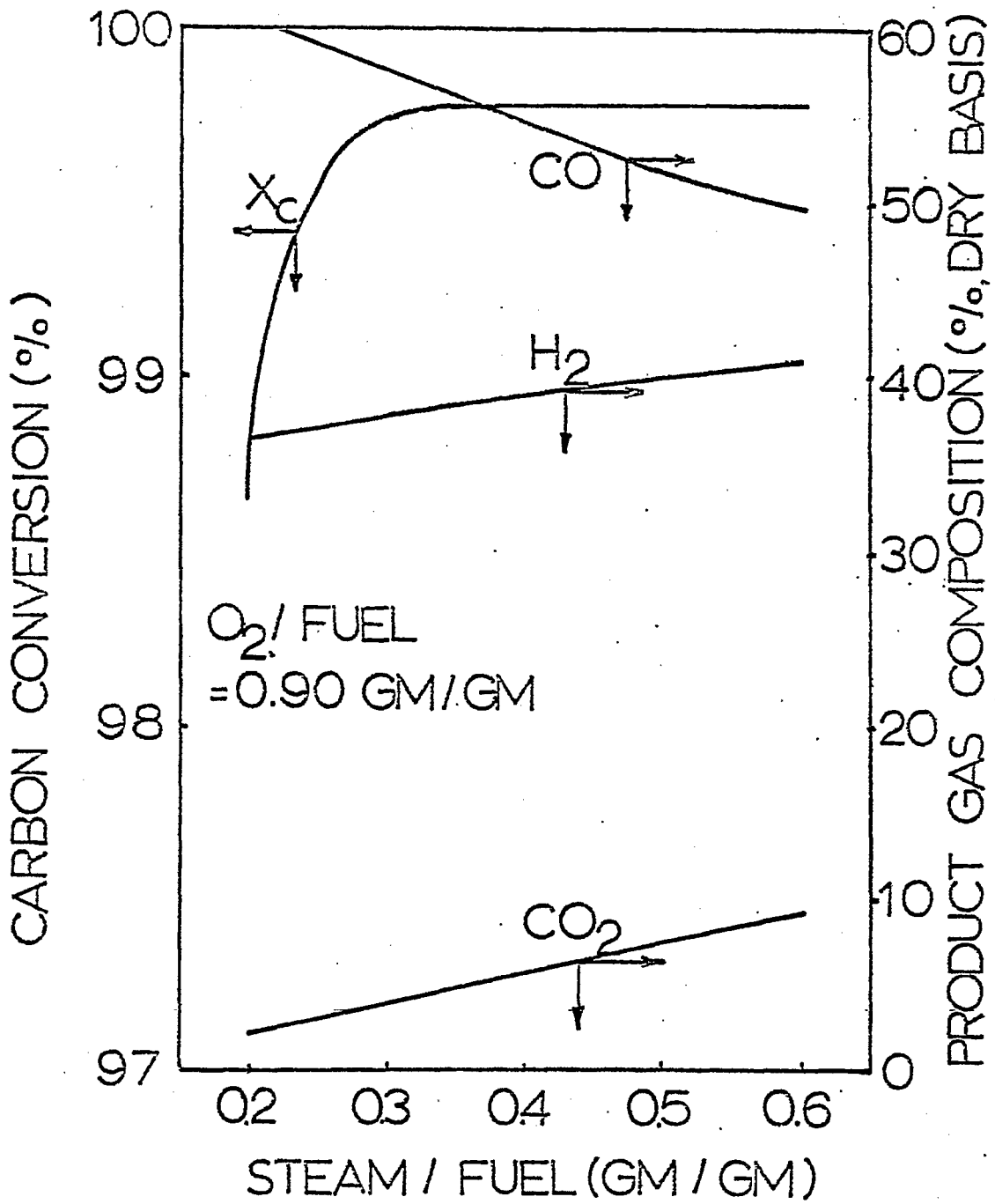

FIGURE 29 EFFECTS OF STEAM/FUEL RATIO ON THE CARBON CONVERSION AND THE MAJOR PRODUCT COMPOSITION AT OXYGEN/FUEL = 0.90 GM/GM (W-1 RUN) FEEDING H-COAL RESIDUE FROM WYODAK COAL IN THE TEXACO PILOT PLANT GASIFIER

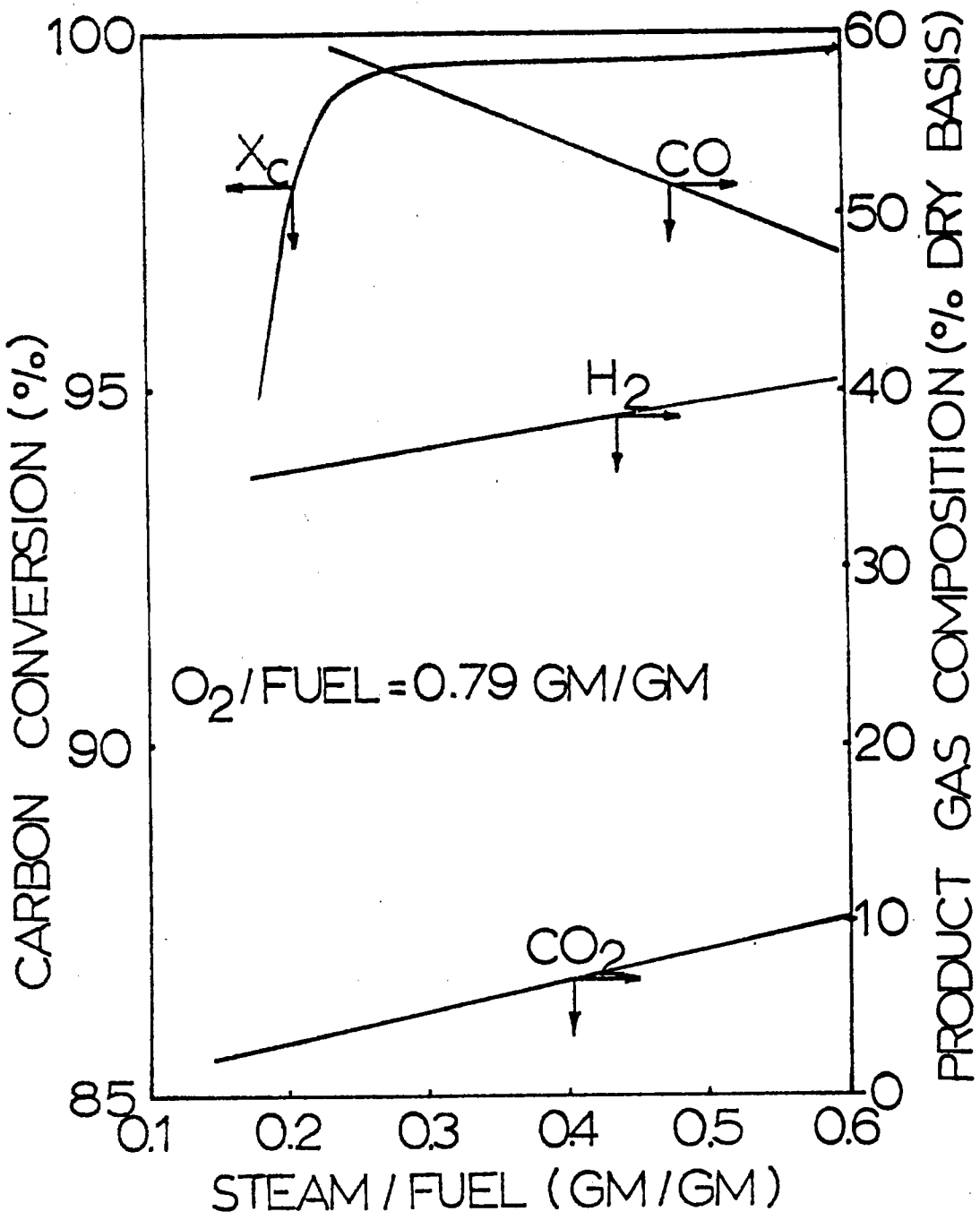

FIGURE 30 EFFECTS OF STEAM/FUEL RATIO ON THE CARBON CONVERSION AND THE MAJOR PRODUCT COMPOSITION AT OXYGEN/FUEL = 0.79 GM/GM FEEDING COAL RESIDUES FROM EXXON DSP VACCUM TOWER BOTTOMS IN THE TEXACO PILOT PLANT GASIFIER

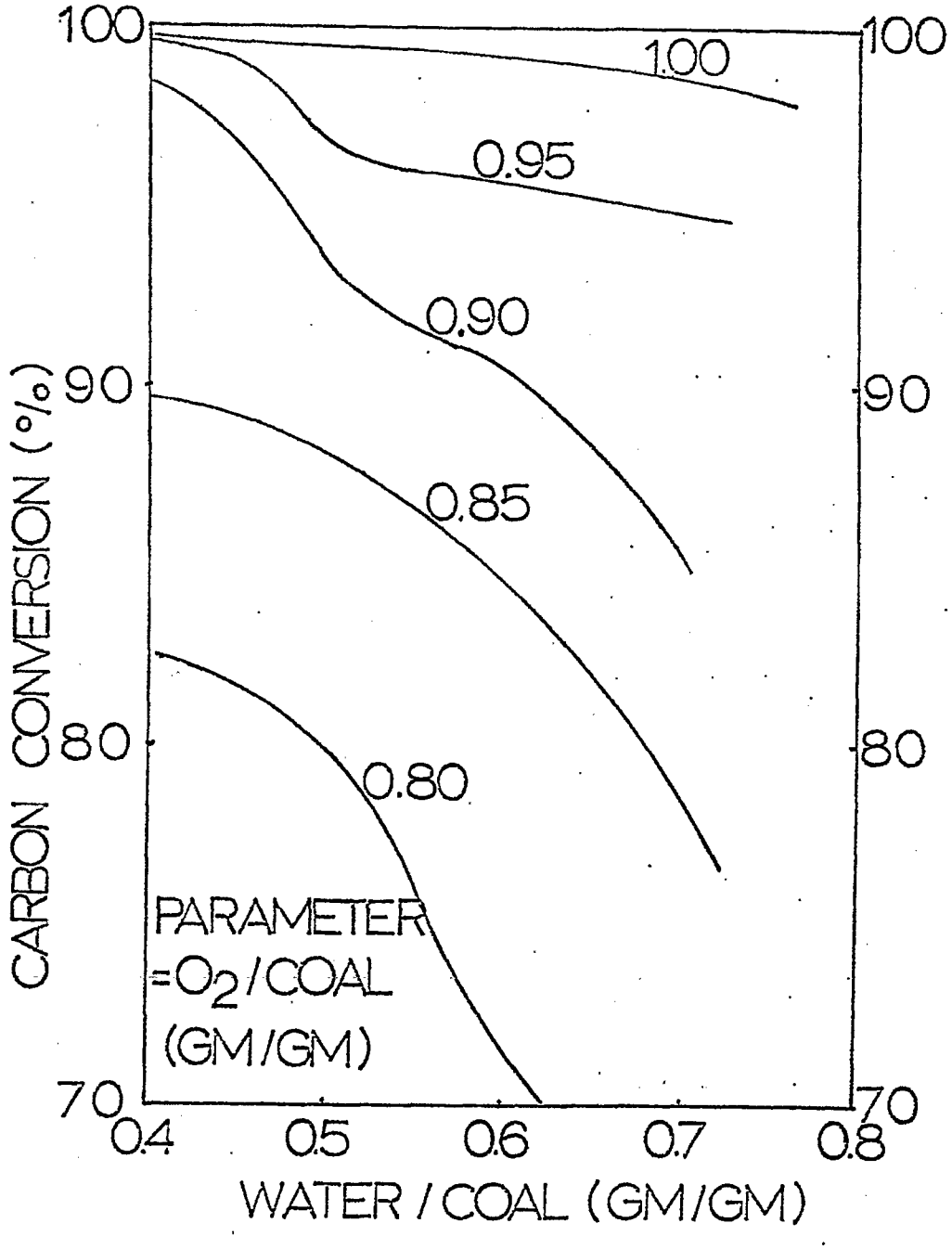

FIGURE 31 EFFECT OF WATER/COAL RATIO ON CARBON CONVERSION AT VARIOUS OXYGEN/COAL RATIO FEEDING WESTERN COAL TEXACO's PILOT PLANT GASIFIER IN COAL-WATER SLURRY RUNS.

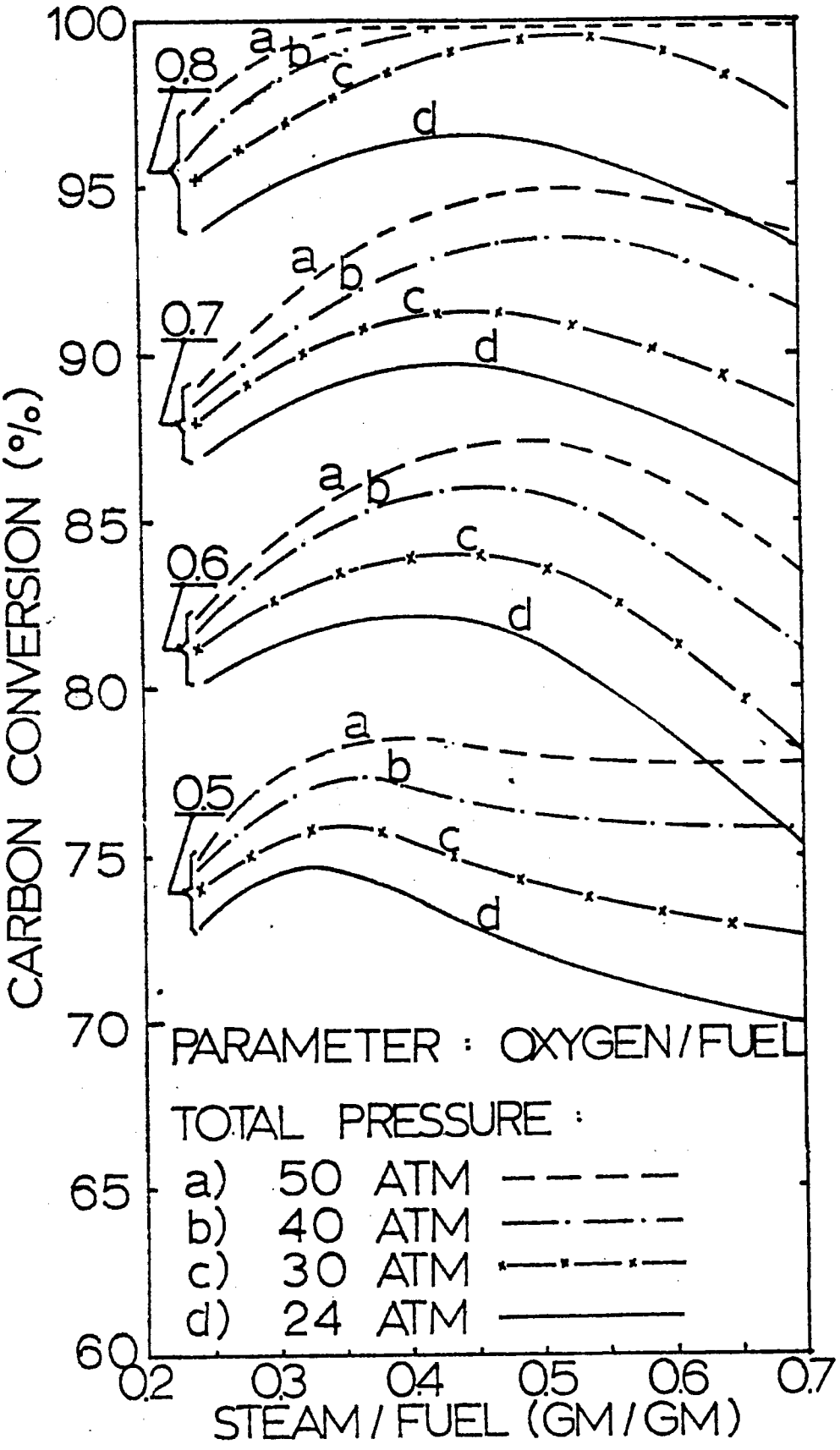

FIGURE 32. EFFECT OF TOTAL PRESSURE ON CARBON CONVERSION AT VARIOUS FEEDING RATIOS USING H-COAL RESIDUE FROM ILLINOIS NO. 6 COAL IN THE TEXACO PILOT PLANT GASIFIER

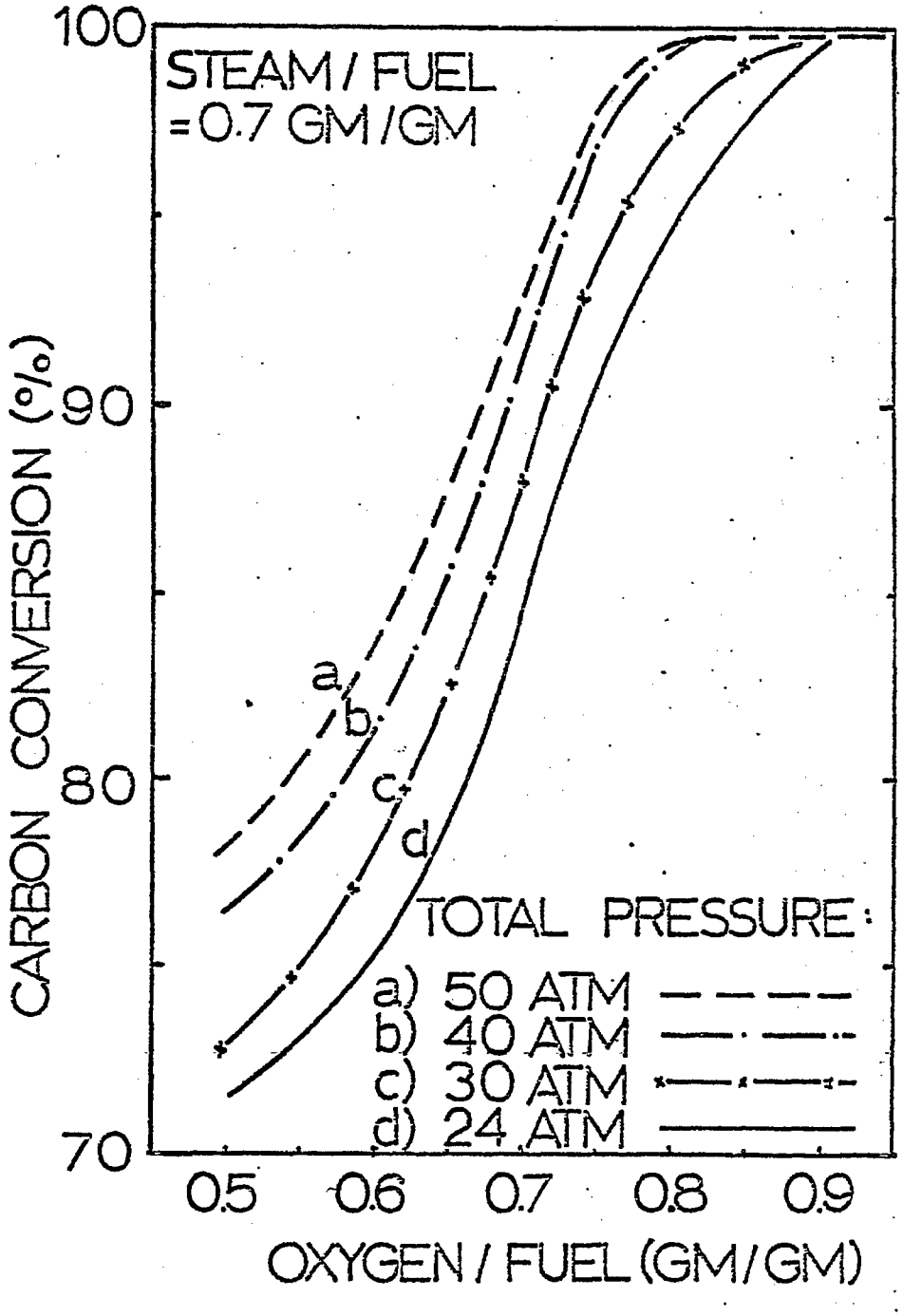

FIGURE 33 EFFECT OF TOTAL PRESSURE ON CARBON CONVERSION AT VARIOUS OXYGEN/FUEL RATIOS WITH STEAM/FUEL = 0.7 GM/GM FEEDING H-COAL RESIDUE FROM ILLINOIS NO. 6 COAL IN THE TEXACO PILOT PLANT GASIFIER.

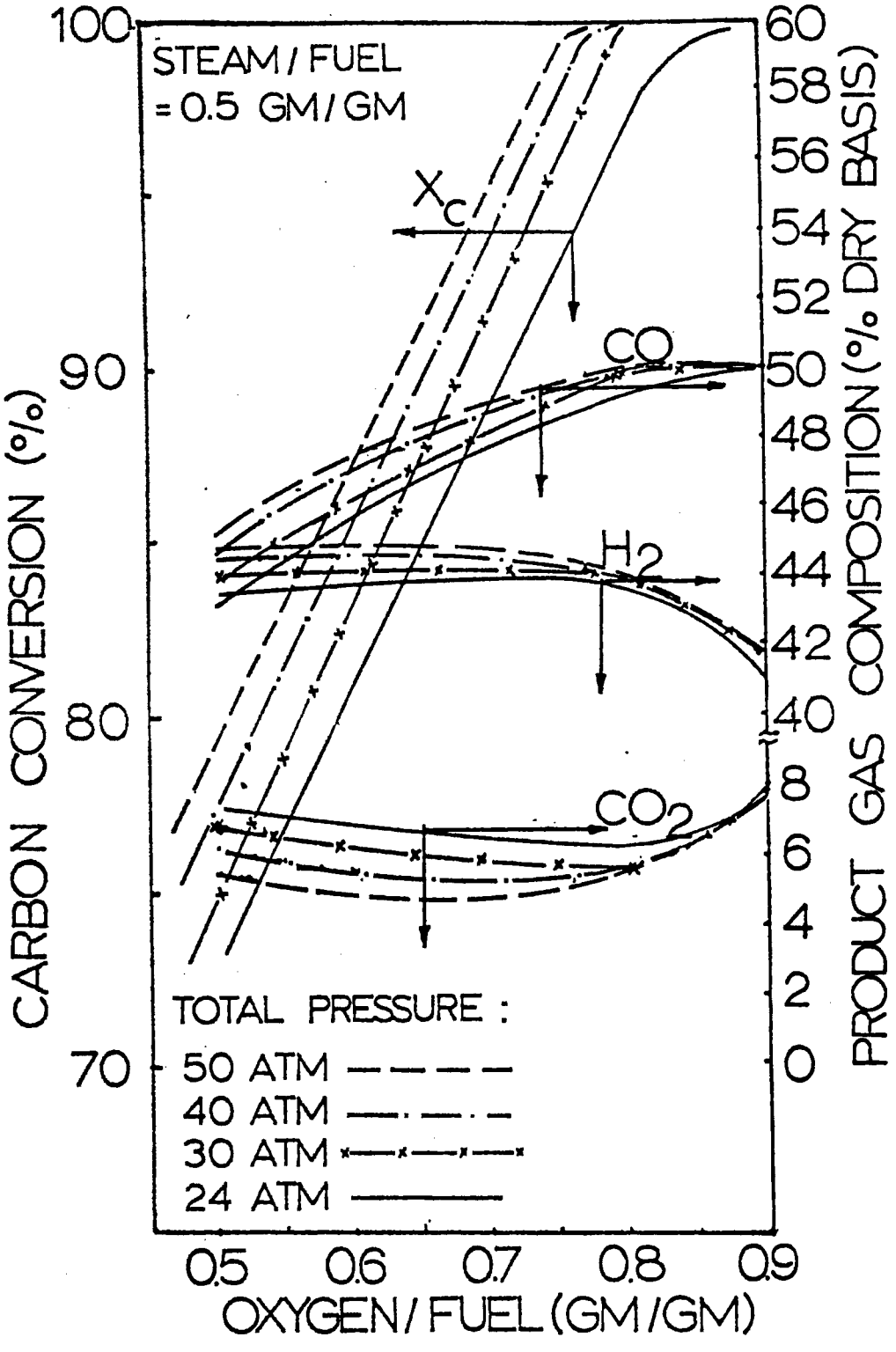

FIGURE 34 EFFECT OF TOTAL PRESSURE ON CARBON CONVERSION AND MAJOR PRODUCT GAS COMPOSITION AT VARIOUS OXYGEN/FUEL RATIOS WITH STEAM/FUEL = 0.5 GM/GM FEEDING H-COAL RESIDUE FROM ILLINOIS NO. 6 COAL IN THE TEXACO PILOT PLANT GASIFIER

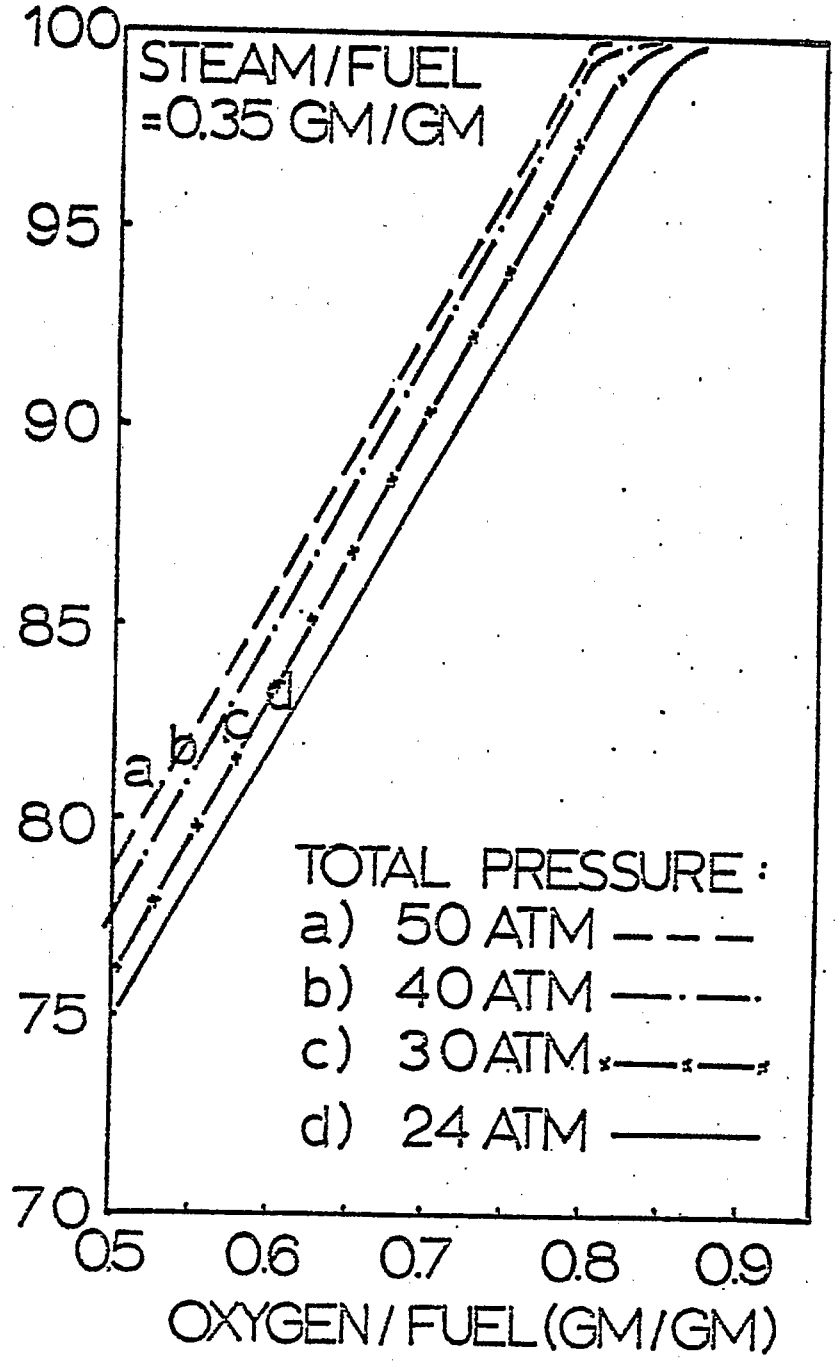

FIGURE 35 EFFECT OF TOTAL PRESSURE ON CARBON CONVERSION AT VARIOUS OXYGEN/FUEL RATIOS WITH STEAM/FUEL = 0.35 GM/GM FEEDING H-COAL RESIDUE FROM ILLINOIS NO. 6 COAL IN THE TEXACO PILOT PLANT GASIFIER.

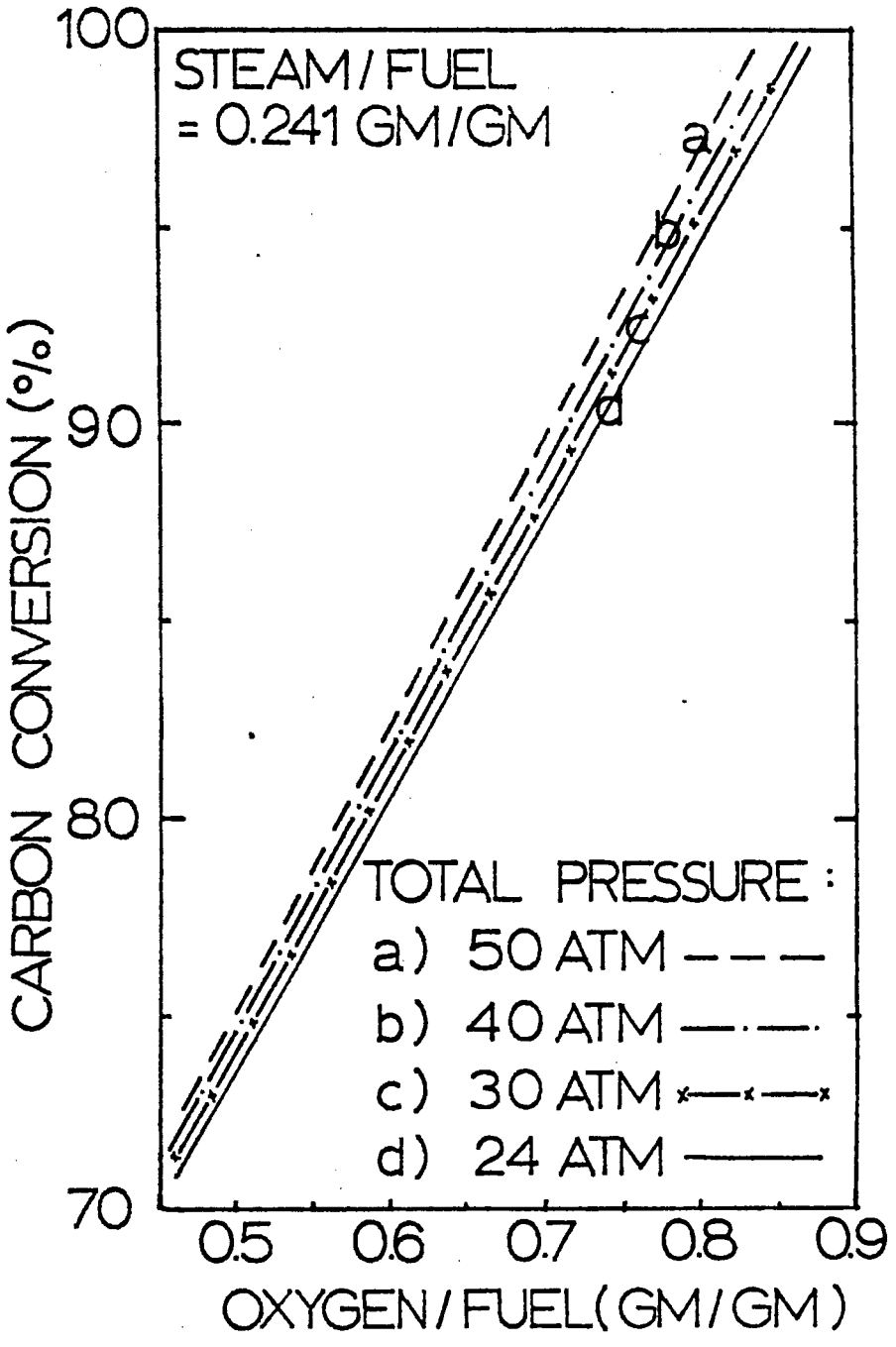

FIGURE 36 EFFECT OF TOTAL PRESSURE ON CARBON CONVERSION AT VARIOUS OXYGEN/FUEL RATIOS WITH STEAM/FUEL = 0.241 GM/GM FEEDING H-COAL RESIDUE FROM ILLINOIS NO. 6 COAL IN THE TEXACO PILOT PLANT GASIFIER.

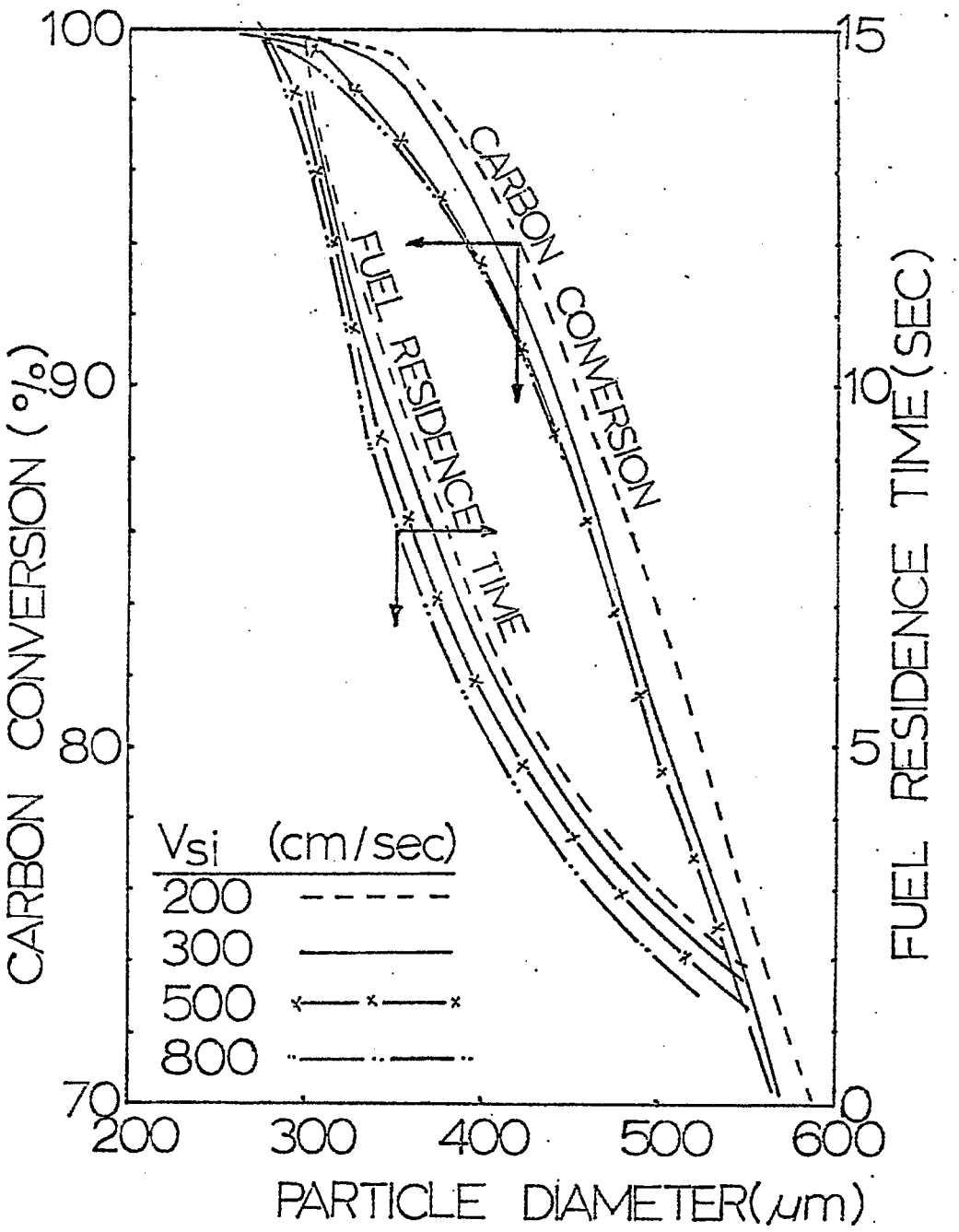

FIGURE 37 EFFECT OF FUEL PARTICLE SIZE ON THE FUEL RESIDENCE TIME AND THE CARBON CONVERSION AT VARIOUS INITIAL SOLID VELOCITIES FEEDING ILLINOIS NO. 6 COAL LIQUEFACTION RESIDUE IN TEXACO PILOT PLANT ENTRAINED GASIFIER.

(A) Compiling Program

```
1.    //ENGRTZCH JOB (CE060266,****),'CHAUNG',TIME=2,REGION=160K
2.    /*JOBPARM I=5,L=4
3.    /*ROUTE  XEQ   CPU2
4.    /*ROUTE  PRINT RMT3
5.    //STEP1 EXEC PGM=IEFBR14
6.    //OLD DD DSN=CE060266.CHAUNG,VOL=SER=DISK00,
7.    // UNIT=3330-1,DISP=(OLD,DELETE)
8.    //*
9.    //STEP2 EXEC FORTGCL
10.   //FORT.SYSIN DD *
11.   C      SIMULATION OF TEXACO PROCESS
12.   C      COMPARTMENT-IN-SERIES MODEL
13.   C      *** SHRINKING-CORE MODEL ***
14.   C      ***TO SPECIFY THE FLOW DIRECTION.
15.   C      ***THE DEFINITION OF 'DIRECT' GIVEN IN SUBROUTINE VSOLID IS USED
16.   C      FOR UPWARD FLOW, 'DIRECT'=1.0
17.   C      FOR DOWNWARD FLOW, 'DIRECT'=-1.0
18.           REAL KS,KV,KDIFF,KOVER
19.           REAL N2F,N2P2,N2P3,N2P5
20.           REAL N2MOL
21.           LOGICAL*1 NAME(12)
22.           DIMENSION HT(20),HTUP(30),CP(30),DTM(5)
23.           DIMENSION TGAS(5),FTG(4),HBL(4),TSOLID(5),FTS(5),DFTS(5),RK(5)
24.           DIMENSION X1(120,2),Y1(120,2),NPT1(2),IC1(2)
25.           DIMENSION X2(120,4),Y2(120,4),NPT2(4),IC2(4)
26.           DIMENSION X3(120,3),Y3(120,3),NPT3(3),IC3(3)
27.           DIMENSION X4(120,1),Y4(120,1),NPT4(1),IC4(1)
29.           DIMENSION X5(120,2),Y5(120,2),NPT5(2),IC5(2)
29.           COMMON /S1/ FCOAL,FOXY,FSTEAM/S2/ TG,TS, DENS,DENG,CPS,PT
30.           COMMON /S3/ TFCOAL,XMOIS
31.           COMMON /A1/ YC,YOXY,YH,YS,YN,YCR,YOXYR,YHR,YSR,YNR
32.           COMMON /A2/ XH2,XCO,XCO2,XH2S,XH20,XN2,XCH4,XTAR
33.           COMMON /A3/ GOXY,GSTEAM,GCO2,GCO,GH2,GH2S,GN2,GCH4
34.   C
35.   C
36.           DATA NAME/'                '/
37.           DATA HL/30./
38.           DATA A,B,C,Q/4.92E5,8900.,0.14,1.25/
39.           DATA VIS,AT/6.E-4,18241.5/
40.           DATA NPT1,IC1/120,120,'$$$$','****'/
41.           DATA NPT2,IC2/120,120,120,120,'1111','2222','3333','4444'/
42.           DATA NPT3,IC3/120,120,120,'5555','6666','7777'/
43.           DATA NPT4,IC4/120,'%%%%'/
44.           DATA NPT5,IC5/120,120,'GGGG','SSSS'/
45.   C
46.           NAMELIST/DATA/NAME,TA,TSTEAM,TOXY,
47.          X              YOXY,YH,YC,YS,YN,YASH,XMOIS,
48.          X              FOXY,FSTEAM,TFCOAL
49.   C
50.       10 READ(5,DATA)
51.   C
52.           WRITE(6,1) (NAME(J),J=1,12)
53.        1 FORMAT('1',T40,12A1,/)
54.   C
55.           WRITE(6,DATA)
```

```
      C
      C     *** FC IS THE FIXED CARBON IN DMMF BASIS ****
            FC=65.0
            DENSI=1.18
            RI=1.75E-2
            CPS=0.45
      C
            CPOXY=8.724
            CPSTM=11.34
            CPCO2=13.83175
            CPCO=8.4765
            CPCH4=20.772
            CPH2=7.73
            CPH2S=4.77
            CPN2=8.39675
      C
            PT=24.
            FCOAL=TFCOAL*(1.-YASH)*(1.-XMOIS)
      C     FCOAL IS THE FEED RATE OF COAL IN DMMF BASIS
      C
      C     ****TOHUP IS CAL/G DMMF COAL FEED
      C     ****FCOAL*TOHUP IS CAL FLOW THROUGH THIS COMPARTMENT/SEC
      C     ****SUBDWL IS G COAL CONSUMED IN THIS COMPARTMENT/G DMMF COAL
      C     ****FCOAL*SUBDWL/100. IS G COAL CONSUMED IN THIS COMP./SEC
      C     ****RHEAT1 IS CAL PRODUCED IN THIS CP./G DMMF COAL
      C     ****RHEAT1*FCOAL IS CAL PRODUCED IN THIS COMP./SEC
      C     ****CWL'S ARE G CARBON CONSUMED IN THIS COMPART./G DMMF COAL
      C     ****RHEAT IS CAL GENERATED IN THIS COMP./G DMMF COAL FEED
      C     ****RHEAT*FCOAL IS CAL GENERATED IN THIS COMPART./SEC
      C     *** FGS IS THE FRACTION OF HEAT GENERATED BY CO AND H2 COMBUSTIO
      C     *** THAT BACK RADIATED TO THE SOLID SURFACE FROM THE FRAME FRONT
      C     *** IN ADDITION TO THOSE FROM THE BULK GAS PHASE.
            FGS=0.25
            SWELL=1.0
            EF=0.9
            SIGMA=1.355E-12
            FASH=YASH/(1.-YASH)
      C
      C     *** RS IS THE FRACTION OF COAL SULPHUR THAT DOES NOT REACTED
      C     *** INTO GASEOUS PRODUCT BUT DEPOSITED TOGETHER WITH ASH ***
      C     *** RN IS THE FRACTION OF COAL NITROGEN THAT DOES NOT REACTED
      C     *** INTO GASEOUS PRODUCT BUT DEPOSITED TOGETHER WITH ASH ***
            RS=0.5
            YS=YS*(1.-RS)
            RN=0.3
            YN=YN*(1.-RN)
      C
            DELH=5.
      C
      C     **** 'FWGS' IS THE FRACTION OF HEAT RELEASED BY WATER-GAS-SHIFT
      C     *** THAT IS ADSORPED BY THE SOLID PHASE.
            FWGS=1.0
      C
```

```
      CALL VOLATL(YC,YOXY,YH,YN,YS,YASH,FC,FO,FH,FN,FS,VH2,R1,R2,VMO)
      VMO=VMO*(1.-0.066*ALOG(PT))
      SWL=Q*VMO*(1.-C)
C
      YCR=YC-(VMO/100.)*(XCO*12./28.+XCO2*12./44.+XCH4*12./16.+XTAR*72/
     1/78.)
      YOXYR=YOXY-VMO*(XCO2*32./44.+XCO*16./28.+XH2O*16./18.)/100.
      YHR=YH-VMO*(XH2+XH2S*2./34.+XH2O*2./18.+XCH4*4./16.+XTAR*6./78.)
     1/100.
      YSR=YS-XH2S*VMO*32./(34.*100.)
      YNR=YN-XN2*VMO/100.
      FLOXY=YOXYR/YCR
      FLH=YHR/YCR
      FLN=YNR/YCR
      FLS=YSR/YCR
      ALPHA=YCR/12.
      BETA=YHR/1.
      GAMA=YOXYR/16.
      DELTA=YNR/14.
      EPSN=YSR/32.
      WRITE(6,547)ALPHA,BETA,GAMA,DELTA,EPSN
  547 FORMAT(//2X,'ALPHA=',F15.5,2X,'BETA=',F15.5,2X,'GAMA=',F15.5,2X,
     1'DELTA=',F15.5,2X,'EPSN=',F15.5)
C
      DENSP=DENSI*(1.+FASH-SWL/100.)/((1.+FASH)*SWELL)
      RP=RI*(SWELL**0.333)
      GOXYIN=FOXY*TFCOAL
      GH2OIN=(FSTEAM+XMOIS)*TFCOAL
C
C     *** ENTHIN IS THE TOTAL INLET ENTHALPY :
      CALL HEATUP(1,TOXY,298.,HTUP,CP)
      CALL HEATUP(2,TSTEAM,298.,HTUP,CP)
      ENTHG=HTUP(1)*GOXYIN/32.+HTUP(2)*TFCOAL*FSTEAM/18.
      CALL HEATUP(2,TA,298.,HTUP,CP)
      ENTHS=CPS*FCOAL*(1.+FASH)*(TA-298.)+TFCOAL*XMOIS*(HTUP(2)-10520.)
     1/18.
      ENTHIN=ENTHG+ENTHS
C     **** NC IS THE NUMBER OF STEP SIZES IN EACH GAS COMPARTMENT
      NC=3
      TMOLE=GOXYIN/32.+GH2OIN/18.
      POXYIN=PT*GOXYIN/(32.*TMOLE)
      PH2OIN=PT*GH2OIN/(18.*TMOLE)
      GCO2IN=0.
      PCO2IN=0.
      GCOIN=0.
      PCOIN=0.
      GH2SIN=0.
      PH2SIN=0.
      GH2IN=0.
      PH2IN=0.
      GN2IN=0.
      PN2IN=0.
```

```
      GCH4IN=0.
      PCH4IN=0.
      TSIN=TA
      TIMEIN=0.
      HSIN=0.
      WLIN=0.
      USIN=300.
      GTARIN=0.
      TGAS(1)=2800.
      TGAS(2)=2900.
      WLCP=SWL
      TG1=(GOXYIN*CPOXY*TOXY/32.+GH2OIN*CPSTM*TSTEAM/18.)/(GOXYIN*CPOXY
     1/32.+GH2OIN*CPSTM/18.)
      X1(1,1)=0.
      X1(1,2)=0.
      Y1(1,1)=TG1
      Y1(1,2)=TA
      X2(1,1)=0.
      X2(1,2)=0.
      X2(1,3)=0.
      X2(1,4)=0.
      Y2(1,1)=(GH2OIN/18.)/TMOLE
      Y2(1,2)=0.
      Y2(1,3)=0.
      Y2(1,4)=0.
      X3(1,1)=0.
      X3(1,2)=0.
      X3(1,3)=0.
      Y3(1,1)=0.
      Y3(1,2)=0.
      Y3(1,3)=0.
      X4(1,1)=0.
      Y4(1,1)=0.
      X5(1,1)=0.
      X5(1,2)=0.
      Y5(1,1)=TMOLE*82.05*TG1/(AT*PT)
      Y5(1,2)=USIN
      I=1
      J=1
      ITERG=1
      M=1
      R=(RI+RF)/2.
C     *** GAS-WALL HEAT TRANSFER ***
C     *** UO IS THE OVERALL HEAT TRANSFER COEFF. BETWEEN GAS AND WALL
C     *** FOR GASIFICATION ZONE SIMULATED AS A HEAT EXCHANGER, CAL/SEC
C     *** FOR GASIFICATION ZONE SIMULATED AS A HEAT EXCHANGER,
C     *** CAL/(SEC.CM.CM.K)
      UO=3.4E-3
      DT=152.4
      TW=1700.
C
```

```
      C
  300 TG=TGAS(I)
      IF(TG.LE.300.)TG=TS+100.
      TIME=TIMEIN
      HS=HSIN
      USI=USIN
      WL=WLIN
      TS=TSIN
      GOXY=GOXYIN
      GSTEAM=GH2OIN
      GCO2=GCO2IN
      GCO=GCOIN
      GH2=GH2IN
      GH2S=GH2SIN
      GN2=GN2IN
      GCH4=GCH4IN
      POXY=POXYIN
      PSTEAM=PH2OIN
      PCO2=PCO2IN
      PCO=PCOIN
      PH2=PH2IN
      PH2S=PH2SIN
      PN2=PN2IN
      PCH4=PCH4IN
      GTAR=GTARIN
      K=1
      TMOLE=GOXY/32.+GSTEAM/18.+GCO2/44.+GCO/28.+GH2/2.+GH2S/34.+GN2/28
     1+GCH4/16.
      GSUM=GOXY+GSTEAM+GCO2+GCO+GH2+GH2S+GN2+GCH4
      RHEAT1=0.
      RHEAT2=0.
      RHEAT3=0.
      RHTS=0.
      SUBDWL=0.
      RHT=0.
      RK(3)=0.
      DWL=(SWL-WL)/SWL
      IF(DWL.LE.0.08) GO TO 500
      C
      C
      C
  140 IF(TS.GT.600.) R=RP
      DP=2.*R
      DENS=DENSI*(1.+FASH-WL/100.)/((1.+FASH)*SWELL)
      CALL VSOLID(DELH,USI,TMOLE,GSUM,DP,TG,PT,AT,VIS,DENS,DELTIM,US,UG
      USI=US
      C
  110 CONDUT=(7.7E-7)*((TG+TS)**0.75)
      CT=-(3./(DENS*CPS*R))*(CONDUT/R+EF*SIGMA*4.*TG**3)*DELTIM
      IF(ABS(CT).GT.25.) GO TO 20
      ECT=EXP(CT)
      GO TO 30
```

```
264.       20   ECT=1.0E-12
265.       30   DELTS=(TG-(TG-TS)*ECT)-TS
266.            TSM=TS+DELTS/2.
267.            TS=TS+DELTS
268.            IF(TSM.GT.1250.) TSM=1250.
269.      C
270.      C
271.            TIME=TIME+DELTIM
272.            HS=HS+DELH
273.            AGU1=-B/TSM
274.            IF(ABS(AGU1).LE.25.) GO TO 12
275.            EAGU1=0.
276.            GO TO 13
277.       12   EAGU1=EXP(AGU1)
278.       13   AK=A*EAGU1
279.      C
280.            AGU2=-AK*DELTIM
281.            IF(ABS(AGU2).LE.25.) GO TO 15
282.            EAGU2=0.
283.            GO TO 16
284.       15   EAGU2=EXP(AGU2)
285.       16   DELWL=(SWL-(SWL-WL)*EAGU2)-WL
286.            WL=WL+DELWL
287.      C
288.            WRITE(6,123) TIME,TS,WL,HS,TG,DELWL
289.       123  FORMAT(///2X,'TIME=',F15.5,5X,'TS=',F15.5,5X,'WL=',F15.5,2X,'HS='
290.           1,F15.5,2X,'TG=',F15.5,2X,'DELWL=',F15.6)
291.            SUBDWL=SUBDWL+DELWL
292.            DENS=DENSI*(1.+FASH-WL/100.)/((1.+FASH)*SWELL)
293.            DWL=(SWL-WL)/SWL
294.            IF(DWL.LE.0.08) WLCP=WL
295.            IF(K.GE.NC) GO TO 400
296.            K=K+1
297.            GO TO 110
298.      C
299.      C
300.       400  YCR=YC-(WLCP/100.)*(XCO*12./28.+XCO2*12./44.+XCH4*12./16.+XTAR*72.
301.           1/78.)
302.      C
303.            DO 404 N=1,4
304.            CALL HEAT(N,TG,HT)
305.       404  CONTINUE
306.            CALL PYROLY(SUBDWL,SWL,GOXY,RHEAT1,DOXY,WATERP,CO2P,H2SP,N2P,COP,
307.           1H2P,CH4P,TARP)
308.            GOXYEX=GOXY-DOXY*FCOAL
309.            IF(GOXYEX.LT.0.) GO TO 424
310.            GOXY=GOXYEX
311.            GO TO 426
312.       424  GOXY=0.
```

```
      426  GSTEAM=GSTEAM+WATERP*FCOAL
           GCO2=GCO2+CO2P*FCOAL
           GH2S=GH2S+H2SP*FCOAL
           GN2=GN2+N2P*FCOAL
           GCO=GCO+COP*FCOAL
           GH2=GH2+H2P*FCOAL
           GCH4=GCH4+CH4P*FCOAL
           GTAR=GTAR+TARP*FCOAL
           GSUM=GOXY+GSTEAM+GCO2+GH2S+GN2+GCO+GH2+GCH4
           TMOLE=GOXY/32.+GSTEAM/18.+GCO2/44.+GCO/28.+GH2/2.+GH2S/34.+GN2/28.
          1+GCH4/16.
           XCARB=100.*(GCO/28.+GCO2/44.+GCH4/16.+GTAR*6./78.)*12./(FCOAL*YC)
           POXY=PT*(GOXY/32.)/TMOLE
           PSTEAM=PT*(GSTEAM/18.)/TMOLE
           PCO2=PT*(GCO2/44.)/TMOLE
           PCO=PT*(GCO/28.)/TMOLE
           PH2=PT*(GH2/2.)/TMOLE
           PCH4=PT*(GCH4/16.)/TMOLE
           PH2S=PT*(GH2S/34.)/TMOLE
           PN2=PT*(GN2/28.)/TMOLE
C
           IF(GOXY.GT.0.) GO TO 433
           GOXY=0.
           POXY=0.
C
      433  CALL ENTHAL(TG,TS,FCOAL,FASH,WL,CPS,ENTH)
           TOHUP=(ENTH-ENTHIN)/FCOAL
C
C
C
           IF(POXYIN.GT.0.05) GO TO 436
           TW=2100.-600.*HS/330.
           HLOSS=UO*3.14*DT*FLOAT(NC)*DELH*(TG-TW)
           GO TO 437
      436  HLOSS=FCOAL*ABS(RHEAT1)*HL/100.
      437  HTEXC=-RHEAT1-TOHUP-HLOSS/FCOAL
      420  DO 410 N=1,8
           CALL HEATUP(N,TG,298.,HTUP,CP)
      410  CONTINUE
           DELTG=(HTEXC*FCOAL)/(GOXY*CP(1)/32.+GSTEAM*CP(2)/18.+GCO2*CP(3)
          1/44.+GCO*CP(4)/28.+GH2*CP(6)/2.+GH2S*CP(7)/34.+GN2*CP(8)/28.)
           ERRTG=DELTG/TG
           DHTEX=HTEXC/TOHUP
           IF(ABS(ERRTG).LE.0.02) GO TO 800
           IF(ABS(HTEXC).LE.5.0) GO TO 800
           IF(ABS(DHTEX).LE.0.10) GO TO 800
C
```

```
360.            DWL=(SWL-WL)/SWL
361.            IF(M.EQ.1) GO TO 302
362.            IF(DWL.GE.0.08) GO TO 302
363.            IF(ITERG.GE.5) GO TO 416
364.            ITERG=ITERG+1
365.            GO TO 302
366.      416   DELH=DELH/2.
367.            TGAS(1)=TGIN-30.
368.            I=1
369.            GO TO 300
370.      C
371.      C
372.      C     USE OF WEGSTEIN METHOD FOR THE SEARCH OF CORRECT TG
373.      C     SEARCH FOR STABLE BALANCE OF HEAT GENERATION AND HEAT REQUIREMENT
374.       302  FTG(I)=TGAS(I)+DELTG
375.            HBL(I)=HTEXC
376.            IF(I.EQ.2) GO TO 319
377.            IF(I.EQ.3) GO TO 339
378.            IF(M.EQ.1) GO TO 311
379.            TGAS(2)=TG+DELTG/2.
380.            IF(TGAS(2).GT.4000.) TGAS(2)=TG+DELTG/5.
381.            I=2
382.            GO TO 300
383.       311  TGAS(2)=TGAS(1)+100.
384.            I=2
385.            GO TO 300
386.       319  CHECKG=HBL(1)*HBL(2)
387.            IF(CHECKG.GT.0.) GO TO 322
388.            TGAS(3)=(TGAS(1)*HBL(2)-TGAS(2)*HBL(1))/(HBL(2)-HBL(1))
389.            I=3
390.            GO TO 300
391.       320  IF(FOXY.LE.0.) GO TO 322
392.            IF(ABS(HBL(1)).GE.ABS(HBL(2))) GO TO 321
393.            TGAS(3)=TGAS(1)-(TGAS(2)-TGAS(1))
394.            I=3
395.            GO TO 300
396.       321  TGAS(3)=TGAS(2)+(TGAS(1)-TGAS(2))
397.            I=3
398.            GO TO 300
399.       322  TGAS(3)=(TGAS(1)*FTG(2)-TGAS(2)*FTG(1))/(TGAS(1)-TGAS(2)+FTG(2)
400.           1-FTG(1))
401.            I=3
402.            GO TO 300
403.       339  CHECK1=HBL(1)*HBL(3)
404.            IF(CHECK1.LT.0.) GO TO 342
405.            GO TO 340
406.       342  TGAS(2)=TGAS(3)
407.            FTG(2)=FTG(3)
408.            HBL(2)=HBL(3)
409.            GO TO 319
410.       340  TGAS(1)=TGAS(2)
```

```
411.            FTG(1)=FTG(2)
412.            HBL(1)=HBL(2)
413.            TGAS(2)=TGAS(3)
414.            FTG(2)=FTG(3)
415.            HBL(2)=HBL(3)
416.            GO TO 319
417.       341  TGAS(1)=TG+DELTG/3.
418.            I=1
419.            GO TO 300
420.       C
421.       C
422.       C
423.       C
424.       500  RHTS=0.
425.            RHEAT2=0.
426.            R=RP
427.            DP=2.*R
428.            IF(WL.GE.99.95) WL=99.95
429.            TI=TS
430.            DENS=DENSI*(1.+FASH-WL/100.)/((1.+FASH)*SWELL)
431.            Y=((1.-WL/100.)/(1.-SWL/100.))**0.333
432.            RC=RP*Y
433.            CALL VSOLID(DELH,USI,TMOLE,GSUM,DP,TG,PT,AT,VIS,DENS,DELTIM,US)
434.            USI=US
435.            IF(GOXY.GT.0.) GO TO 505
436.       C
437.            GOXY=0.
438.            POXY=0.
439.            GO TO 600
440.       C
441.       C    ***** WHEN OXYGEN IS STILL EXISTED *****
442.       C    IF OXYGEN IS STILL ENOUGH THE PARTIAL PRESSURE OF CO IS ALMOST
443.       C    ZERO AND THE WATER-GAS-SHIFT REACTION CAN BE NEGLECTED
444.       C
445.       C
446.       505  TSOLID(1)=TS
447.       C
448.            IF(WL.GE.99.95) GO TO 560
449.            IF(XCARB.GE.99.75) GO TO 560
450.       C
451.            Y=((1.-WL/100.)/(1.-SWL/100.))**0.333
452.            RC=RP*Y
453.            R=RP
454.            DP=2.*R
455.            CALL HEAT(1,TG,HT)
456.            CALL HEAT(2,TG,HT)
457.       C    *** RUNGE-KUTTA-GILL METHOD
458.            DO 510 L=1,4
459.            TS=TSOLID(L)
460.            IF(TS.LE.0.) GO TO 506
461.            CALL COMBUS(TG,TS,PT,RP,POXY,SWL,Y,DENSP,RATE,CWL,PHI,QRH,FAS
462.           1,DELTIM,Q1,Q2)
```

```
      CALL CBSTM(DELTIM,PSTEAM,PH2,PCO,RP,PT,DENSP,TG,TS,SWL,Y,FASH
     1,RATE2,CWL2,QCSM,WL)
      CALL CBCO2(PCO2,DELTIM,WL,SWL,RP,PT,DENSP,TG,TS,FASH,Y,RATE3,CWL3
     1,QCBCO2)
      QCCDG=(RATE3/12.)*(2.*HT(2)+HT(1)*(BETA/2.-GAMA-EPSN)/ALPHA)
      QCSG=(RATE2/12.)*(HT(2)+HT(1)*(ALPHA-GAMA+BETA/2.-EPSN)/ALPHA)
      QCOMG=(RATE/12.)*(2.-2./PHI)*HT(2)
      CONDUT=(7.7E-7)*((TS+TG)**0.75)
      RK(L)=(3./(DENS*CPS*R))*(CONDUT*(TG-TS)/R+EF*SIGMA*(TG**4-TS**4)
     1+QRH*RATE-QCSM*RATE2/12.-QCBCO2*RATE3/12.-FGS*(QCOMG+QCSG+QCCDG))
      GO TO 507
  506 CONDUT=(7.7E-7)*(TG**0.75)
      RK(L)=(3./(DENS*CPS*R))*(CONDUT*TG/R+EF*SIGMA*(TG**4))
  507 IF(L.EQ.1) GO TO 5071
      IF(L.EQ.2) GO TO 5072
      IF(L.EQ.3) GO TO 5073
      IF(L.EQ.4) GO TO 510
 5071 TSOLID(2)=TSOLID(1)+(DELTIM/2.)*RK(1)
      GO TO 510
 5072 TSOLID(3)=TSOLID(1)+0.2071*DELTIM*RK(1)+0.2929*DELTIM*RK(2)
      GO TO 510
 5073 TSOLID(4)=TSOLID(1)-0.7071*DELTIM*RK(2)+1.7071*DELTIM*RK(3)
  510 CONTINUE
      TS=TSOLID(1)+(DELTIM/6.)*(RK(1)+0.58578*RK(2)+3.41422*RK(3)+RK(4)
      Y=((1.-WL/100.)/(1.-SWL/100.))**0.333
      RC=RP*Y
      CALL COMBUS(TG,TS,PT,RP,POXY,SWL,Y,DENSP,RATE,CWL,PHI,QRH,FASH
     1,DELTIM,Q1,Q2)
      CALL CBSTM(DELTIM,PSTEAM,PH2,PCO,RP,PT,DENSP,TG,TS,SWL,Y,FASH
     1,RATE2,CWL2,QCSM,WL)
      CALL CBCO2(PCO2,DELTIM,WL,SWL,RP,PT,DENSP,TG,TS,FASH,Y,RATE3,CWL3
     1,QCBCO2)
C
C
      YCR=YCR-(CWL+CWL2+CWL3)
      WL=WL+(CWL+CWL2+CWL3)*(1.+FLOXY+FLH+FLS+FLN)*100.
C
C     CHAR-OXYGEN REACTION
      DOXY1=(ALPHA+BETA/4.-EPSN/2.-GAMA/2.)*32.
      CO2P1=ALPHA*44.
      H2OP1=(BETA/2.-EPSN)*18.
      N2P1=(DELTA/2.)*28.
      H2SP1=EPSN*34.
C
C     CHAR-STEAM REACTION FOLLOWED BY CO AND H2(PRODUCT) COMBUSTION
      DOXY2=(ALPHA+BETA/4.-GAMA/2.-EPSN/2.)*32.
      CO2P2=ALPHA*44.
      H2OP2=(BETA/2.-EPSN)*18.
      N2P2=(DELTA/2.)*28.
      H2SP2=EPSN*34.
C
```

```
514.      C
515.      C      CHAR-CO2 REACTION FOLLOWED BY CO COMBUSTION
516.             DOXY3=(ALPHA+BETA/4.-GAMA/2.-EPSN/2.)*32.
517.      C      CO2 DECREASED BY ALPHA BUT INCREASED BY TWO ALPHAS
518.             CO2P3=ALPHA*44.
519.             H2OP3=(BETA/2.-EPSN)*18.
520.             N2P3=(DELTA/2.)*28.
521.             H2SP3=EPSN*34.
522.      C
523.      C      PARTIAL PRESSURE AND FLOW RATE CALCULATION
524.             GOXYEX=GOXY-FCOAL*(CWL*DOXY1+CWL2*DOXY2+CWL3*DOXY3)/(12.*ALPHA)
525.             IF(GOXYEX.LT.0.) GO TO 524
526.             GOXY=GOXYEX
527.             COP=0.
528.             GCO=0.
529.             PCO=0.
530.             RHTD=0.
531.             GO TO 526
532.       524   GOXY=0.
533.             COP=ABS(GOXYEX)*(28./16.)/FCOAL
534.             COPMAX=(28./12.)*(CWL*(2.-2./PHI)+CWL2+CWL3)
535.             IF(COP.LE.COPMAX) GO TO 5251
536.             DELH=DELH/2.
537.             GO TO 300
538.       5251  RHTD=COP*HT(2)/28.
539.       526   GSTEAM=GSTEAM+FCOAL*(CWL*H2OP1+CWL2*H2OP2+CWL3*H2OP3)/(12.*ALPHA
540.             GCO2=GCO2+FCOAL*(CWL*CO2P1+CWL2*CO2P2+CWL3*CO2P3)/12./ALPHA-FCOP
541.            1*COP*(44./28.)
542.             GN2=GN2+FCOAL*(CWL*N2P1+CWL2*N2P2+CWL3*N2P3)/12./ALPHA
543.             GH2S=GH2S+FCOAL*(CWL*H2SP1+CWL2*H2SP2+CWL3*H2SP3)/12./ALPHA
544.             GCO=GCO+FCOAL*COP
545.             TMOLE=GOXY/32.+GSTEAM/18.+GCO2/44.+GN2/28.+GH2S/34.+GCO/28.
546.             XCARB=100.*(GCO/28.+GCO2/44.+GCH4/16.+GTAR*6./78.)*12./(FCOAL*YC
547.             POXY=PT*GOXY/(32.*TMOLE)
548.             PSTEAM=PT*GSTEAM/(18.*TMOLE)
549.             PCO2=PT*GCO2/(44.*TMOLE)
550.             PCO=PT*GCO/(28.*TMOLE)
551.             PN2=PT*GN2/(28.*TMOLE)
552.             PH2S=PT*GH2S/(34.*TMOLE)
553.             GH2=0.
554.             PH2=0.
555.             GCH4=0.
556.             PCH4=0.
557.      C
558.      C      TOTAL HEAT OF REACTION GENERATED IN THE GASEOUS PHASE=HEAT OF
559.      C      COMBUSTION OF CO AND HYDROGEN THAT PRODUCED FROM CHAR-OXYGEN
560.      C      REACTION, AHAR-STEAM REACTION, AND CHAR-CO2 REACTION.
561.             RHTA=(Q1/12.+QRH)*CWL
562.             DO 1000 N=1,2
563.             CALL HEAT(N,TG,HT)
564.       1000  CONTINUE
565.             RHTB=HT(1)*(ALPHA-GAMA+BETA/2.-EPSN)*CWL2/(ALPHA*12.)+HT(2)
566.            1*CWL2/12.
```

```
      RHTC=HT(1)*(BETA/2.-GAMA-EPSN)*CWL3/(12.*ALPHA)+2.*HT(2)*CWL3/12.
      RHEAT2=RHEAT2+RHTA+RHTB+RHTC-RHTD
      RHTS=RHTS+CWL*QRH-CWL2*QCSM/12.-CWL3*QCBCO2/12.
      GO TO 700
C
  560 IF(WL.GE.99.95) WL=99.95
      IF(XCARB.GE.99.95) XCARB=99.95
      IF(FOXY.GE.0.02) GO TO 8010
      CONDUT=(7.7E-7)*((TG+TS)**0.75)
      CT=-(3./(DENS*CPS*R))*(CONDUT/R+EF*SIGMA*4.*TG**3)*DELTIM
      IF(ABS(CT).GT.25.) GO TO 562
      ECT=EXP(CT)
      GO TO 564
  562 ECT=1.0E-12
  564 TS=TG-(TG-TS)*ECT
      CALL WGSHIF(TS,PCO,PSTEAM,PCO2,PH2,RATE4,QWG,GCO,GSTEAM,GCO2,GH2
     1,DELTIM,FCOAL,FASH,WGL,TG,PT)
C     WATER-GAS-SHIFT REACTION
      DCO4=WGL*FCOAL*28.
      DH2O4=WGL*FCOAL*18.
      CO2P4=WGL*FCOAL*44.
      H2P4=WGL*FCOAL*2.
C
      CALL CH4REF(TS,GCH4,FCOAL,DELTIM,DCH46,QMREF)
C
C     *** METHANE REFORMING REACTION ***
      DH2O6=DCH46*18./16.
      COP6=DCH46*28./16.
      H2P6=3.*DCH46*2./16.
C
      RHEAT2=RHEAT2+QMREF*DCH46/16.
      RHEAT3=RHEAT3+QWG*WGL
C
      GSTEAM=GSTEAM-DH2O4-FCOAL*DCH46
      GCO=GCO-DCO4+FCOAL*COP6
      GH2=GH2+H2P4+FCOAL*H2P6
      GCH4=GCH4-FCOAL*DCH46
      GCO2=GCO2+CO2P4
      IF(GSTEAM.LT.0.) GSTEAM=0.
      IF(GCO2.LE.0.) GCO2=0.
      IF(GCO.LT.0.) GCO=0.
      IF(GH2.LT.0.) GH2=0.
C
      GSUM=GOXY+GSTEAM+GCO2+GCO+GH2+GH2S+GN2+GCH4
      TMOLE=GOXY/32.+GSTEAM/18.+GCO2/44.+GCO/28.+GH2/2.+GH2S/34.+GN2/28
     1+GCH4/16.
      PSTEAM=PT*GSTEAM/(18.*TMOLE)
      PCO2=PT*GCO2/(44.*TMOLE)
      PCO=PT*GCO/(28.*TMOLE)
      PN2=PT*GN2/(28.*TMOLE)
      PH2=PT*GH2/(2.*TMOLE)
      PH2S=PT*GH2S/(34.*TMOLE)
      PCH4=PT*GCH4/(16.*TMOLE)
```

```
      RHTS=0.
      GO TO 700
C
C     WHEN OXYGEN IS CONSUMED
C
  600 IF(WL.GE.99.95) GO TO 560
      IF(XCARB.GE.99.75) GO TO 560
C
      Y=((1.-WL/100.)/(1.-SWL/100.))**0.333
      RC=RP*Y
C     *** RUNGE-KUTTA-GILL METHOD ***
      TSOLID(1)=TS
      DO 610 L=1,4
      TS=TSOLID(L)
      IF(TS.LE.0.) GO TO 606
      CALL CBSTM(DELTIM,PSTEAM,PH2,PCO,RP,PT,DENSP,TG,TS,SWL,Y,FASH
     1,RATE2,CWL2,QCSM,WL)
      CALL CBCO2(PCO2,DELTIM,WL,SWL,RP,PT,DENSP,TG,TS,FASH,Y,RATE3,CWL3
     1,QCBCO2)
      CALL WGSHIF(TS,PCO,PSTEAM,PCO2,PH2,RATE4,QWG,GCO,GSTEAM,GCO2,GH2
     1,DELTIM,FCOAL,FASH,WGL,TG,PT)
      RATEW=WGL*RP*DENSP/(3.*(1.+FASH-SWL/100.)*DELTIM)
      CALL CBHYM(PH2,PCH4,DELTIM,WL,SWL,Y,RP,DENSP,PT,TG,TS,CWL5,RATE5
     1,QCBHY,FASH)
C     CWL'S ARE THE GM CARBON CONSUMED PER GM DMMF COAL FOR EACH
C     SPECIFIC REACTION IN EACH COMPARTMENT
C     WGL IS THE GMOLE CONVERSION FOR WATER-GAS-SHIFT REACTION IN EACH
C     COMPARTMENT PER GM DMMF COAL
      CONDUT=(7.7E-7)*((TS+TG)**0.75)
      RK(L)=(3./(DENS*CPS*R))*(CONDUT*(TG-TS)/R+EF*SIGMA*(TG**4-TS**4)
     1+(-QWG)*RATEW*FWGS-RATE2*QCSM/12.-RATE3*QCBCO2/12.+(-QCBHY)*
     2RATE5/12.)
      IF(WL.GE.95..AND.ABS(RK(L)).GT.8000.) GO TO 620
      GO TO 607
  606 CONDUT=(7.7E-7)*(TG**0.75)
      RK(L)=(3./(DENS*CPS*R))*(CONDUT*TG/R+EF*SIGMA*(TG**4))
  607 IF(L.EQ.1) GO TO 6071
      IF(L.EQ.2) GO TO 6072
      IF(L.EQ.3) GO TO 6073
      IF(L.EQ.4) GO TO 610
 6071 TSOLID(2)=TSOLID(1)+(DELTIM/2.)*RK(1)
      GO TO 610
 6072 TSOLID(3)=TSOLID(1)+0.2071*DELTIM*RK(1)+0.2929*DELTIM*RK(2)
      GO TO 610
 6073 TSOLID(4)=TSOLID(1)-0.7071*DELTIM*RK(2)+1.7071*DELTIM*RK(3)
  610 CONTINUE
      TS=TSOLID(1)+(DELTIM/6.)*(RK(1)+0.58578*RK(2)+3.41422*RK(3)+RK(4
      GO TO 630
C
```

```
      620  TS=TI
           CONDUT=(7.7E-7)*((TG+TS)**0.75)
           CT=-(3./(DENS*CPS*R))*(CONDUT/R+EF*SIGMA*4.*TG**3)*DELTIM
           IF(ABS(CT).GT.25.) GO TO 622
           ECT=EXP(CT)
           GO TO 624
      622  ECT=1.0E-12
      624  TS=TG-(TG-TS)*ECT
      630  Y=((1.-WL/100.)/(1.-SWL/100.))**0.333
           RC=RP*Y
           CALL CBSTM(DELTIM,PSTEAM,PH2,PCO,RP,PT,DENSP,TG,TS,SWL,Y,FASH
          1,RATE2,CWL2,QCSM,WL)
           CALL CBCO2(PCO2,DELTIM,WL,SWL,RP,PT,DENSP,TG,TS,FASH,Y,RATE3,CWL3
          1,QCBCO2)
           CALL WGSHIF(TS,PCO,PSTEAM,PCO2,PH2,RATE4,QWG,GCO,GSTEAM,GCO2,GH2
          1,DELTIM,FCOAL,FASH,WGL,TG,PT)
           RATEW=WGL*RP*DENSP/(3.*(1.+FASH-SWL/100.)*DELTIM)
           CALL CBHYM(PH2,PCH4,DELTIM,WL,SWL,Y,RP,DENSP,PT,TG,TS,CWL5,RATE5
          1,QCBHY,FASH)
C
           WL=WL+(CWL2+CWL3+CWL5)*(1.+FLOXY+FLH+FLS+FLN)*100.
           YCR=YCR-(CWL2+CWL3+CWL5)
C
C          CHAR-STEAM REACTION
           DH2O2=(ALPHA-GAMA)*18.
           COP2=ALPHA*28.
           H2P2=(ALPHA-GAMA+BETA/2.-EPSN)*2.
           N2P2=(DELTA/2.)*28.
           H2SP2=EPSN*34.
C
C          CHAR-CO2 REACTION
           DCO23=ALPHA*44.
           COP3=2.*ALPHA*28.
           H2OP3=GAMA*18.
           H2P3=(BETA/2.-GAMA-EPSN)*2.
           N2P3=(DELTA/2.)*28.
           H2SP3=EPSN*34.
C
C          WATER-GAS-SHIFT REACTION
           DCO4=WGL*FCOAL*28.
           DH2O4=WGL*FCOAL*18.
           CO2P4=WGL*FCOAL*44.
           H2P4=WGL*FCOAL*2.
C
C          CARBON-HYDROGEN REACTION
           DH25=(2.*ALPHA+GAMA-EPSN-BETA/2.)*2.
           CH4P5=ALPHA*16.
           H2OP5=GAMA*18.
           N2P5=(BETA/2.)*28.
           H2SP5=EPSN*34.
C
           CALL CH4REF(TS,GCH4,FCOAL,DELTIM,DCH4S,DMREF)
```

```
721.      C
722.      C      *** METHANE REFORMING REACTION ***
723.             DH2O6=DCH46*18./16.
724.             COP6=DCH46*28./16.
725.             H2P6=3.*DCH46*2./16.
726.      C
727.      C      PARTIAL PRESSURE AND FLOW RATE CALCULATION
728.             GOXY=0.
729.             FOXY=0.
730.      C
731.             GSTEAM=GSTEAM+FCOAL*(CWL3*H2OP3-CWL2*DH2O2+H2OP5*CWL5)/(12.*ALPHA
732.            1-DH2O4-FCOAL*DCH46
733.             GCO=GCO+FCOAL*(CWL2*COP2+CWL3*COP3)/(12.*ALPHA)-DCO4+FCOAL*COP6
734.             GH2=GH2+FCOAL*(CWL2*H2P2+CWL3*H2P3-CWL5*DH25)/(12.*ALPHA)+H2P4
735.            1+FCOAL*H2P6
736.             GCH4=GCH4+FCOAL*CWL5*CH4P5/(12.*ALPHA)-FCOAL*DCH46
737.             GCO2=GCO2-FCOAL*CWL3*DCO23/(12.*ALPHA)+CO2P4
738.             GN2=GN2+FCOAL*(CWL2*N2P2+CWL3*N2P3+CWL5*N2P5)/(12.*ALPHA)
739.             GH2S=GH2S+FCOAL*(CWL2*H2SP2+CWL3*H2SP3+CWL5*H2SP5)/(12.*ALPHA)
740.      C
741.             IF(GSTEAM.LT.0.) GSTEAM=0.
742.             IF(GCO2.LE.0.) GCO2=0.
743.             IF(GCO.LE.0.) GCO=0.
744.             IF(GH2.LE.0.) GH2=0.
745.      C
746.             TMOLE=GCO2/44.+GSTEAM/18.+GCO/28.+GN2/28.+GH2S/34.+GH2/2.+GCH4/16
747.             XCARB=100.*(GCO/28.+GCO2/44.+GCH4/16.+GTAR*6./78.)*12./(FCOAL*YC)
748.             PSTEAM=PT*GSTEAM/(18.*TMOLE)
749.             PCO2=PT*GCO2/(44.*TMOLE)
750.             PCO=PT*GCO/(28.*TMOLE)
751.             PN2=PT*GN2/(28.*TMOLE)
752.             PH2=PT*GH2/(2.*TMOLE)
753.             PH2S=PT*GH2S/(34.*TMOLE)
754.             PCH4=PT*GCH4/(16.*TMOLE)
755.             RHEAT2=RHEAT2+QMREF*DCH46/16.
756.             RHEAT3=RHEAT3+QWG*WGL*(1.-FWGS)
757.             RHTS=RHTS+(-QWG)*WGL*FWGS-CWL2*QCSM/12.-CWL3*QCBCO2/12.+CWL5*
758.            1(-QCBHY)/12.
759.      C
760.      C
761.       700   GSUM=GOXY+GSTEAM+GCO2+GCO+GH2+GH2S+GN2+GCH4
762.             TMOLE=GOXY/32.+GSTEAM/18.+GCO2/44.+GCO/28.+GH2/2.+GH2S/34.+GN2/28
763.            1+GCH4/16.
764.             IF(WL.GE.99.95) WL=99.95
765.             IF(XCARB.GE.99.95) XCARB=99.95
766.             TI=TS
767.             R=RP
768.             DP=2.*R
769.             DENS=DENSI*(1.+FASH-WL/100.)/((1.+FASH)*SWELL)
770.             Y=((1.-WL/100.)/(1.-SWL/100.))**0.333
771.             RC=RP*Y
772.             CALL VSOLID(DELH,USI,TMOLE,GSUM,DP,TG,PT,AT,VIS,DENS,DELTIM,US,UG
773.             USI=US
```

```
      TIME=TIME+DELTIM
      HS=HS+DELH
C
      IF(K.GE.NC) GO TO 515
      K=K+1
      IF(GOXY.GT.0.) GO TO 505
      GOXY=0.
      POXY=0.
      GO TO 600
C
  515 RHEAT=RHEAT1+RHEAT2+RHEAT3+(-RHTS)
      CALL ENTHAL(TG,TS,FCOAL,FASH,WL,CPS,ENTH)
      TOHUP=(ENTH-ENTHIN)/FCOAL
C
      IF(POXYIN.GT.0.05) GO TO 736
      TW=2100.-600.*HS/330.
      HLOSS=U0*3.14*DT*FLOAT(NC)*DELH*(TG-TW)
      GO TO 737
  736 HLOSS=FCOAL*ABS(RHEAT)*HL/100.
  737 HTEXC=-RHEAT-TOHUP-HLOSS/FCOAL
      GO TO 420
C
C     CORRECTION OF TG BY HALF DELTG
  800 TG=TG+DELTG/2.
      IF(WL.GE.99.99) GO TO 8010
      DHS=HS-325.
      IF(ABS(DHS).GT.10.) GO TO 806
 8010 WRITE(6,801) M
  801 FORMAT(///2X,'*****FOR GASEOUS COMPARTMENT',I3,'**********')
      WRITE(6,802)TG,TIME,TS,GOXY,GSTEAM,GCO2,GCO,GN2,GH2,GH2S,POXY,
     1PSTEAM,PCO2,PCO,PN2,PH2,PH2S,WL,HS,GCH4,PCH4
  802 FORMAT(///2X,'CORRECTED GAS TEMP=',F15.5,//2X,'TIME=',E10.3,//2X,
     1'TS OUTLET=',F10.4,//2X,'OXYGEN FLOW RATE=',F15.5,'GM/SEC',//2X
     2,'STEAM FLOW RATE=',F15.5,'G/SEC',//2X,'CO2 FLOW RATE=',F15.5,'G
     3/SEC',',//2X,'CO FLOW RATE=',F15.5,'GM/SEC',//2X,'N2 FLOW RATE=',
     4F15.5,'GM/SEC',//2X,'H2 FLOW RATE=',F15.5,'GM/SEC',//2X,'H2S FLOW
     5RATE=',F15.5,'GM/SEC',//2X,'OXYGEN PRESSURE=',F15.5,'ATM',//2X,
     6'STEAM PRESSURE=',F15.5,'ATM',//2X,'CO2 PRESSURE=',F15.5,'ATM',//2
     7X,'CO PRESSURE=',F15.5,'ATM',//2X,'N2 PRESSURE=',F15.5,'ATM',//2X
     8,'HYDROGEN PRESSURE=',F15.5,'ATM',//2X,'H2S PRESSURE=',F15.5,'ATM
     9',//2X,'TOTAL WEIGHT LOSS=',F15.5,'%',//2X,'ENTRAINED HEIGHT=',
     $F15.5,'CM',//2X,'GCH4=',F15.5,2X,'PCH4=',F15.5,'ATM')
      WRITE(6,805) GTAR
  805 FORMAT(//2X,'TAR YIELD=',F15.5,'G/SEC')
      DRYP=PT-PSTEAM
      COMOL=(PCO/DRYP)*100.
      CO2MOL=(PCO2/DRYP)*100.
      H2MOL=(PH2/DRYP)*100.
      CH4MOL=(PCH4/DRYP)*100.
      N2MOL=(PN2/DRYP)*100.
      H2SMOL=(PH2S/DRYP)*100.
```

```
      WRITE(6,862) COMOL,H2MOL,CO2MOL,CH4MOL,N2MOL,H2SMOL
  862 FORMAT(//2X,'CO MOL %=',F7.3,2X,'H2 MOL %=',F7.3,2X,'CO2 MOL %='
     1,F7.3,/2X,'CH4 MOL %=',F7.3,2X,'N2 MOL %=',F7.3,2X,'H2S MOL %=',
     2F7.3)
      WRITE(6,808) XCARB
  808 FORMAT(/2X,'CARBON CONVERSION=',F10.4,2X,'%')
C
C
  806 IP=M+1
      X1(IP,1)=HS
      X1(IP,2)=HS
      Y1(IP,1)=TG
      Y1(IP,2)=TS
      X2(IP,1)=HS
      X2(IP,2)=HS
      X2(IP,3)=HS
      X2(IP,4)=HS
      Y2(IP,1)=PSTEAM/PT
      Y2(IP,2)=PCO2/PT
      Y2(IP,3)=PCO/PT
      Y2(IP,4)=PH2/PT
      X3(IP,1)=HS
      X3(IP,2)=HS
      X3(IP,3)=HS
      Y3(IP,1)=PN2/PT
      Y3(IP,2)=PH2S/PT
      Y3(IP,3)=PCH4/PT
      X4(IP,1)=HS
      Y4(IP,1)=XCARB
      X5(IP,1)=HS
      X5(IP,2)=HS
      Y5(IP,1)=UG
      Y5(IP,2)=US
C
C
      IF(WL.GE.99.99.AND.POXY.GE.0.02) GO TO 900
      IF(TG.LE.200.) GO TO 900
      IF(TS.LE.200.) GO TO 900
      IF(M.EQ.119) GO TO 840
      M=M+1
C     COMPARTMENT SIZE ADJUSTMENT
      DELH=1.0
      IF(US.LE.100.) DELH=1.0
      IF(POXY.GT.0.01) DELH=0.5
      IF(HS.LE.40.) DELH=0.5
      DWL=(SWL-WL)/SWL
      IF(DWL.GT.0.08) DELH=0.5
C
      TGIN=TG
      TSIN=TS
      ENTHIN=ENTH
      K=1
      ITERG=1
      RHEAT1=0.
```

```
      RHEAT2=0.
      RHEAT3=0.
      RHTS=0.
      RHEAT=0.
      SUBOWL=0.
      USIN=US
      GOXYIN=GOXY
      GH2OIN=GSTEAM
      GCO2IN=GCO2
      GCOIN=GCO
      GH2IN=GH2
      GCH4IN=GCH4
      GH2SIN=GH2S
      GN2IN=GN2
      FH2OIN=PSTEAM
      FOXYIN=POXY
      FCO2IN=PCO2
      FCOIN=PCO
      FH2IN=PH2
      FCH4IN=PCH4
      FN2IN=PN2
      FH2SIN=PH2S
      GTARIN=GTAR
      TIMEIN=TIME
      HSIN=HS
      WLIN=WL
C
      IF(GOXY.LE.0.) GO TO 880
      TGAS(1)=TGIN+50.
      TGAS(2)=TGAS(1)+100.
C
      GO TO 890
  880 TGAS(1)=TGIN-10.
      TGAS(2)=TGAS(1)-10.
  890 I=1
      GO TO 300
C
  840 CALL FPPLOT(X1,Y1,NPT1,IC1,2,120)
      CALL FPPLOT(X2,Y2,NPT2,IC2,4,120)
      CALL FPPLOT(X3,Y3,NPT3,IC3,3,120)
      CALL FPPLOT(X4,Y4,NPT4,IC4,1,120)
      CALL FPPLOT(X5,Y5,NPT5,IC5,2,120)
      GO TO 10
  900 STOP
      END
      SUBROUTINE VOLATL(YC,YOXY,YH,YN,YS,YASH,FC,FO,FH,FN,FS,VH2,R1,R2
     1,VNO)
      COMMON /A2/ XH2,XCO,XCO2,XH2S,XH2O,XN2,XCH4,XTAR
C     ***FC,FH,FN,FS ARE THE % OF O2,H2,N2,S RESPECTIVELY REMAINED IN
C        CHAR AFTER DEVOLATILIZATION***
      FO=5.
      FH=10.
      FS=50.
      FN=50.
```

```
      C     ***VH2 IS THE AMOUNT OF H2 IN VOLATILE AS % OF DMMF COAL, WHICH
      C        CAN BE ESTIMATED BY LOISON-CHAUVIN CORRELATION***
      C     *** R1=XCO/XCO2
      C     *** R2=XH2O/XCO2, R1 AND R2 CAN BE ESTIMATED BY LOISON-CHAUVIN
      C        CORRELATION FOR A GIVEN COAL****
            R1=2.0
            R2=2.667
            VH2=1.0
      C     *** FC IS THE FIXED CARBON OF THE GIVEN DMMF COAL,% ***
            VC=YC*100.-FC
            VH=YH*(100.-FH)
            VN=YN*(100.-FN)
            VS=YS*(100.-FS)
            VO=YOXY*(100.-FO)
            VCO2=VO/(32./44.+R1*16./28.+R2*16./18.)
      C     OXYGEN BALANCE ***
            VCO=R1*VCO2
            VH2O=R2*VCO2
            VH2S=VS*34./32.
            VN2=VN
      C     *** HYDROGEN BALANCE AND CARBON BALANCE TO SOLVE VCH4 AND VTAR ***
            H=VH-VH2-VH2O*2./18.-VH2S*2./34.
            C=VC-VCO*12./28.-VCO2*12./44.
            VCH4=(12.*H-C)/(12.*4./16.-12./16.)
            VTAR=(H-VCH4*4./16.)/(6./78.)
            VMO=VH2+VCO+VCO2+VH2O+VH2S+VN2+VCH4+VTAR
            XH2=VH2/VMO
            XCO=VCO/VMO
            XCO2=VCO2/VMO
            XH2O=VH2O/VMO
            XH2S=VH2S/VMO
            XN2=VN2/VMO
            XCH4=VCH4/VMO
            XTAR=VTAR/VMO
            WRITE(6,100) XH2,XCO,XCO2,XH2S,XN2,XCH4,XTAR,XH2O,VMO
        100 FORMAT(//2X,'XH2=',E10.4,2X,'XCO=',E10.4,2X,'XCO2=',E10.4,2X
           1,'XH2S=',E10.4,/2X,'XN2=',E10.4,2X,'XCH4=',E10.4,2X,'XTAR=',E10.4
           2,2X,'XH2O=',E10.4,2X,'VMO=',F10.4)
            RETURN
            END
```

```
            SUBROUTINE VSOLID(DELH,USI,TMOLE,OSUM,DP,TG,PT,AT,VIS,DENS,RDTIME
           1,US,UG)
      C
      C     FOR UPWARD FLOW, "DIRECT"=1.0
      C     FOR DOWNWARD FLOW, "DIRECT"=-1.0
      C
```

```
      C
      C     DOWNWARD FLOW
            DIRECT=-1.0
      C
            UG=(TMOLE*82.05*TG)/(AT*PT)
            DENG=PT*GSUM/(TMOLE*82.05*TG)
            ACONT=18.*VIS/(DENS*DP**2)
            UT=(DENS-DENG)*980.*(DP**2)/(18.*VIS)
            IF(USI.EQ.0.) GO TO 10
            US=USI
            GO TO 20
   10       US=UG-UT*DIRECT
   20       TIME=DELH/US
   30       BCONT=-ACONT*TIME
            IF(ABS(BCONT).LE.25.) GO TO 22
            EB=0.
            GO TO 28
   22       EB=EXP(BCONT)
   28       FTIME=DELH-USI*(1.-EB)/ACONT-(UG-UT*DIRECT)*(TIME-(1.-EB)/ACONT)
            DFTIME=-USI*EB-(UG-UT*DIRECT)*(1.-EB)
            DTIME=FTIME/DFTIME
            TIME=TIME-DTIME
            IF(ABS(DTIME).LE.0.02) GO TO 35
            GO TO 30
   35       RDTIME=TIME
            US=-DFTIME
            RETURN
            END
            SUBROUTINE HEAT(N,TEMP,HT)
            DIMENSION HT(20)
      C     N=1 IS H2 COMBUSTION, N=2 IS CO COMBUSTION, N=3 IS CH4 COMBUSTION,
      C     N=4 IS C6H6 COMBUSTION
      C     THE UNIT OF HT IS CAL/GMOLE
            DIMENSION HT298(20), DALPHA(20), DBETA(20), DGAMA(20)
            HT298(1)=-57798.
            HT298(2)=-66911.6
            HT298(3)=-191760.
            HT298(4)=-749420.
            DALPHA(1)=-2.765
            DALPHA(2)=-3.28
            DALPHA(3)=5.049
            DALPHA(4)=13.351
            DBETA(1)=0.947E-3
            DBETA(2)=7.18E-3
            DBETA(3)=-9.256E-3
            DBETA(4)=-3.1616E-2
            DGAMA(1)=2.636E-7
            DGAMA(2)=-2.8875E-6
            DGAMA(3)=9.501E-6
            DGAMA(4)=1.293E-5
            HT(N)=HT298(N)+DALPHA(N)*(TEMP-298.)+DBETA(N)*(TEMP**2-298.**2)
           1/2.+DGAMA(N)*(TEMP**3-298.**3)/3.
            RETURN
            END
```

```
      SUBROUTINE PYROLY(WL,SWL,GOXY,RHEAT1,DOXY,WATERP,CO2P,H2SP,N2P,
     1COP,H2P,CH4P,TARP)
      COMMON /S1/ FCOAL,FOXY,FSTEAM/S2/ TG,TS, DENS,DENG,CPS,PT
      COMMON /A1/ YC,YOXY,YH,YS,YN,YCR,YOXYR,YHR,YSR,YNR
      COMMON /A2/ XH2,XCO,XCO2,XH2S,XH2O,XN2,XCH4,XTAR
      DIMENSION HT(20)
      REAL N2P
      DO 402 N=1,4
      CALL HEAT(N, TG, HT)
  402 CONTINUE
C
      IF(GOXY.GT.0.) GO TO 123
      H2P=WL*XH2/100.
      CO2P=WL*XCO2/100.
      COP=WL*XCO/100.
      WATERP=WL*XH2O/100.
      H2SP=WL*XH2S/100.
      N2P=WL*XN2/100.
      CH4P=WL*XCH4/100.
      TARP=WL*XTAR/100.
      RHEAT1=0.
      GO TO 130
  123 DOXY=WL*(XH2/4.+XCO/56.+XCH4/8.+XTAR/10.4)*(32./100.)
      TARP=0.
      GOXYEX=GOXY-DOXY*FCOAL
      IF(GOXYEX.LT.0.) GO TO 124
      COP=0.
      CH4P=0.
      H2P=0.
      GO TO 126
  124 COP=(ABS(GOXYEX)/FCOAL)*(28./16.)
      COPMAX=WL*XCO/100.
      IF(COP.GT.COPMAX) GO TO 125
      H2P=0.
      CH4P=0.
      GO TO 126
  125 CH4P=(COP-COPMAX)*(16./(4.*28.))
      COP=COPMAX
      CH4PMX=WL*XCH4/100.
      IF(CH4P.GT.CH4PMX) GO TO 128
      H2P=0.
      GO TO 126
  128 H2P=(CH4P-CH4PMX)*(4.*2./16.)
      CH4P=CH4PMX
      H2PMAX=WL*XH2/100.
      IF(H2P.GT.H2PMAX) H2P=H2PMAX
  126 CO2P=WL*(XCO2/44.+XCO/28.+XCH4/16.+XTAR/13.)*(44./100.)-COP*(44.
     1/28.)-CH4P*(44./16.)
      WATERP=WL*(XH2/2.+XH2O/18.+XCH4/8.+XTAR/26.)*(18./100.)-H2P*18.
     1/2.-CH4P*36./16.
      H2SP=XH2S*(WL/100.)
      N2P=XN2*(WL/100.)
      RHEAT1=WL*(XH2*HT(1)/2.+XCO*HT(2)/28.+XCH4*HT(3)/16.
     1+XTAR*HT(4)/78.)/100.-COP*HT(2)/28.-CH4P*HT(3)/16.-H2P*HT(1)/2.
  130 RETURN
      END
```

```
      SUBROUTINE HEATUP(N,TEMP,TI,HTUP,CP)
      DIMENSION HTUP(30),ALPHA(30),BETA(30),GAMA(30),CP(30)
C     N=1 IS OXYGEN, N=2 IS STEAM, N=3 IS CO2, N=4IS CO,
C     N=5 IS CH4,  N=6 IS H2
C     N=5 IS CH4,  N=6 IS H2,  N=7 IS H2S,  N=8 IS N2
C     THE UNIT OF TEMP IS K,  THE UNIT OF HTUP IS CAL/GMOLE
      ALPHA(1)=6.148
      ALPHA(2)=7.256
      ALPHA(3)=6.214
      ALPHA(4)=6.42
      ALPHA(5)=3.381
      ALPHA(6)=6.947
      ALPHA(7)=6.662
      ALPHA(8)=6.524
      BETA(1)=3.102E-3
      BETA(2)=2.298E-3
      BETA(3)=1.0396E-2
      BETA(4)=1.665E-3
      BETA(5)=1.8044E-2
      BETA(6)=-0.2E-3
      BETA(7)=5.134E-3
      BETA(8)=1.25E-3
      GAMA(1)=-0.923E-6
      GAMA(2)=0.283E-6
      GAMA(3)=-3.545E-6
      GAMA(4)=-0.196E-6
      GAMA(5)=-4.3E-6
      GAMA(6)=0.481E-6
      GAMA(7)=-0.854E-6
      GAMA(8)=-0.001E-6
      CP(N)=ALPHA(N)+BETA(N)*TEMP+GAMA(N)*(TEMP**2)
      HTUP(N)=ALPHA(N)*(TEMP-TI)+BETA(N)*(TEMP**2-TI**2)/2.
     1+GAMA(N)*(TEMP**3-TI**3)/3.
      RETURN
      END
```

```
1124.            SUBROUTINE ENTHAL(TG,TS,FCOAL,FASH,WL,CPS,ENTH)
1125.            DIMENSION HTUP(30),ALPHA(30),BETA(30),GAMA(30),CP(30)
1126.            COMMON /A3/ GOXY,GSTEAM,GCO2,GCO,GH2,GH2S,GN2,GCH4
1127.            DO 50 N=1,8
1128.            CALL HEATUP(N,TG,298.,HTUP,CP)
1129.        50  CONTINUE
1130.            ENTHG=HTUP(1)*GOXY/32.+HTUP(2)*GSTEAM/18.+HTUP(3)*GCO2/44.+HTUP(4
1131.           1*GCO/28.+HTUP(5)*GCH4/16.+HTUP(6)*GH2/2.+HTUP(7)*GH2S/34.+HTUP(8)
1132.           2*GN2/28.
1133.            ENTHS=CPS*FCOAL*(1.+FASH-WL/100.)*(TS-298.)
1134.            ENTH=ENTHG+ENTHS
1135.            RETURN
1136.            END
1137.            SUBROUTINE COMBUS(TG,TS,PT,RP,POXY,SWL,Y,DENSP,RATE,CWL,PHI,QRH
1138.           1,FASH,DELTIM,Q1,Q2)
1139.            REAL KS,KDIFF,KDASH,KOVER
1140.            DP=2.*RP
1141.            VOID=0.75
1142.            TM=(TS+TG)/2.
1143.            Q1=-94051.-3.964*(TS-298.)+(3.077E-3)*(TS*TS-298.*298.)
1144.           1-(0.874E-6)*(TS**3-298.**3)
1145.            Q2=-26414.-0.684*(TS-298.)-(0.513E-3)*(TS*TS-298.*298.)
1146.           1+(8.85E-8)*(TS**3-298.**3)
1147.            Z=2500.*EXP(-6249./TM)
1148.            IF(DP.LE.5.0E-3) GO TO 10
1149.            IF(DP.LE.0.1) GO TO 20
1150.            GO TO 30
1151.        10  PHI=(2.*Z+2.)/(Z+2.)
1152.            GO TO 40
1153.        20  PHI=((2.*Z+2.)-Z*(DP-0.005)/0.095)/(Z+2.)
1154.            GO TO 40
1155.        30  PHI=1.0
1156.        40  QRH=-(Q1/12.)*(2./PHI-1.)-(Q2/12.)*(2.-2./PHI)
1157.            IF(POXY.LE.0.) GO TO 55
1158.            IF(TS.LT.273.) GO TO 55
1159.            ATS=-17967./TS
1160.            IF(ABS(ATS).GT.49.) GO TO 33
1161.            EATS=EXP(ATS)
1162.            GO TO 44
1163.        33  EATS=1.E-15
1164.        44  KS=8710.*EATS
1165.            DIFF=(4.26/PT)*(TG/1800.)**1.75
1166.            KDIFF=(PHI*0.292*DIFF)/(DP*TM)
1167.            IF(Y.GE.0.95) GO TO 45
1168.            KDASH=KDIFF*(VOID**2.5)
1169.            KOVER=1./(1./KDIFF+1./(Y*Y*KS)+(1./KDASH)*(1./Y-1.).
1170.            GO TO 50
1171.        45  KOVER=1./(1./KDIFF+1./KS)
1172.        50  RATE=KOVER*POXY
1173.            CWL=RATE*3.*(1.+FASH-SWL/100.)*DELTIM/(DENSP*RP)
1174.            GO TO 66
1175.        55  RATE=0.
1176.            CWL=0.
1177.        66  RETURN
1178.            END
```

```
1179.            SUBROUTINE CBSTM(DELTIM,PSTEAM,PH2,PCO,RP,PT,DENSP,TG,TS,SWL,Y
1180.           1,FASH,RATE2,CWL2,QCSM,WL)
1181.            REAL KS,KDIFF,KDASH,KOVER
1182.            VOID=0.75
1183.            DP=2.*RP
1184.            IF(PSTEAM.LT.0.001) GO TO 10
1185.            IF(WL.GE.99.9) GO TO 10
1186.            IF(PH2.LE.0.) GO TO 5
1187.            IF(PCO.LE.0.) GO TO 5
1188.            CTS=17.644-30260./(TS*1.8)
1189.            IF(ABS(CTS).GT.16.) GO TO 10
1190.            CSEQK=EXP(CTS)
1191.            IF(CSEQK.GT.10000.) GO TO 5
1192.            PEXC=PSTEAM-PH2*PCO/CSEQK
1193.            GO TO 6
1194.       5    PEXC=PSTEAM
1195.       6    IF(PEXC.LE.0.) GO TO 10
1196.            GO TO 20
1197.      10    CWL2=0.
1198.            RATE2=0.
1199.            QCSM=0.
1200.            GO TO 30
1201.      20    TM=(TS+TG)/2.
1202.            IF(TM.LE.200.) GO TO 10
1203.            ATS=-21060./TS
1204.            IF(ABS(ATS).GT.25.) GO TO 10
1205.            EATS=EXP(ATS)
1206.            KS=247.*EATS
1207.            KDIFF=(10.E-4)*(TM/2000.)**0.75/(DP*PT)
1208.            IF(Y.GE.0.95) GO TO 45
1209.            KDASH=KDIFF*(VOID**2.5)
1210.            KOVER=1./(1./KDIFF+1./(Y*Y*KS)+(1./KDASH)*(1./Y-1.))
1211.            GO TO 50
1212.      45    KOVER=1./(KDIFF+1./KS)
1213.      50    RATE2=KOVER*PEXC
1214.            CWL2=RATE2*3.*(1.+FASH-SWL/100.)*DELTIM/(DENSP*RP)
1215.     150    QCSM=31382.+2.011*(TS-298.)-(0.733E-3)*(TS**2-298.**2)/2.
1216.      30    RETURN
1217.            END
```

```
1218.            SUBROUTINE CBCO2(PCO2,DELTIM,WL,SWL,RP,FT,DENSP,TG,TS,FASH,
1219.           1,RATE3,CWL3,QCBCO2)
1220.            REAL KS,KDIFF,KDASH,KOVER
1221.            DP=2.*RP
1222.            VOID=0.75
1223.            IF(TS.LE.850.) GO TO 10
1224.            IF(PCO2.LE.0.) GO TO 10
1225.            IF(WL.GE.99.9) GO TO 10
1226.            GO TO 100
1227.       10   CWL3=0.
1228.            RATE3=0.
1229.            QCBCO2=0.
1230.            GO TO 200
1231.       100  TM=(TS+TG)/2.
1232.            IF(TM.LE.200.) GO TO 10
1233.            BTS=-21060./TS
1234.            IF(ABS(BTS).GT.25.) GO TO 10
1235.            EBTS=EXP(BTS)
1236.            KS=247.*EBTS
1237.            KDIFF=(7.45E-4)*(TM/2000.)**0.75/(DP*FT)
1238.            IF(Y.GE.0.95) GO TO 45
1239.            KDASH=KDIFF*(VOID**2.5)
1240.            KOVER=1./(1./KDIFF+1./(Y*Y*KS)+(1./KDASH)*(1./Y-1.))
1241.            GO TO 50
1242.       45   KOVER=1./(1./KDIFF+1./KS)
1243.       50   RATE3=KOVER*PCO2
1244.            CWL3=RATE3*3.*(1.+FASH-SWL/100.)*DELTIM/(DENSP*RP)
1245.       150  QCBCO2=41220.+2.256*(TS-298.)-(7.066E-3)*(TS**2-298.**2)/2.
1246.           $+(3.153E-6)*(TS**3-298.**3)/3.
1247.       200  RETURN
1248.            END
```

```
      SUBROUTINE WGSHIF(TS,PCO,PSTEAM,PCO2,PH2,RATE4,QWG,GCO,GSTEAM,
     1GCO2,GH2,DELTIM,FCOAL,FASH,WGL,TG,PT)
C     WATER-GAS-SHIFT REACTION
      F=0.2
      IF(TS.LE.1000.) GO TO 10
      TM=(TG+TS)/2.
      CKWG=EXP(-3.6893+7234./(1.8*TM))
      EK=EXP(-27760./(1.987*TS))
      EP=0.5-PT/250.
      PF=PT**EP
      RAT=EXP(-8.91+5553./TS)
      GO TO 20
   10 RATE4=0.
      QWG=0.
      GO TO 30
   20 PEXC=PCO-PCO2*PH2/(CKWG*PSTEAM)
      RATE4=F*(2.877E5)*EK*(PEXC/PT)*PF*RAT
      WGL=RATE4*DELTIM*FASH
C     THE UNIT OF RATE4 IS GMOLE/SEC-GM OF ASH
C
      A=1.-CKWG
      B=GCO2/44.+GH2/2.+CKWG*(GCO/28.+GSTEAM/18.)
      C=(GCO2/44.)*(GH2/2.)-CKWG*(GCO/28.)*(GSTEAM/18.)
      D=B*B-4.*A*C
      IF(D.LT.0.) GO TO 10
      IF(PEXC.LT.0.) GO TO 25
      X=(-B+SQRT(D))/(2.*A)
      GO TO 26
   25 X=(-B-SQRT(D))/(2.*A)
   26 WGLMAX=X/FCOAL
      CHECK=WGL*WGLMAX
      IF(CHECK.LT.0.) GO TO 10
      IF(ABS(WGL).GT.ABS(WGLMAX)) GO TO 27
      GO TO 28
   27 WGL=WGLMAX
      RATE4=WGL/(DELTIM*FASH)
   28 QWG=-9839.-0.515*(TS-298.)+(6.233E-3)*(TS**2-298.**2)/2.-(3.151E-
     $)*(TS**3-298.**3)/3.
   30 RETURN
      END
```

```
      SUBROUTINE CBHYM(PH2,PCH4,DELTIM,WL,SWL,Y,RP,DENSP,PT,TG,TS,CWL5
     1,RATE5,QCBHY,FASH)
      REAL KV,KEQ,KS,KDIFF,KDASH,KOVER
      IF(TS.LE.1200.) GO TO 10
      IF(WL.GE.99.9) GO TO 10
      IF(WL.LE.SWL) GO TO 10
      VOID=0.75
      DP=2.*RP
      TM=(TG+TS)/2.
      IF(PH2.LE.0.001) GO TO 10
      IF(PCH4.LE.0.) GO TO 5
      ATS=18400./(1.8*TS)
      IF(ABS(ATS).GE.25.) GO TO 5
      KEQ=(0.175/34713.)*EXP(ATS)
      PEQ=PCH4/KEQ
      PEQMAX=PH2*PH2
      IF(PEQ.GE.PEQMAX) GO TO 10
      PEQMIN=PEQMAX/10000.
      IF(PEQ.LE.PEQMIN) GO TO 5
      GO TO 6
5     PEXC=PH2
      GO TO 7
6     PEXC=PH2-SQRT(PEQ)
7     IF(PEXC.LE.0.001) GO TO 10
      BTS=-17921./TS
      IF(ABS(BTS).GE.25.) GO TO 10
      KS=0.120*EXP(BTS)
      KDIFF=(1.33E-3)*(TM/2000.)**0.75/(DP*PT)
      IF(Y.GE.0.95) GO TO 20
      KDASH=KDIFF*(VOID**2.5)
      KOVER=1./(1./KDIFF+1./(Y*Y*KS)+(1./KDASH)*(1./Y-1.))
      GO TO 30
20    KOVER=1./(1./KDIFF+1./KS)
30    RATE5=KOVER*PEXC
      CWL5=RATE5*3.*(1.+FASH-SWL/100.)*DELTIM/(DENSP*RP)
      QCBHY=-17889.-14.613*(TS-298.)+(1.7424E-2)*(TS*TS-298.*298.)/2.
     1-(5.26E-6)*(TS**3-298.**3)/3.
      GO TO 100
10    RATE5=0.
      CWL5=0.
      QCBHY=0.
100   RETURN
      END
      SUBROUTINE CH4REF(TS,GCH4,FCOAL,DELTIM,DCH46,QMREF)
      IF(TS.LE.1000.) GO TO 10
      EK=312.*EXP(-30000./(1.987*TS))
      DCH46=GCH4*(1.-EXP(-EK*DELTIM))/FCOAL
      QMREF=45126.55+16.624*TS-(9.6385E-3)*TS*TS+(1.7546E-6)*(TS**3)
      GO TO 50
10    DCH46=0.
      QMREF=0.
50    RETURN
      END
/*
//LKED.SYSLMOD DD DSNAME=CE060266.CHAUNG(CBHS),
// VOL=SER=DISK00,UNIT=3330-1,DISP=(NEW,KEEP,DELETE),
// SPACE=(1024,(20,10,1),RLSE),DCB=BLKSIZE=7294
//
```

(B) Executing Program

```
1.      //ENGRTZCH JOB (CE060266,****),'CHAUNG',REGION=192K,TIME=5
2.      /*ROUTE  XEQ   CPU2
3.      /*ROUTE  PRINT LOCAL
4.      /*JOBPARM I=15,L=15
4.1     //*
5.      //JOBLIB DD DSN=CE060266.CHAUNG,VOL=SER=DISK00,
6.      // UNIT=3330-1,DISP=(OLD,KEEP)
6.1     //*
7.      //GO EXEC PGM=CGAS
8.      //FT05F001 DD DDNAME=SYSIN
9.      //FT06F001 DD SYSOUT=A
10.     //SYSIN DD *
11.      &DATA NAME='TEXACO I-1',TA=505.22,TSTEAM=696.67,TOXY=298.,
12.      YOXY=.0156956,YH=.0743163,YC=0.8802616,YS=0.0210464,YN=0.0084423,
13.      YASH=.159,XMOIS=0.002,FOXY=0.866,FSTEAM=0.241,TFCOAL=76.66
14.      &END
15.      &DATA NAME='TEXACO I-2',TA=496.33,TSTEAM=676.33,TOXY=298.,
16.      YOXY=.0205587,YH=.070383,YC=0.8833,YS=.016568,YN=.008828,
17.      YASH=.1731,XMOIS=.002,FOXY=.76818,FSTEAM=0.314,TFCOAL=81.18
18.      &END
19.      &DATA NAME='TEXACO I-3',TA=501.3,TSTEAM=668.,TOXY=298.0,
20.      YOXY=.024276,YH=.066913,YC=0.877634,YS=0.02144,YN=0.0093853,
21.      YASH=.1885,XMOIS=0.002,FOXY=0.813,FSTEAM=0.309,TFCOAL=82.2017
22.      &END
23.      &DATA NAME='TEXACO I-4A',TA=503.55,TSTEAM=751.89,TOXY=298.0,
24.      YOXY=.03479,YH=.067723,YC=0.873468,YS=0.015228,YN=0.0085427,
25.      YASH=.1923,XMOIS=0.002,FOXY=0.80713,FSTEAM=0.323,TFCOAL=79.456
26.      &END
27.      &DATA NAME='TEXACO I-4B',TA=500.22,TSTEAM=706.89,TOXY=298.,
28.      YOXY=.0344827,YH=0.06723,YC=0.87455,YS=0.01508,YN=0.0084043,
29.      YASH=.1909,XMOIS=0.002,FOXY=0.7972,FSTEAM=0.310,TFCOAL=81.846
30.      &END
31.      &DATA NAME='TEXACO I-5A',TA=503.0,TSTEAM=714.7,TOXY=298.0,
32.      YOXY=.0268456,YH=.065374,YC=.87584,YS=.022,YN=.0094456,
33.      YASH=.1954,XMOIS=.002,FOXY=.8263,FSTEAM=.352,TFCOAL=71.63
34.      &END
35.      &DATA NAME='TEXACO I-5B',TA=500.78,TSTEAM=715.78,TOXY=298.,
36.      YOXY=.0267346,YH=.06665,YC=0.87441,YS=0.022134,YN=0.0095747,
37.      YASH=.1958,XMOIS=0.002,FOXY=0.81712,FSTEAM=0.392,TFCOAL=65.0
38.      &END
39.      &DATA NAME='TEXACO I-5C',TA=497.44,TSTEAM=714.67,TOXY=298.0,
40.      YOXY=.0268824,YH=0.0665837,YC=0.874051,YS=0.022402,YN=0.0097075,
41.      YASH=.1965,XMOIS=0.002,FOXY=0.832,FSTEAM=0.429,TFCOAL=56.264
42.      &END
43.      &DATA NAME='TEXACO I-6 ',TA=504.1,TSTEAM=681.89,TOXY=298.0,
44.      YOXY=.0254344,YH=.066482,YC=0.8738353,YS=0.02417527,YN=0.0096952,
45.      YASH=.2058,XMOIS=0.002,FOXY=0.77376,FSTEAM=0.291,TFCOAL=87.7317
46.      &END
47.      &DATA NAME='TEXACO I-7A',TA=504.67,TSTEAM=686.89,TOXY=298.,
48.      YOXY=.02971657,YH=.068548,YC=0.87077,YS=.0208515,YN=0.009739,
49.      YASH=.1991,XMOIS=.002,FOXY=.7757,FSTEAM=0.282,TFCOAL=90.0736
50.      &END
```

```
51.       &DATA NAME='TEXACO I-7B',TA=509.67,TSTEAM=686.89,TOXY=298.,
52.       YOXY=.01970,YH=0.0672478,YC=0.8727273,YS=0.020548,YN=0.0097135,
53.       YASH=.1970,XMOIS=0.002,FOXY=0.782,FSTEAM=0.267,TFCOAL=95.3917
54.       &END
55.       &DATA NAME='TEXACO I-8A',TA=506.89,TSTEAM=680.22,TOXY=298.0,
56.       YOXY=.0315077,YH=0.06634,YC=0.87212,YS=0.02006,YN=0.009478,
57.       YASH=.1875,XMOIS=0.002,FOXY=0.797,FSTEAM=0.247,TFCOAL=92.13
58.       &END
59.       &DATA NAME='TEXACO I-8B',TA=510.22,TSTEAM=685.78,TOXY=298.,
60.       YOXY=.0313653,YH=0.06617466,YC=0.8726937,YS=0.0200492,YN=0.009471,
61.       YASH=.187,XMOIS=0.002,FOXY=0.8016,FSTEAM=0.239,TFCOAL=95.0676
62.       &END
63.       &DATA NAME='TEXACO I-8C',TA=508.55,TSTEAM=684.67,TOXY=298.,
64.       YOXY=.0317969,YH=0.06655,YC=0.8717,YS=0.020212,YN=0.0094897,
65.       YASH=.1886,XMOIS=.002,FOXY=.80028,FSTEAM=0.246,TFCOAL=92.86
66.       &END
67.       &DATA NAME='TEXACO I-9 ',TA=501.33,TSTEAM=667.44,TOXY=298.,
68.       YOXY=.03531,YH=0.065915,YC=0.87164,YS=0.017222,YN=0.00954,
69.       YASH=.1929,XMOIS=0.002,FOXY=0.78725,FSTEAM=0.268,TFCOAL=87.79
70.       &END
71.       &DATA NAME='TEXACO I-10',TA=481.33,TSTEAM=708.00,TOXY=298.0,
72.       YOXY=.0213949,YH=0.069624,YC=0.88396,YS=0.0168,YN=0.0078568,
73.       YASH=.1727,XMOIS=0.002,FOXY=0.83457,FSTEAM=0.276,TFCOAL=129.77
74.       &END
75.       &DATA NAME='TEXACO I-11',TA=477.44,TSTEAM=677.44,TOXY=298.,
76.       YOXY=.02142,YH=0.07104,YC=0.882246,YS=0.016943,YN=0.0079874,
77.       YASH=.1737,XMOIS=0.002,FOXY=0.84843,FSTEAM=0.279,TFCOAL=132.7937
78.       &END
79.       &DATA NAME='TEXACO HCOAL',TA=503.,TSTEAM=714.7,TOXY=298.,
80.       YOXY=.016326,YH=0.06122,YC=0.887,YS=0.02313,YN=0.012244,
81.       YASH=.2650,XMOIS=0.002,FOXY=0.72871,FSTEAM=0.3188,TFCOAL=127.37
82.       &END
83.       &DATA NAME='TEXACO SRCII',TA=503.,TSTEAM=714.7,TOXY=298.,
84.       YOXY=.02283,YH=0.04902,YC=0.87161,YS=0.039753,YN=0.0167875,
85.       YASH=.2554,XMOIS=0.00,FOXY=0.770,FSTEAM=0.300,TFCOAL=126.11
86.       &END
87.       &DATA NAME='TEXACO EXXON',TA=503.,TSTEAM=714.7,TOXY=298.,
88.       YOXY=.04743,YH=0.056076,YC=0.849423,YS=0.0329,YN=0.01417,
89.       YASH=.1672,XMOIS=0.00,FOXY=0.79,FSTEAM=0.500,TFCOAL=126.11
90.       &END
91.      /*
```

☆U.S. GOVERNMENT PRINTING OFFICE:1979 -640 -014/ 4649 REGION NO. 4

U.S. DEPARTMENT OF COMMERCE
Technology Administration
National Technical Information Service
Springfield, VA 22161 (703) 605-6000